Fermilab, October 02 , 2012

Particle Physics' Contribution to Dedicated Innovative Brain PET Imagers

Stan Majewski, PhD (HEP)

Director, Nuclear Medicine Imaging Instrumentation Program
Center for Advanced Imaging
Department of Radiology, West Virginia University
Morgantown, WV

Groupe Charpak-Amerique (West)

Leon bitten by a bee

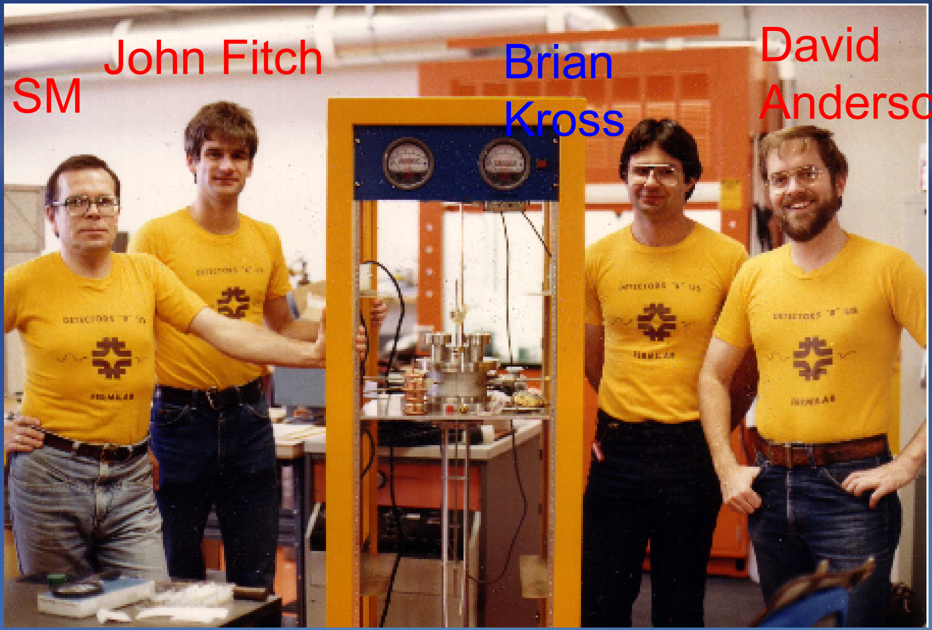

Leon

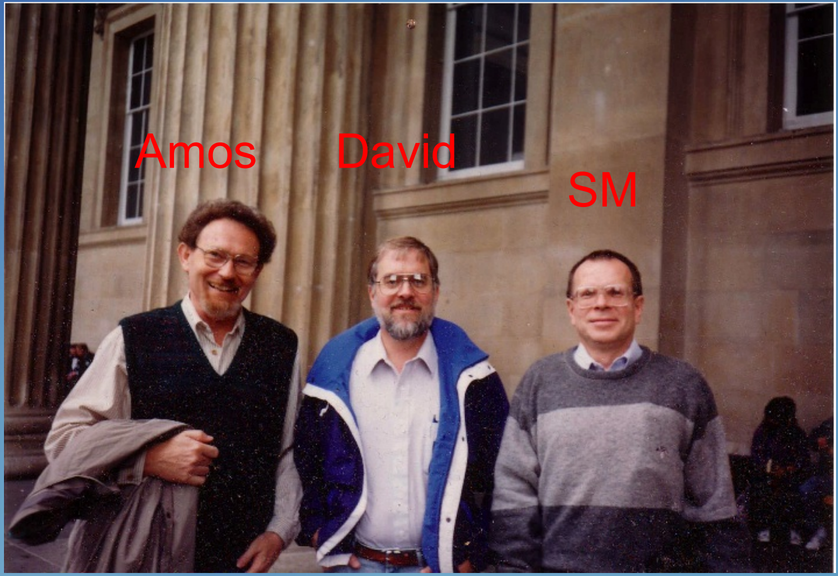

Nobel for Leon

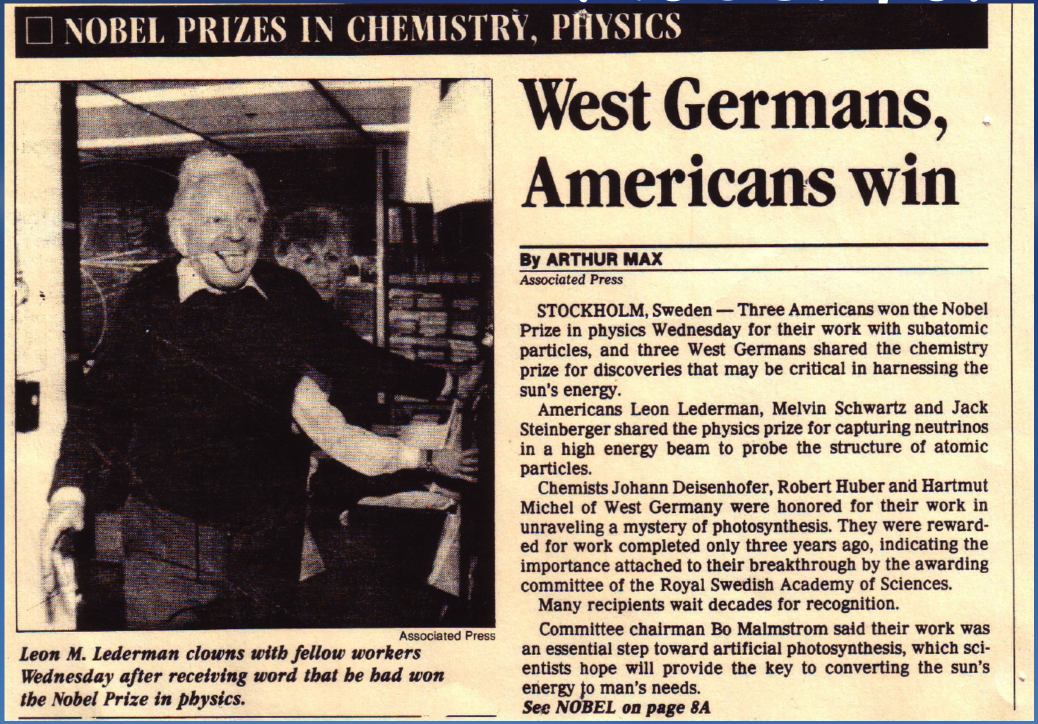

☐ NOBEL PRIZES IN CHEMISTRY, PHYSICS

West Germans, Americans win

By ARTHUR MAX
Associated Press

STOCKHOLM, Sweden — Three Americans won the Nobel Prize in physics Wednesday for their work with subatomic particles, and three West Germans shared the chemistry prize for discoveries that may be critical in harnessing the sun's energy.

Americans Leon Lederman, Melvin Schwartz and Jack Steinberger shared the physics prize for capturing neutrinos in a high energy beam to probe the structure of atomic particles.

Chemists Johann Deisenhofer, Robert Huber and Hartmut Michel of West Germany were honored for their work in unraveling a mystery of photosynthesis. They were rewarded for work completed only three years ago, indicating the importance attached to their breakthrough by the awarding committee of the Royal Swedish Academy of Sciences.

Many recipients wait decades for recognition.

Committee chairman Bo Malmstrom said their work was an essential step toward artificial photosynthesis, which scientists hope will provide the key to converting the sun's energy to man's needs.

See NOBEL on page 8A

Associated Press

Leon M. Lederman clowns with fellow workers Wednesday after receiving word that he had won the Nobel Prize in physics.

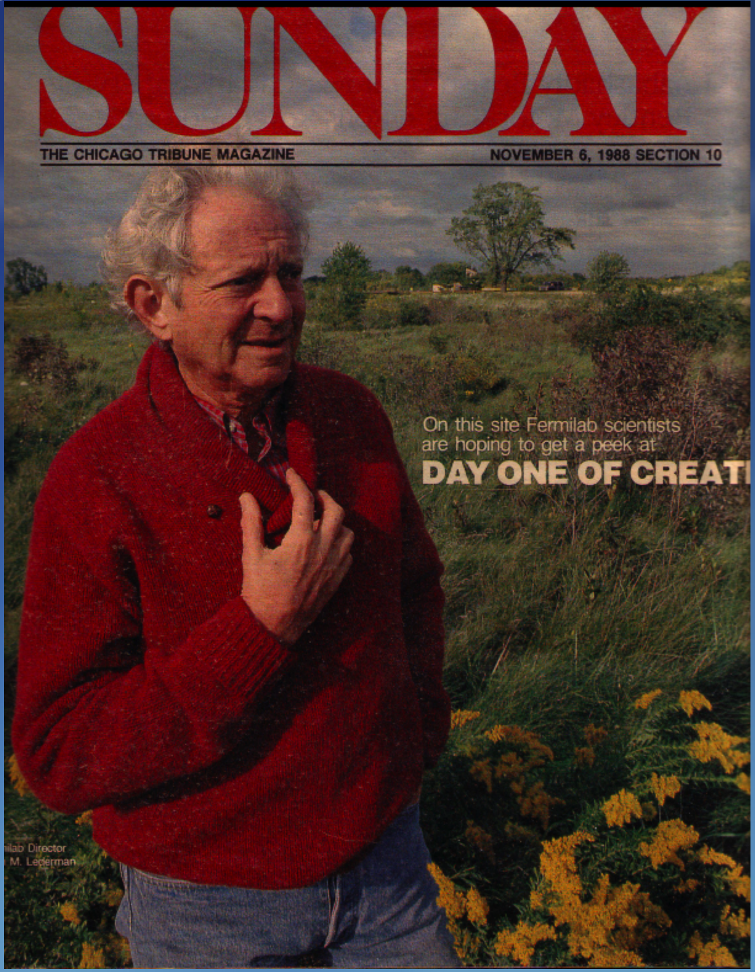

Plan

- A short “spirit-lifting” history introduction
- Motivation for dedicated PET systems
- Motivation for MRI-compatibility
- SiPM enabling technology
- Organ specific imagers
- Main emerging application focus: brain
- Examples of implementations, prior art
- TOFPET option
- Unique opportunity for particle physics community: Fermilab, Berkeley, Brookhaven, Jefferson Lab, ..

Spin-off from ~~particle physics~~ Higgs ?

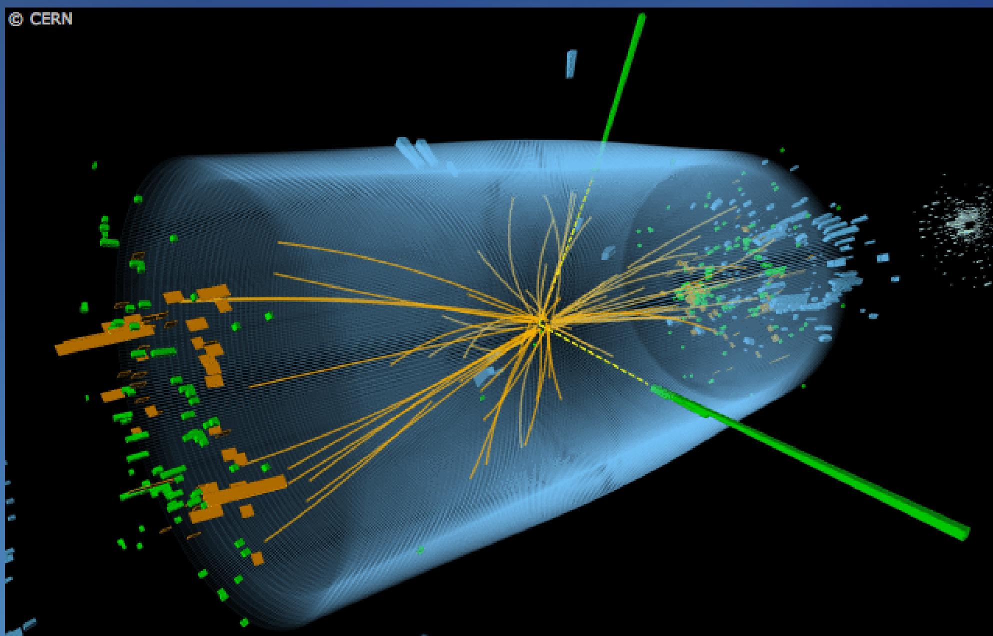

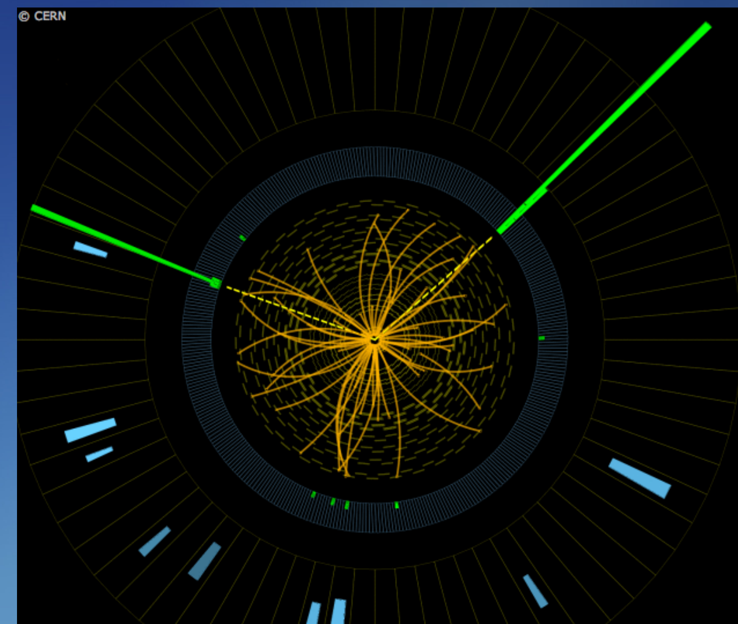

Candidate Higgs event in the CMS at LHC

Why PET ?

Similarities and differences

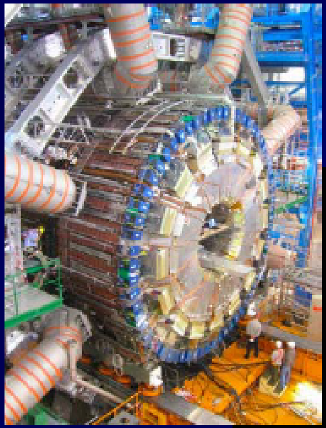

Calorimeter

HEP

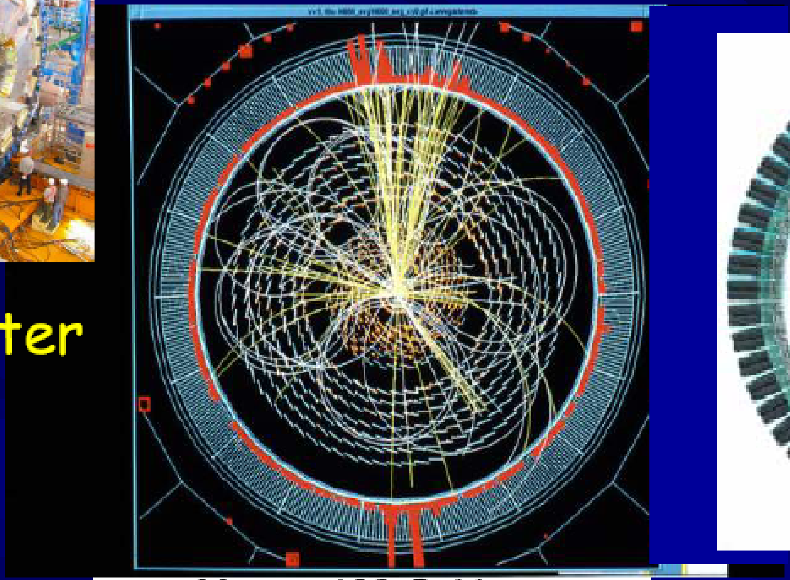

M_{Higgs} = 100 GeV

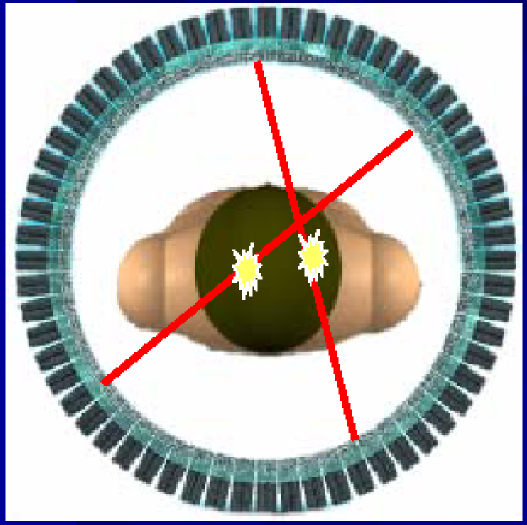

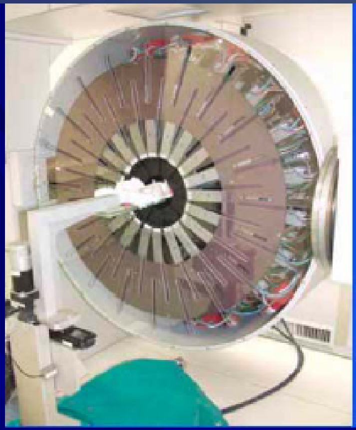

PET Camera

Biomedical Imaging

Similarities

- Geometry and granularity
- Detector (Crystals & scintillator)
- Photo Sensor (PM,APD)
- Electronics: Fast and compact
- Event rate & Data volume

Differences

- Energy range (10GeV-511keV)
- No synchronisation
- --> free running electronics

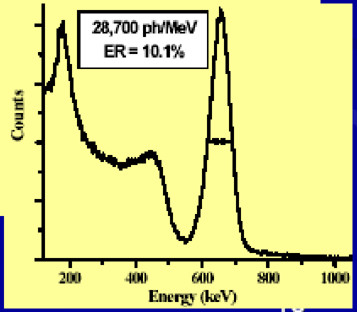

Rationale

-Spin-offs from the "big physics" projects are popular and expected by all the "stakeholders", even if not part of the main "mission"

-Scientists involved are to a large extent "normal" people sharing the concerns of the society

-Medical imaging was and is a natural spin-off from the particle physics community via:

- Relevant technical expertise
- Radiation detection instrumentation
- Fast readout electronics and data acquisition systems
- Fast computers
- Computing algorithms, including simulations ("Monte Carlo")

-Special opening is in the dedicated organ specific imagers, where the technology advancements (compact, mobile, offer new opportunities to implement what particle physics is using or developed initially for the main mission.

Positron Emission Tomography (PET)

Ring of Photon Detectors

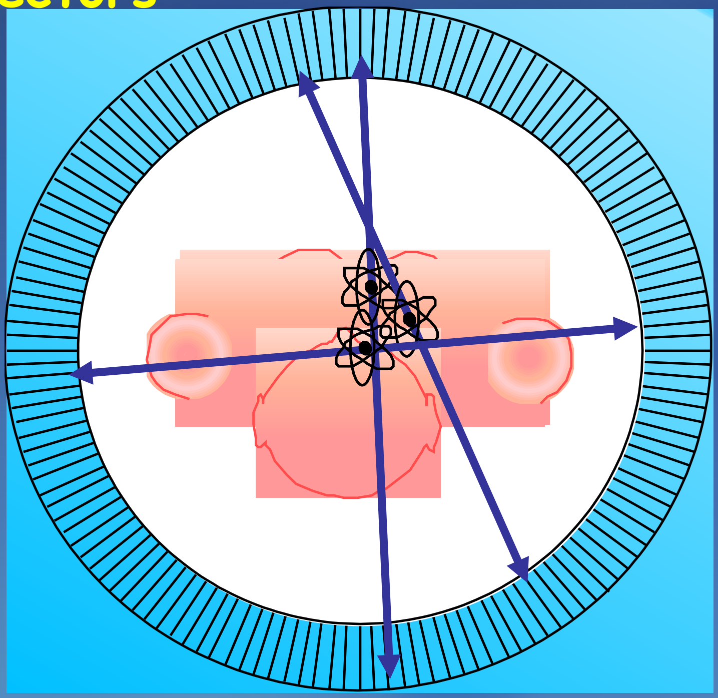

- Radionuclide decays by emitting a positron (β+).
- β+ annihilates with e- from tissue, forming back-to-back 511 keV photon pair.
- 511 keV photon pairs detected via time coincidence.
- Positron lies on line defined by detector pair.

- Detects Pairs of Back-to-Back 511 keV Photons
  - No Collimator Needed ⇒ High Efficiency

(Bill Moses, LBL)

Historically: BGO "Block Detector"

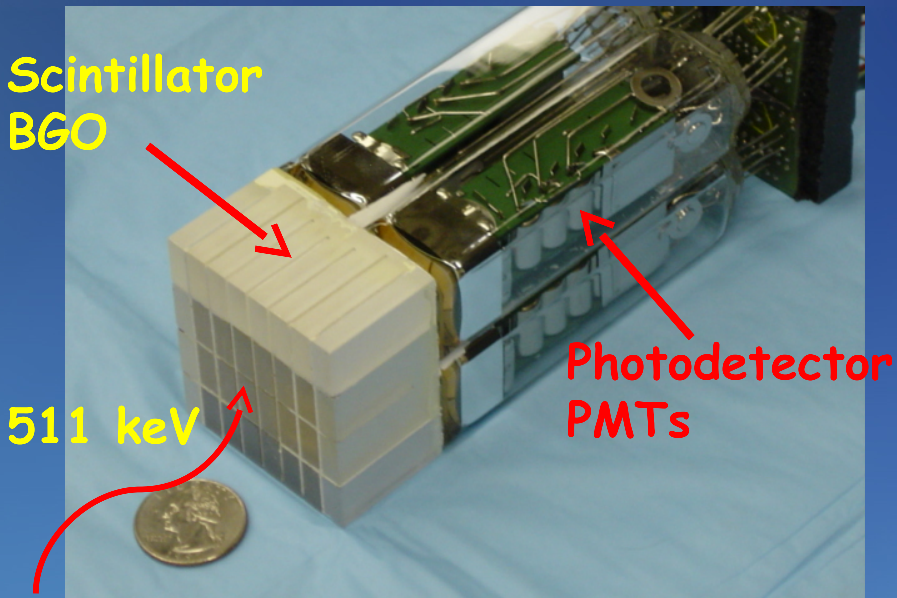

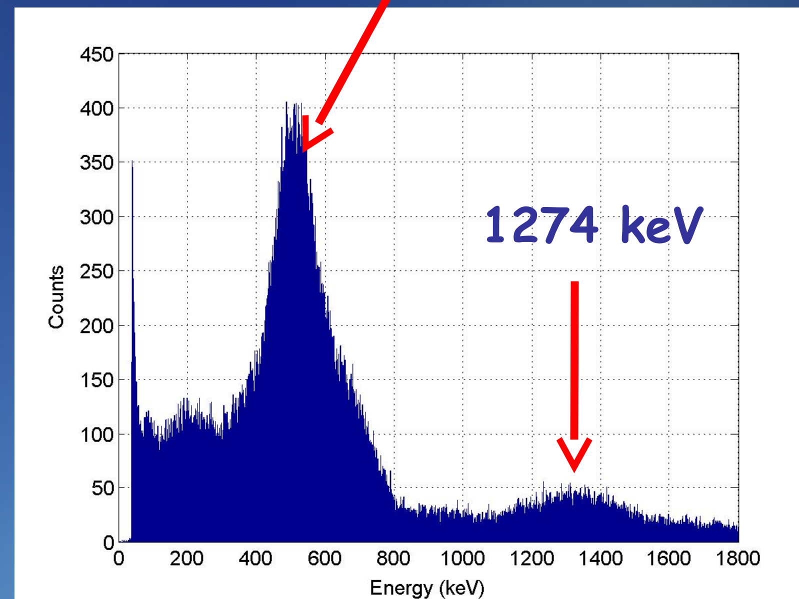

5.3 cm × 5 cm and 3 cm thick
8×4 array, 12.5 mm × 5.25 mm crystal size

(Bill Moses, LBL)

PET Hardware Development

The HIDAC Camera Project at CERN, 1977-1982

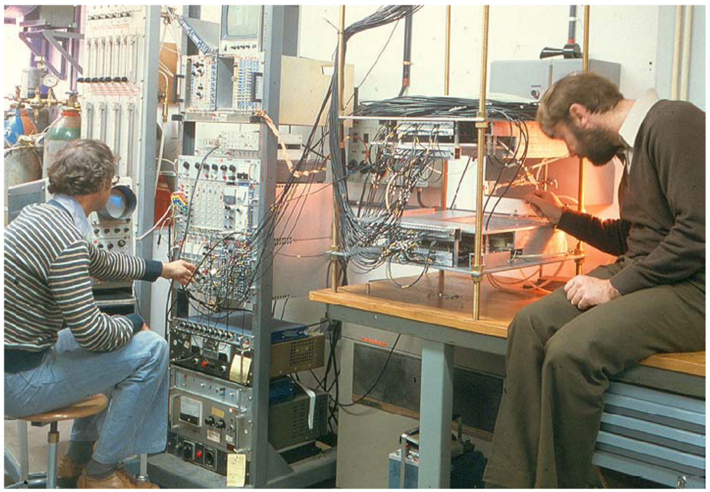

1978

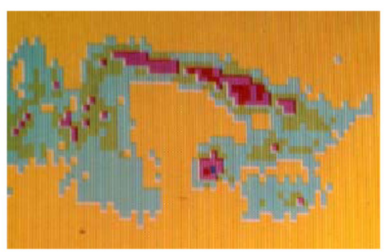

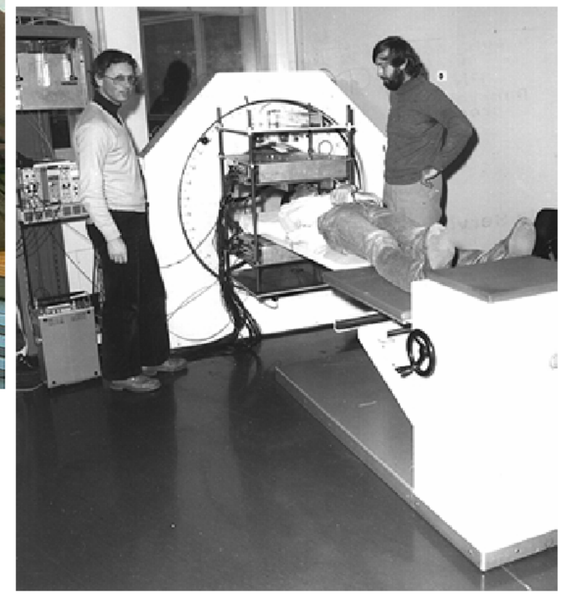

1982

Reconstruction Software

Phys. Med. Biol., 1983, Vol. 28, No. 9, 1009–1019. Printed in Great Britain

A general method for three-dimensional filter computation

B Schorr†, D Townsend‡ and R Clack‡

† DD Division, CERN, Geneva, Switzerland

‡ Department of Nuclear Medicine, Cantonal Hospital, Geneva, Switzerland

Received 24 September 1982, in final form 7 February 1983

Abstract. Application of the Fourier space deconvolution algorithm to three-dimensional (3D) reconstruction problems necessitates the computation of a frequency space filter; which requires taking the 3D Fourier transform of the system response function. In this paper, it is shown that for system response functions of the specific form $d(\theta, \varphi)/r^2$, with $d(\theta, \varphi)$ an angular function describing the imaging system, the filter computation can always be reduced to a single integration which, in many cases, may be performed analytically. Complete expressions are derived for the general 3D filter, and two examples are given to illustrate the use of such expressions.

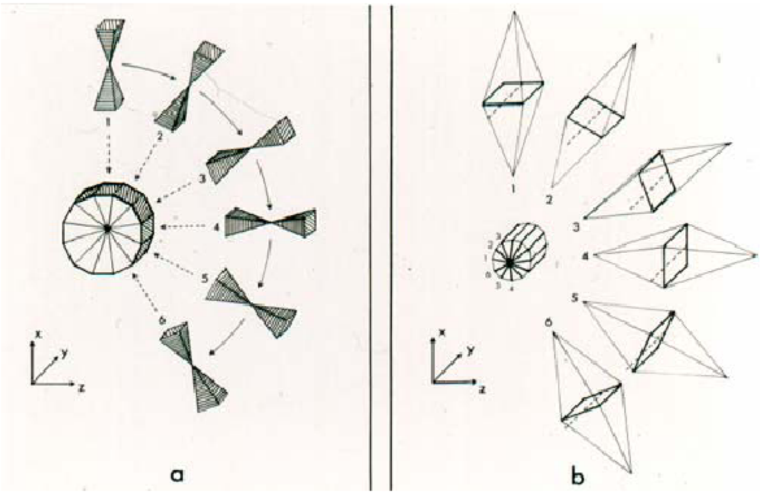

equation (28) may be written

$$D(\Theta, \Phi) = \frac{1}{\cos\Theta} \int_{\Phi-\varphi_0}^{\Phi+\varphi_0} \int_{-\theta_0}^{\theta_0} \delta(\cos\varphi + \tan\theta \tan\Theta)\, d(\theta, \Phi-\varphi)\, d\theta\, d\varphi. \quad (32)$$

Setting $t = \cos\varphi + \tan\theta \tan\Theta$, $\theta = \tan^{-1}[(t - \cos\varphi)/\tan\Theta]$ equation (32) becomes

$$D(\Theta, \Phi) = \frac{\tan\Theta}{\cos\Theta} \int_{\Phi-\varphi_0}^{\Phi+\varphi_0} \int_{t_1}^{t_2} \delta(t) \frac{d(\tan^{-1}[(t-\cos\varphi)/\tan\Theta], \Phi-\varphi)}{\tan^2\Theta + (t-\cos\varphi)^2}\, dt\, d\varphi \quad (33)$$

where

$$t_1 = \cos\varphi - \tan\theta_0 \tan\Theta$$

$$t_2 = \cos\varphi + \tan\theta_0 \tan\Theta.$$

Since

$$\int_a^b \delta(t) f(t)\, dt = \tfrac{1}{2}[\mathrm{sign}(b) - \mathrm{sign}(a)] f(0) \quad (34)$$

with $\mathrm{sign}(0) = 0$, equation (33) may be written

$$D(\Theta, \Phi) = \int_{\Phi-\varphi_0}^{\Phi+\varphi_0} s(\varphi, \theta_0, \Theta)\, g(\varphi, \Theta, \Phi)\, d\varphi \quad (35)$$

for $0 < \Theta < \pi/2$, $0 \leq \Phi \leq \pi/2$ where the functions s and g are given by

$$s(\varphi, \theta_0, \Theta) = \tfrac{1}{2}[\mathrm{sign}(\cos\varphi + \tan\theta_0 \tan\Theta) - \mathrm{sign}(\cos\varphi - \tan\theta_0 \tan\Theta)] \quad (36)$$

$$g(\varphi, \Theta, \Phi) = \frac{\tan\Theta}{\cos\Theta} \frac{d(\tan^{-1}(\cos\varphi/\tan\Theta), \Phi-\varphi)}{\tan^2\Theta + \cos^2\varphi} \quad (37)$$

since $d(-\theta, \varphi) = d(\theta, \varphi)$. Equation (24) is thus reduced to a single integration, equation (35), with the functions s and g given by equations (36) and (37). Computer implementation of equation (35) may be made more efficient by a detailed analysis of equation (36). The function $s(\varphi, \theta_0, \Theta)$, with a value of $+1$, $+\frac{1}{2}$ or 0, has the effect of segmenting Fourier space into at most four regions, as follows:

$$D(\Theta, \Phi) = 0 \qquad 0 < \Theta < \pi/2 - \theta_0,\ 0 \leq \Phi < l - \varphi_0 \quad (38)$$

$$D(\Theta, \Phi) = \int_{\Phi-\varphi_0}^{\Phi+\varphi_0} g(\varphi, \Theta, \Phi)\, d\varphi \qquad \begin{matrix} \pi/2 - \theta_0 \leq \Theta < \pi/2 \\ 0 \leq \Phi \leq \pi/2 \end{matrix} \quad (39)$$

$$D(\Theta, \Phi) = \int_a^b g(\varphi, \Theta, \Phi)\, d\varphi \qquad \begin{matrix} 0 < \Theta < \pi/2 - \theta_0 \\ |l - \varphi_0| \leq \Phi \leq \pi/2 \end{matrix} \quad (40)$$

$$D(\Theta, \Phi) = \int_{\Phi-\varphi_0}^{-l} g(\varphi, \Theta, \Phi)\, d\varphi + \int_l^{\Phi+\varphi_0} g(\varphi, \Theta, \Phi)\, d\varphi \qquad \begin{matrix} 0 < \Theta < \pi/2 - \theta_0 \\ 0 \leq \Phi < \varphi_0 - l \end{matrix} \quad (41)$$

with

$$a = \max(\Phi - \varphi_0, l)$$

$$b = \min(\Phi + \varphi_0, l - \pi/2)$$

and

$$l = \cos^{-1}(\tan\theta_0 \tan\Theta), \qquad 0 \leq l \leq \pi/2.$$

Good Publicity

The HIDAC Camera Project at HCUG, 1983-1988


Une nouvelle technique pour soigner le cerveau et le cœur
Mieux voir pour mieux soigner

Le Courrier, January 1988

Tribune de Genève, January 1988

Scientists Press Plans for New Brain and Heart Research *UNI* News 1988

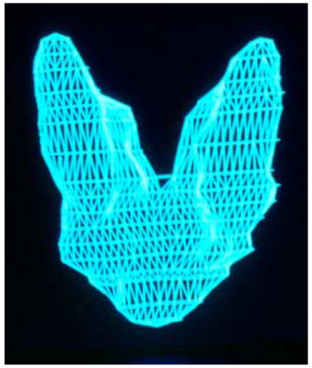

Thyroid imaging with ^{124}I

Financially supported by the Fonds National Suisse

Advances in PET

PET in 1986

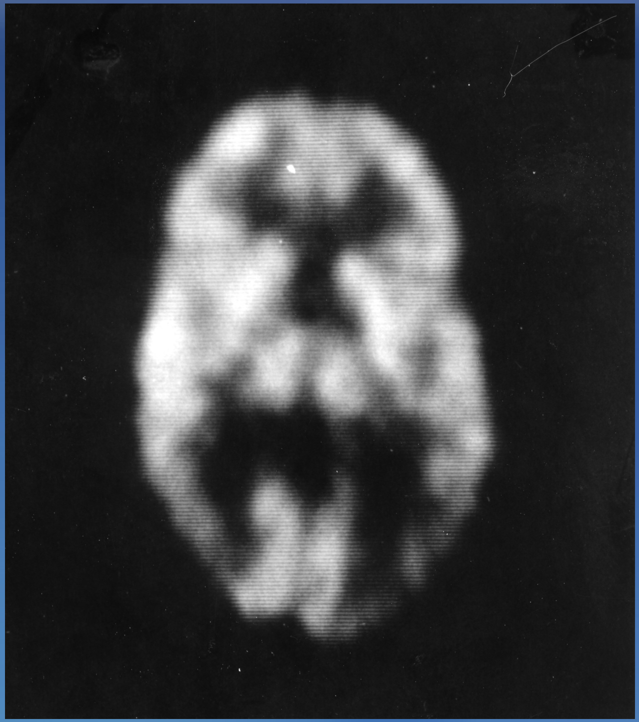

- 8 mm Resolution
- 5 cm Axial Extent
- Cardiology / Neurology
- Academic Research

PET in 2006

- 4 mm Resolution
- >15 cm Axial Extent
- Oncology
- Routine Clinical

Dual-Modality PET/CT Imaging

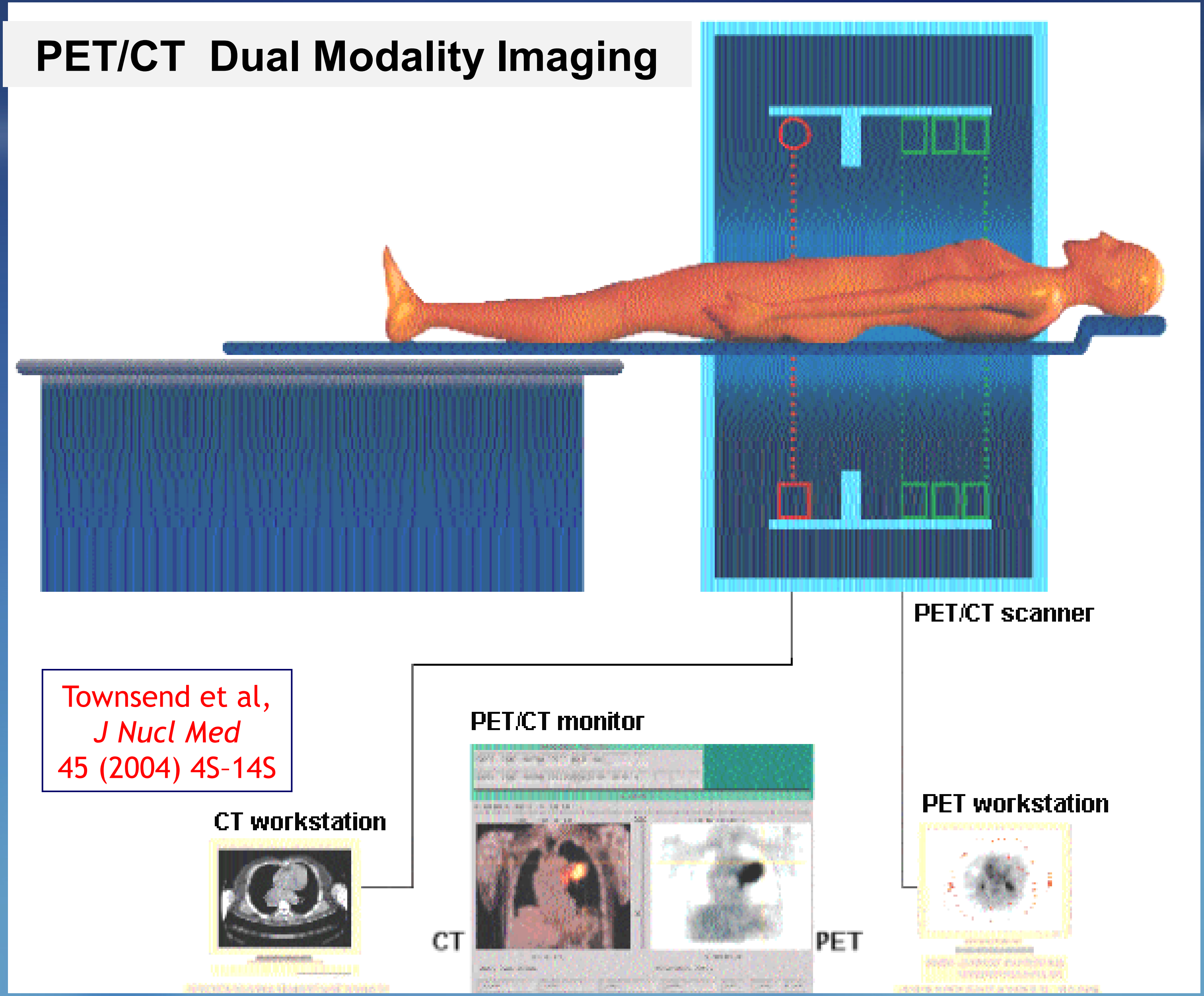

Townsend et al,
J Nucl Med
45 (2004) 4S-14S

Form + function

Fused image accurately localizes uptake into a lymph node and thus demonstrates spread of disease.

- to image different aspects of disease
- to identify tracer uptake
- to simplify the image interpretation
- to give added value to CT and

Why combine form and function?

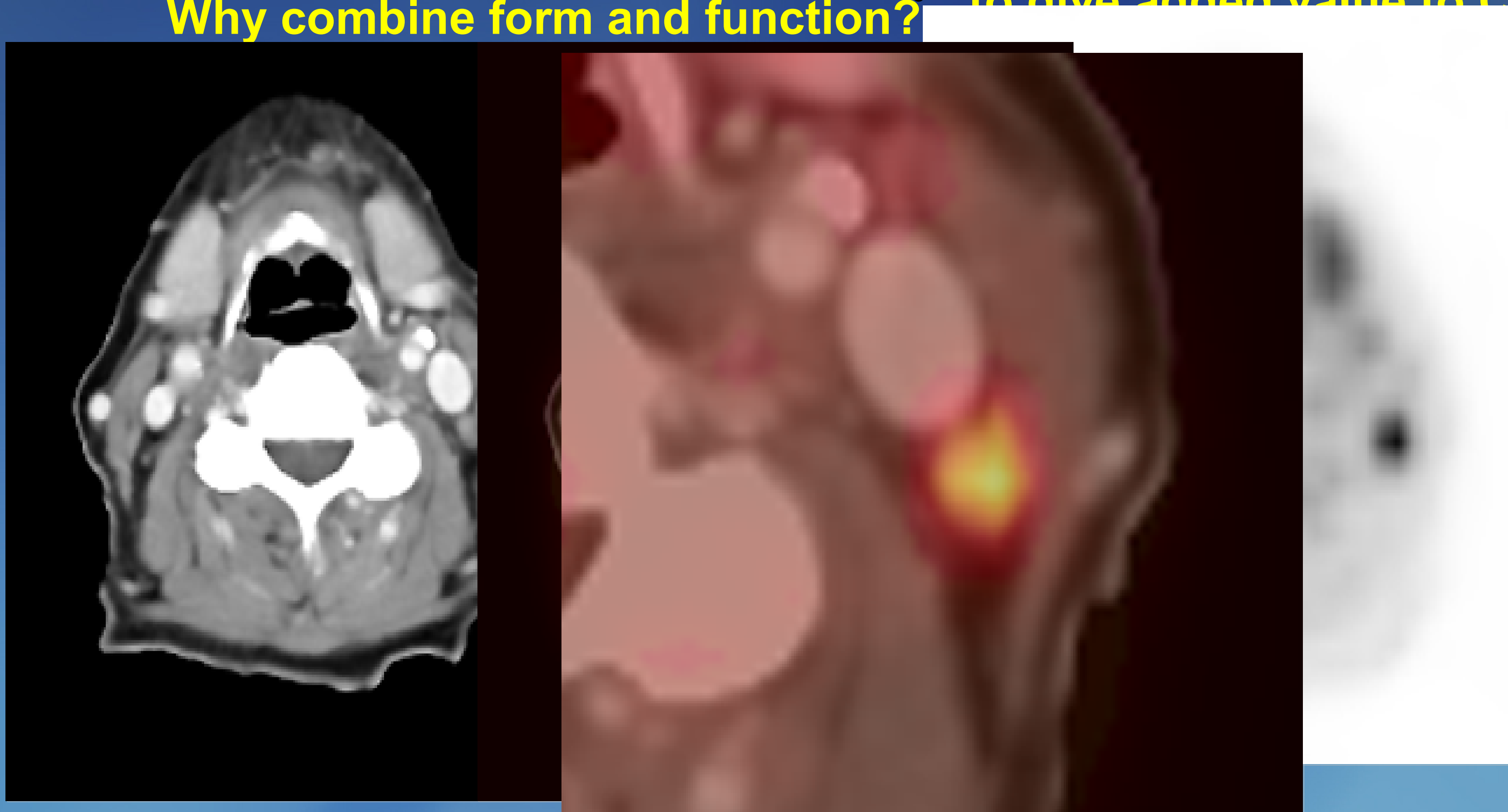

CT (anatomy) **PET/CT** **PET (function)**

Courtesy of David Townsend, Ph.D.
University of Tennessee Medical Center

Combined MR/PET: Potential Realizations

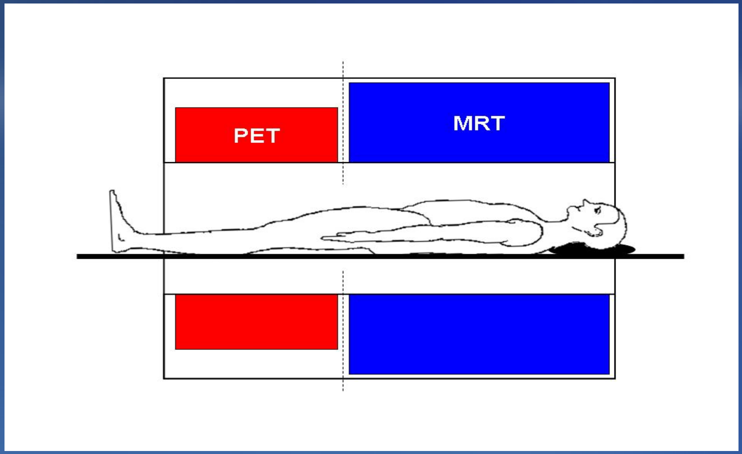

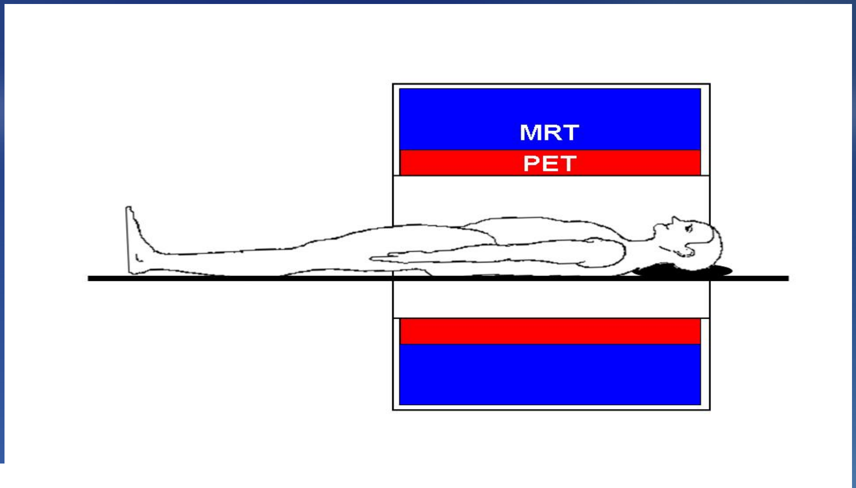

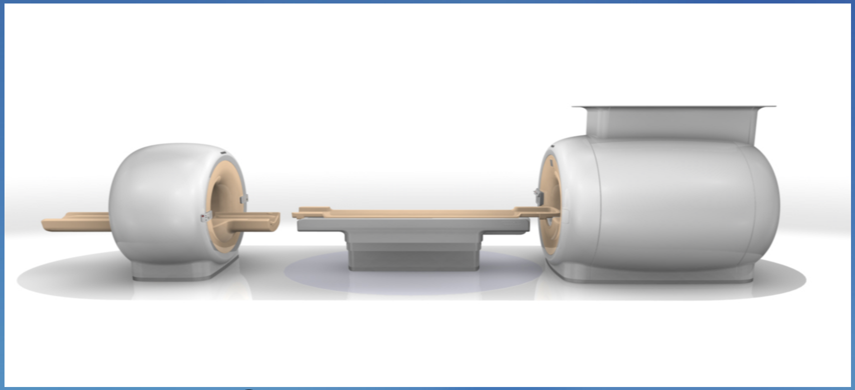

Courtesy: Philips

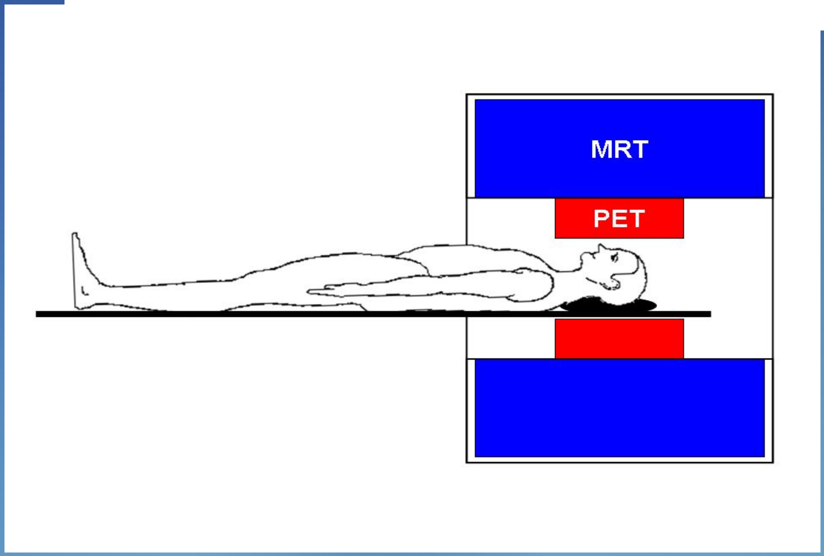

Department of
Preclinical Imaging and
Radiopharmacy

Reference: Siemens mMR whole body PET/MR

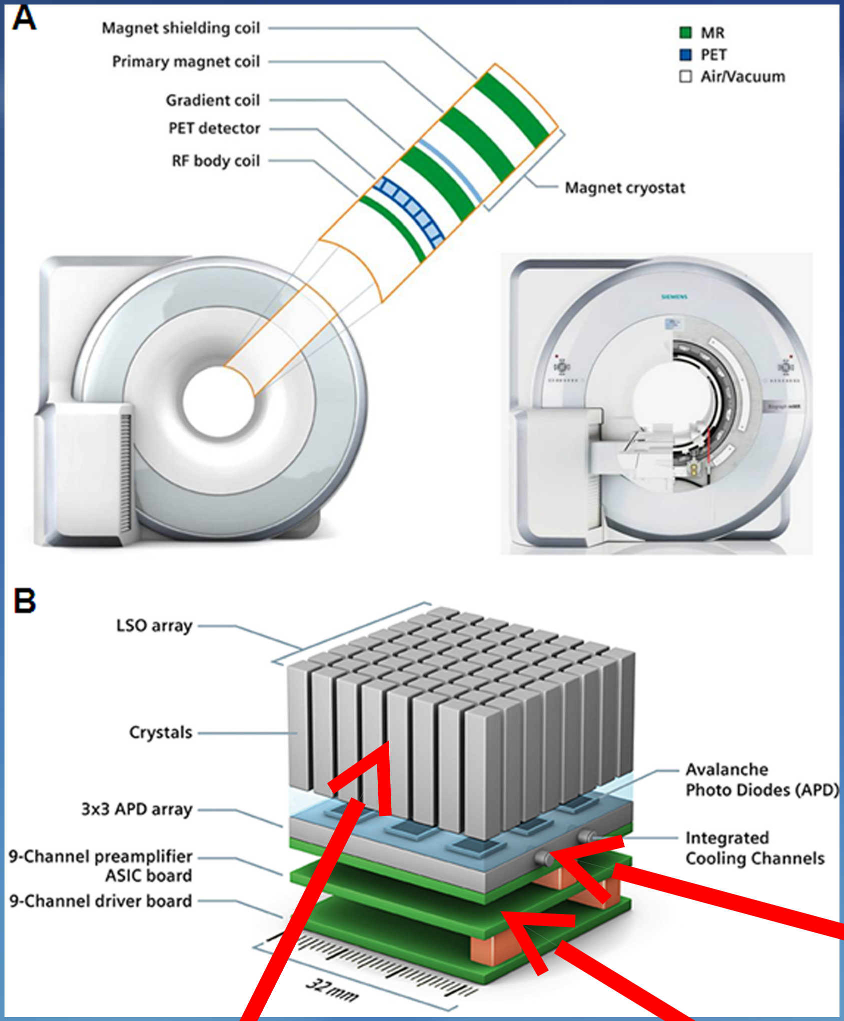

Artistic view of the whole-body mMR MR-PET prototype (a) showing the basic components of the system where the PET detector ring is placed
between the RF coil and the RF body coil. (b). Configuration of the detector block consisting of 88 LSO crystals read-out by a matrix of 33 APDs. Courtesy of Siemens Healthcare.

APDs

LSO array

ASIC

(Habib Zaidi)

Why PET/MRI

Why combine PET and MRI:

MRI

- high resolution
- high soft tissue contrast

+

PET

- high sensitivity
- target specific tracer

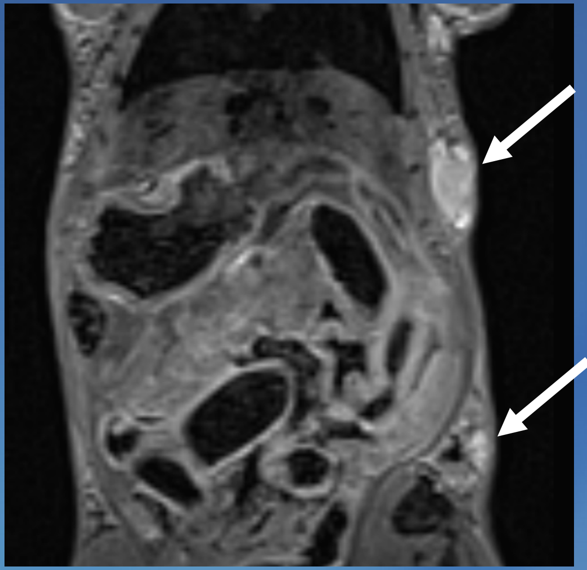

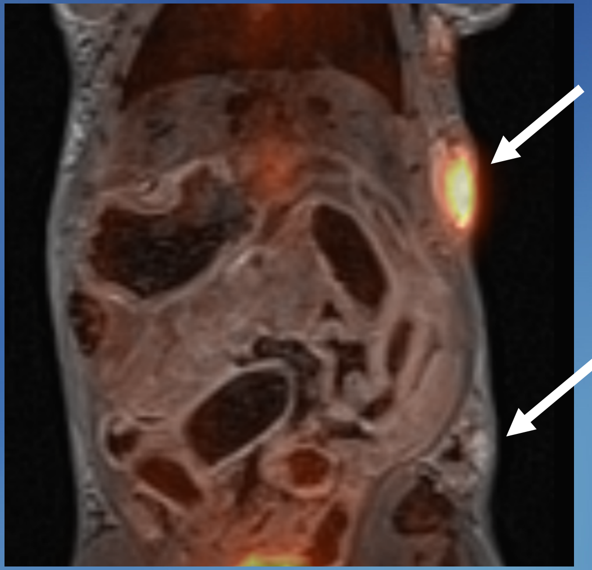

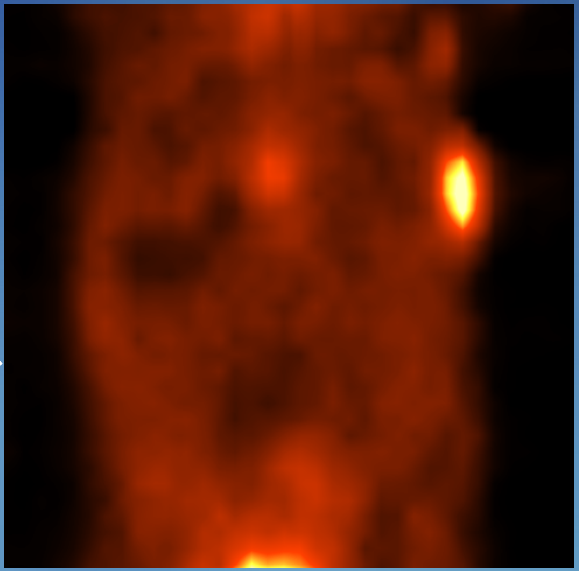

Department of Preclinical Imaging and Radiopharmacy

Added value by PET/MRI

The Search for the Killer Application in PET/MR

Bernd J. Pichler

Department of Preclinical Imaging and Radiopharmacy Tuebingen U.

Brain Function as a Result of Receptor Activation

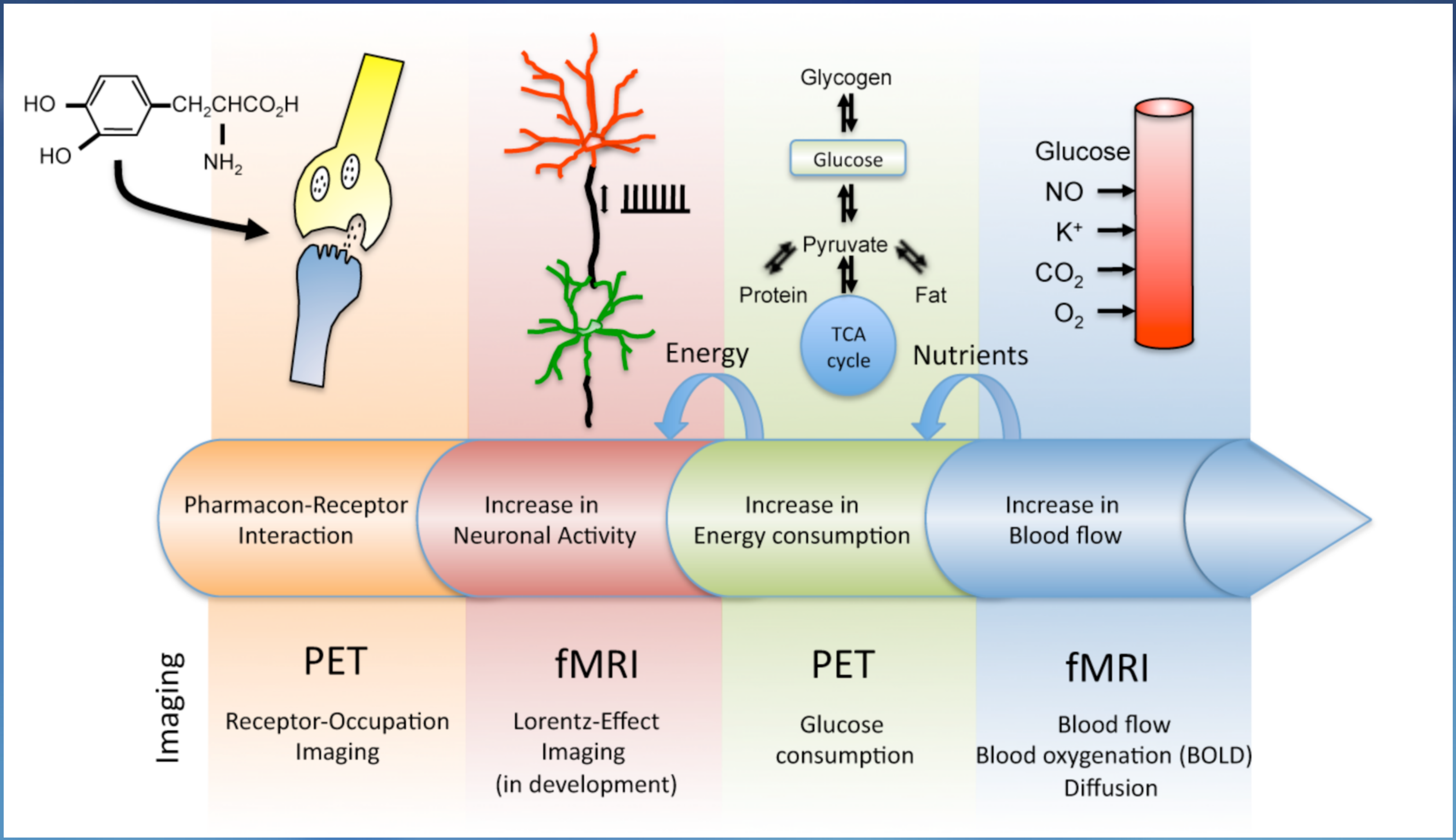

Department of
Preclinical Imaging and
Radiopharmacy

Whole-body PET/MR

Patient: 77 y - BC

CT

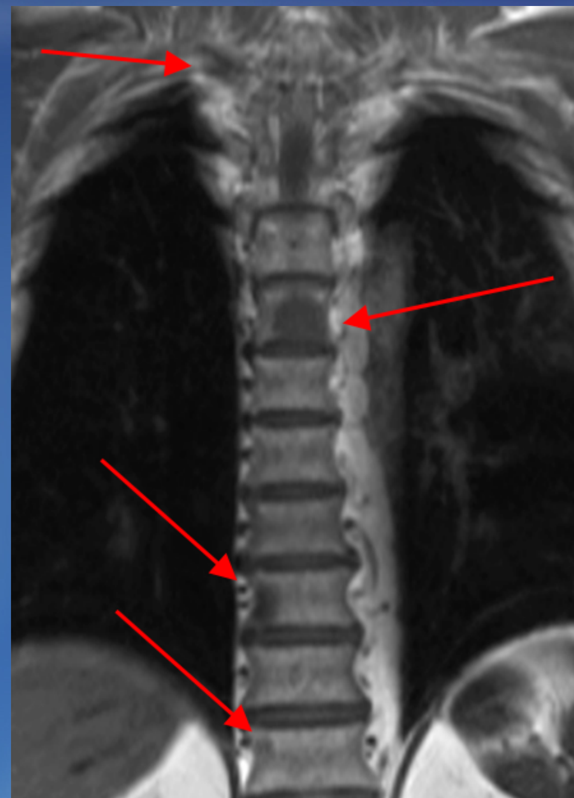

T1w MR
(TSE, TE/TR=9.4/441 ms)

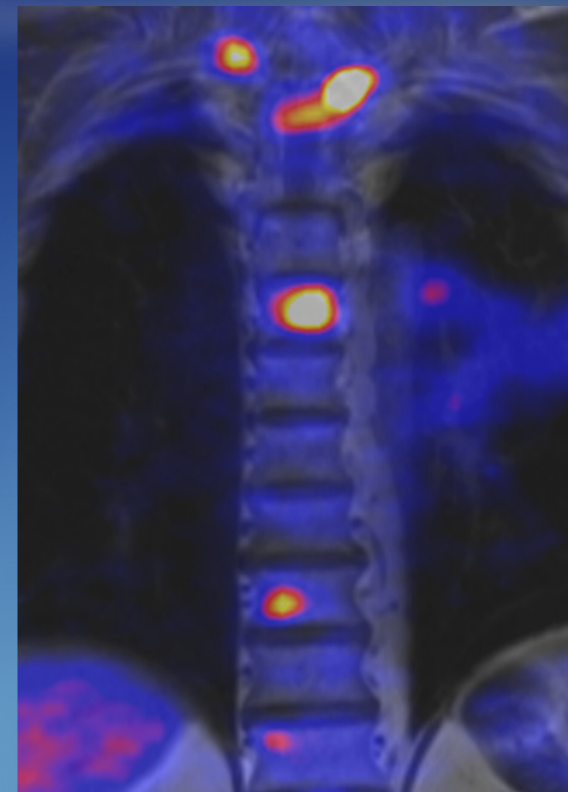

PET/MR

Department of
Preclinical Imaging and
Radiopharmacy

First Clinical PET/MR: System Setup

- Brain/Head only
- 32x6 detectors
- LSO crystals:

  2.5x2.5x20 mm3
- APD Light detectors
- MRI-PET FOV:

  19x28 cm2

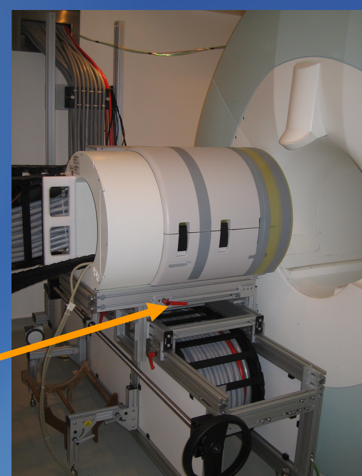

3 T clincial MR scanner

Handling device:
change PET Insert in ca. 10 min

Department of
Preclinical Imaging and
Radiopharmacy

Comparison PET/CT versus PET/MRI

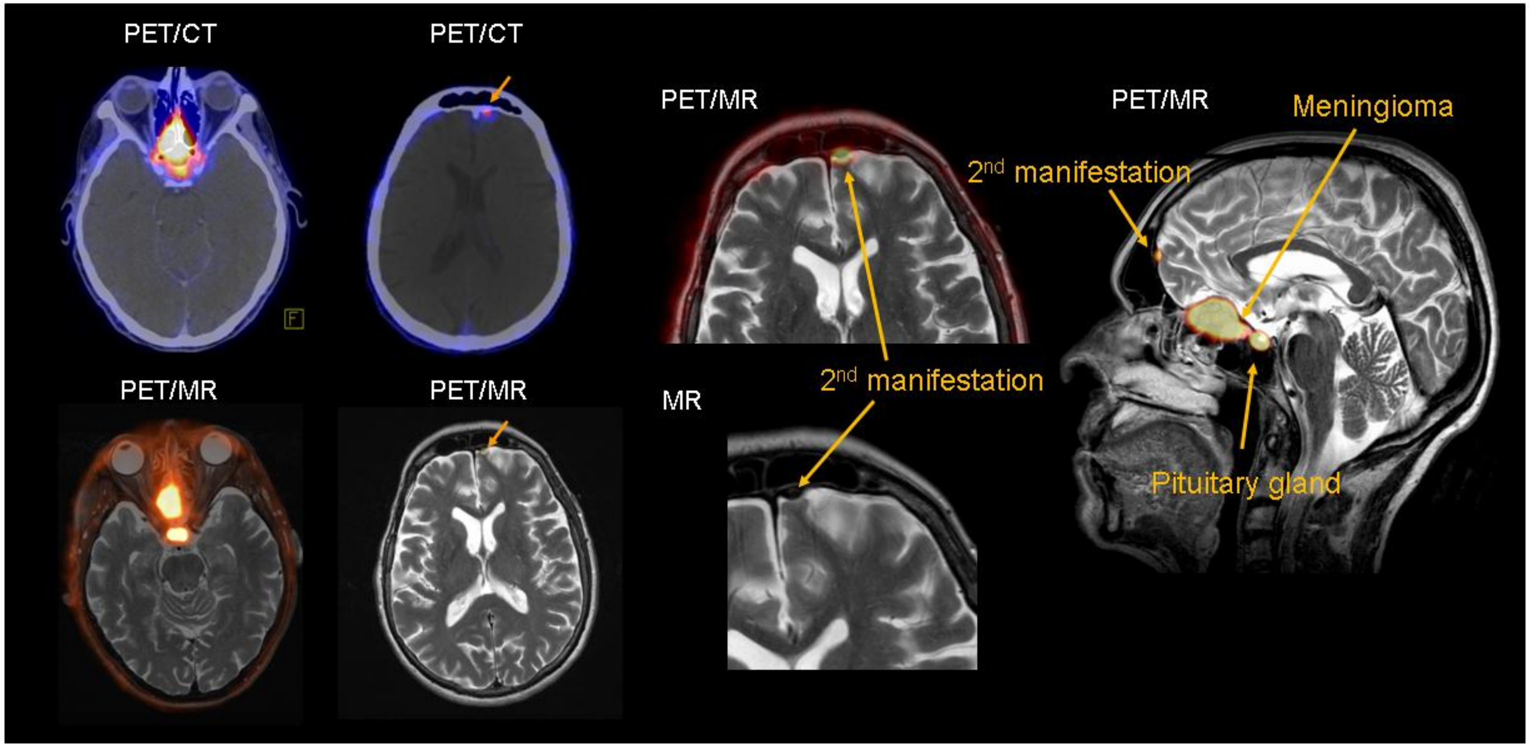

Department of
Preclinical Imaging and
Radiopharmacy

PET/MR Killer Applications

List of PET/MR Killer Applications:

1.Preclinical Imaging

3.Prostate Tumors
4.Pediatric
5.Brain Tumors

6.More will follow…

Potential of PET/MR goes far beyond of current applications…

PET Detector Blocks

- 8 rings with 56 detector blocks each (ø 65.6 cm, transaxial FOV: 59.4 cm, axial FOV: 25.8 cm)
- Each detector block contains:
  - 8 x 8 LSO crystals (4 x 4 x 20 mm3)
  - Crystal read-out by 3 x 3 APDs
  - Cooling channels
  - Pre-amplifiers, etc.
- Total number of
  - detector blocks: 448
  - crystals: 28,672
  - APDs: 4,032

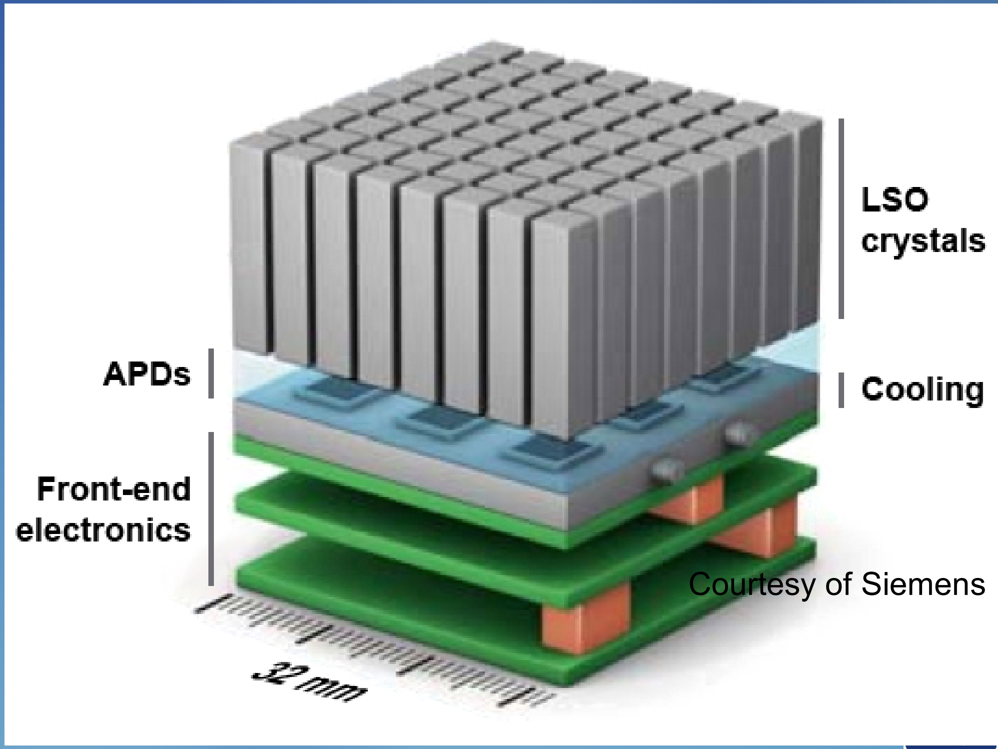

Courtesy of Siemens

Silicon Photo-Multiplier: a revolutionary enabling technology

- Immune to magnetic fields
- Gain = (105-106) at low voltage (<100V)
- (typical APD gain: ~100)
- High photon detection efficiency (up to 50%)
- Dark count (0.1 to 1 MHz)
- Micro APDs in Geiger mode (>breakdown voltage)

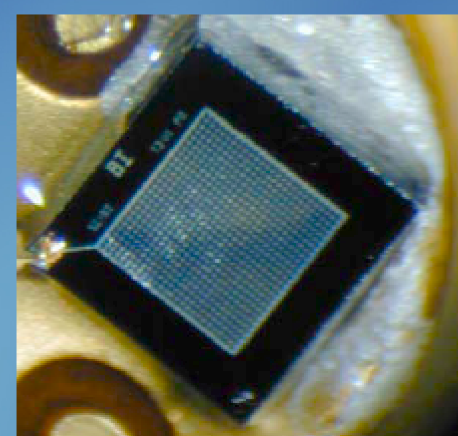

SiPMs come in different sizes ….

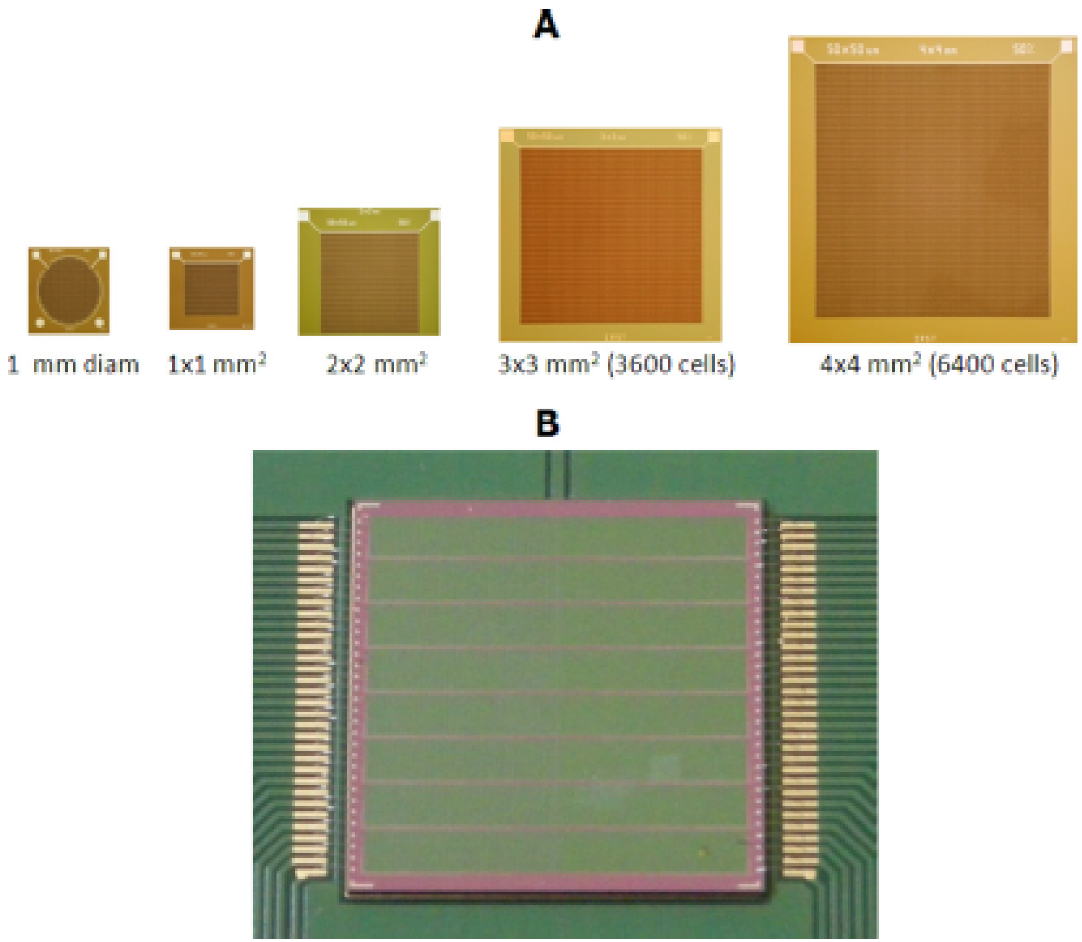

FIG. 7. (a) Photograph of various sizes of SiPM samples. (b). Photograph of the 8 × 8 matrix of 1.5 mm × 1.5 mm pixel with lateral read-out from two sides only, as developed by FBK-irst (Trento, Italy). Adapted with permission from Llosa *et al.*, Phys. Med. Biol., **55**, 23, 7299–7315, 2010 (Ref. 207).

Medical Physics, Vol. 38, No. 10, October 2011

(Habib Zaidi)

Detector & Roadmap Summary

Sumary					*LYSO**			*BGO**		
Product Name	*Process*	*Status*	*Avail Pixel Sizes*	*Available Pkg's*	*~PDE*	*~Eng. Res.*	*~Timing*	*~PDE*	*~Eng. Res.*	*~Timing*
SL	"L"	General Release	1mm 3mm	X13 TO Array4 Array4p9	4%	14%	750ps	14%	18%	5ns
SM	"M"	General Release	6mm	X13 ArraySM-8	9%	13%	700ps	20%	<16%	<5ns
FM	"M"	Sampling	.25mm 1mm 3mm 6mm	TO (.25 & 1mm) X13-ENG SMT	9%	13%	300ps	20%	<16%	2ns
FB/SB	"B"	In Lab & Select sampling	3mm 6mm	SMT Array's	>40%	<10%	<250ps	>30%	<10%	<2ns

* Detector and Crystals sizes vary slightly between measuments. See detailed ppt for specific graphs

** FB measurements are simulation objectives on 3x3x20 crystals

New 4 Side Tileable SMT Package (-SMT)

- 4 Side tileable
- <500um from detector edge to package edge
- Molded smooth top surface
- 3mm Available Now
  - 6mm September
  - 1mm October

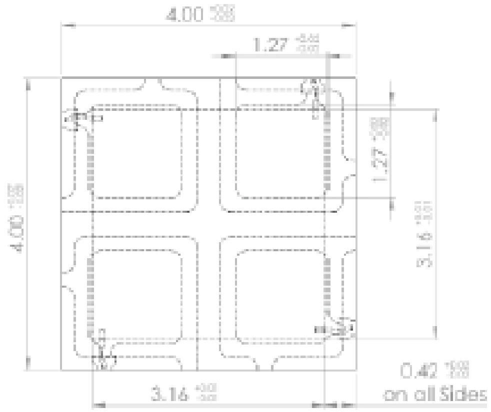

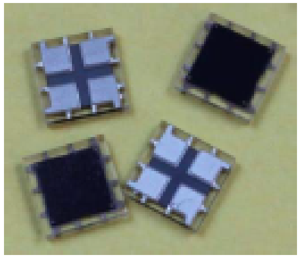

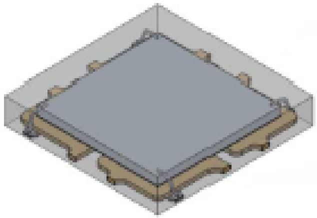

3x3 Array Example:

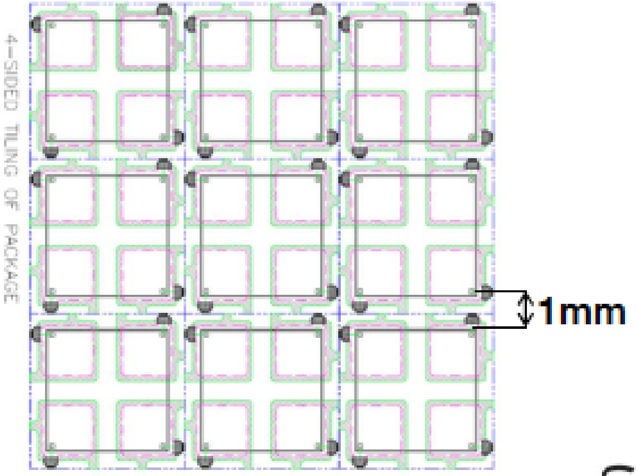

Linear Array Example:

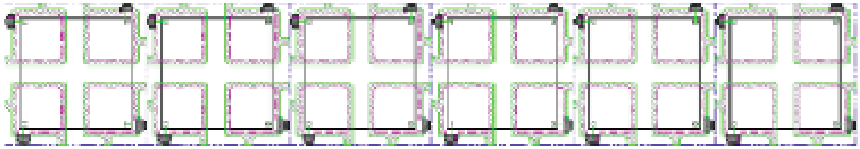

FB Coincidence Resolving Time
("F" Output)

3x3x15mm³ LYSO

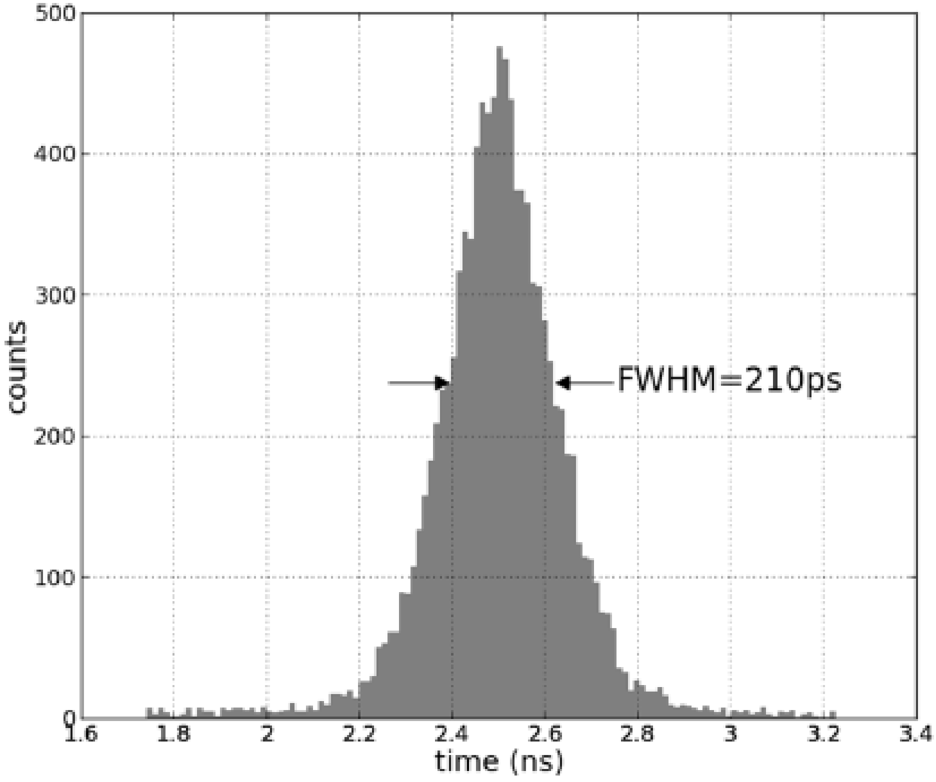

3x3x10mm³ LYSO

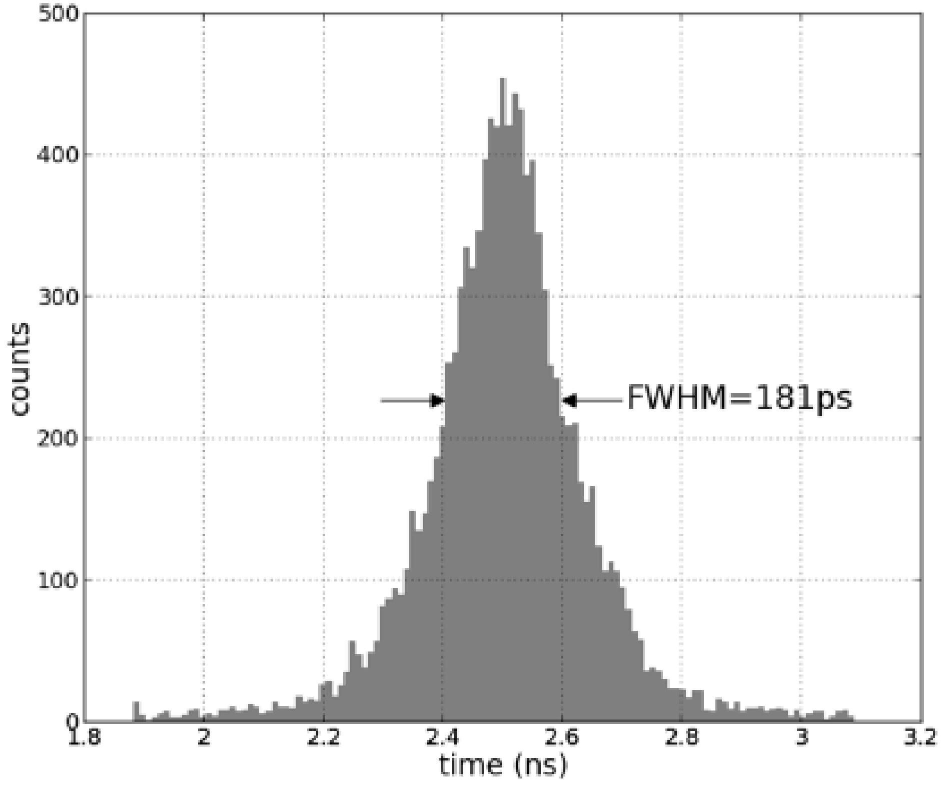

sensL
sense light

SensL Released and Roadmap SPM Products

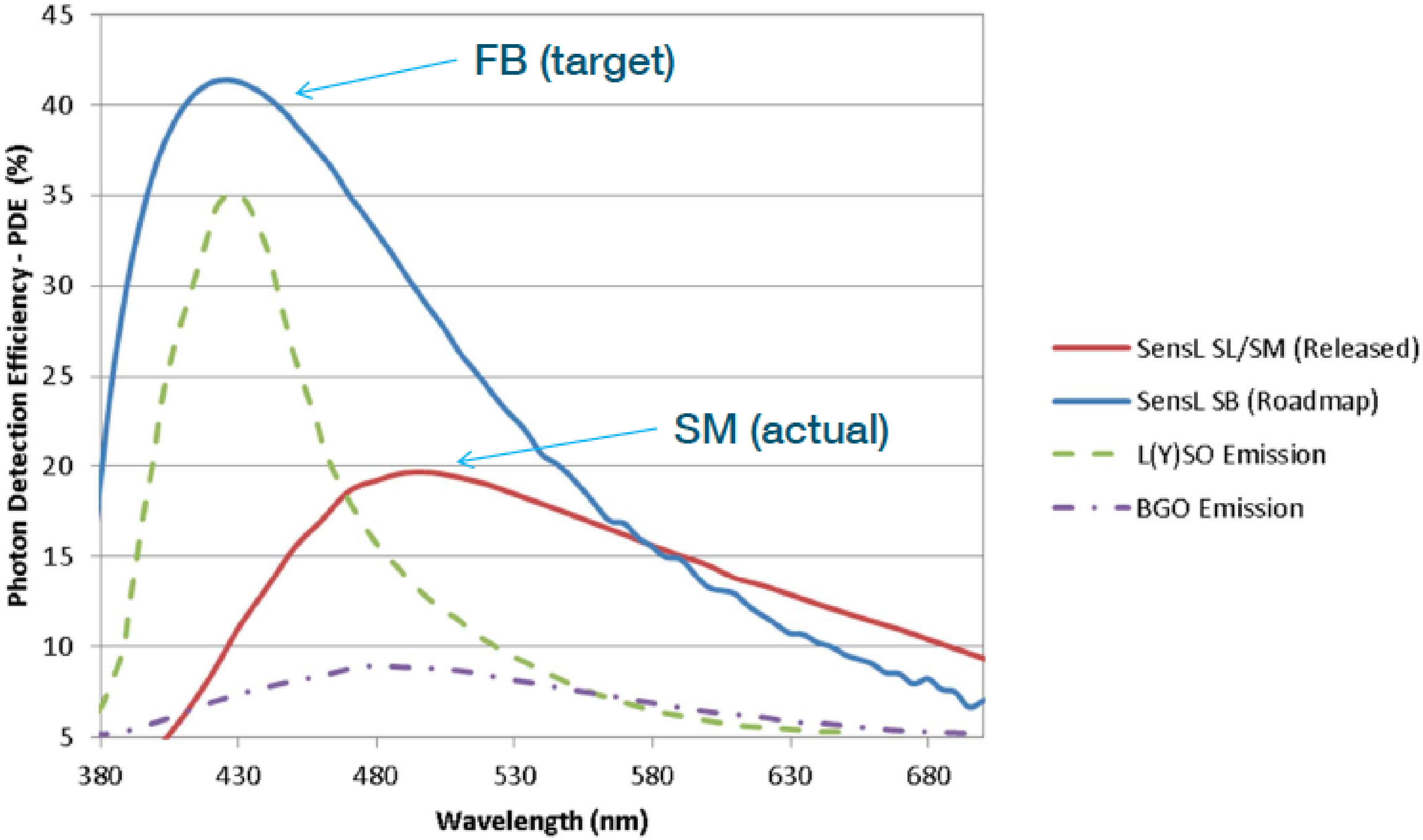

sensL
sense light

TOFPET - How does TOF help?

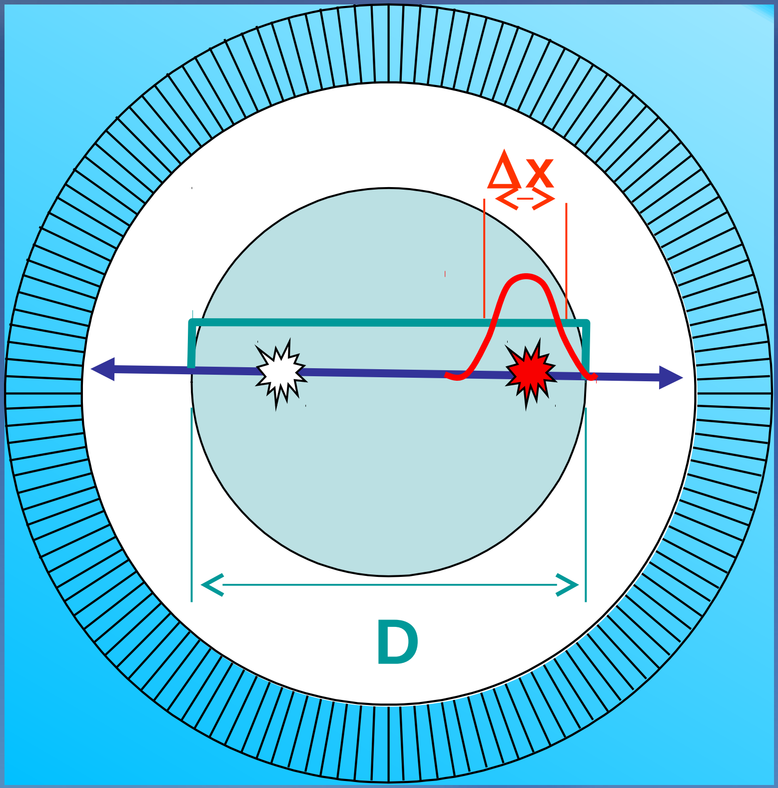

Δt = uncertainty in measurement of t1-t2

Δx = uncertainty in position along LOR
= c . Δt/2

D/Δx ~ reduction in variance
or gain in sensitivity

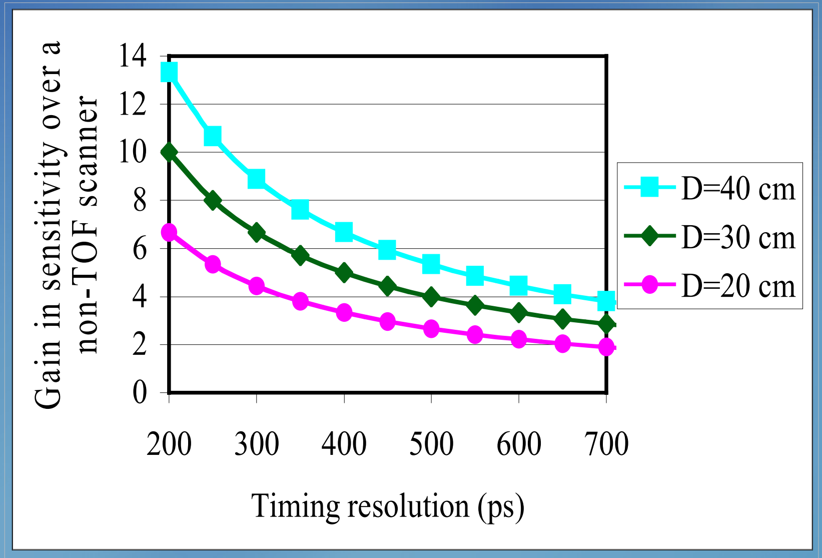

(Joel Karp, U. Penn)

Impact of microcell size on PET timing resolution

$$PDE = Q.E.\,\mathrm{x}\,\Pr(avalanche)\,\mathrm{x}\,fill\ factor$$

$$Fill\ factor \propto Microcell\ size$$

Hammatsu SiPM Microcell size (um)	Hamamatsu SiPM Fill factor (%)
25	30.8
50	61.5
100	78.5

Expectation: PET detector using 100 um SSPM should optimize timing resolution

Correlation with higher dark current

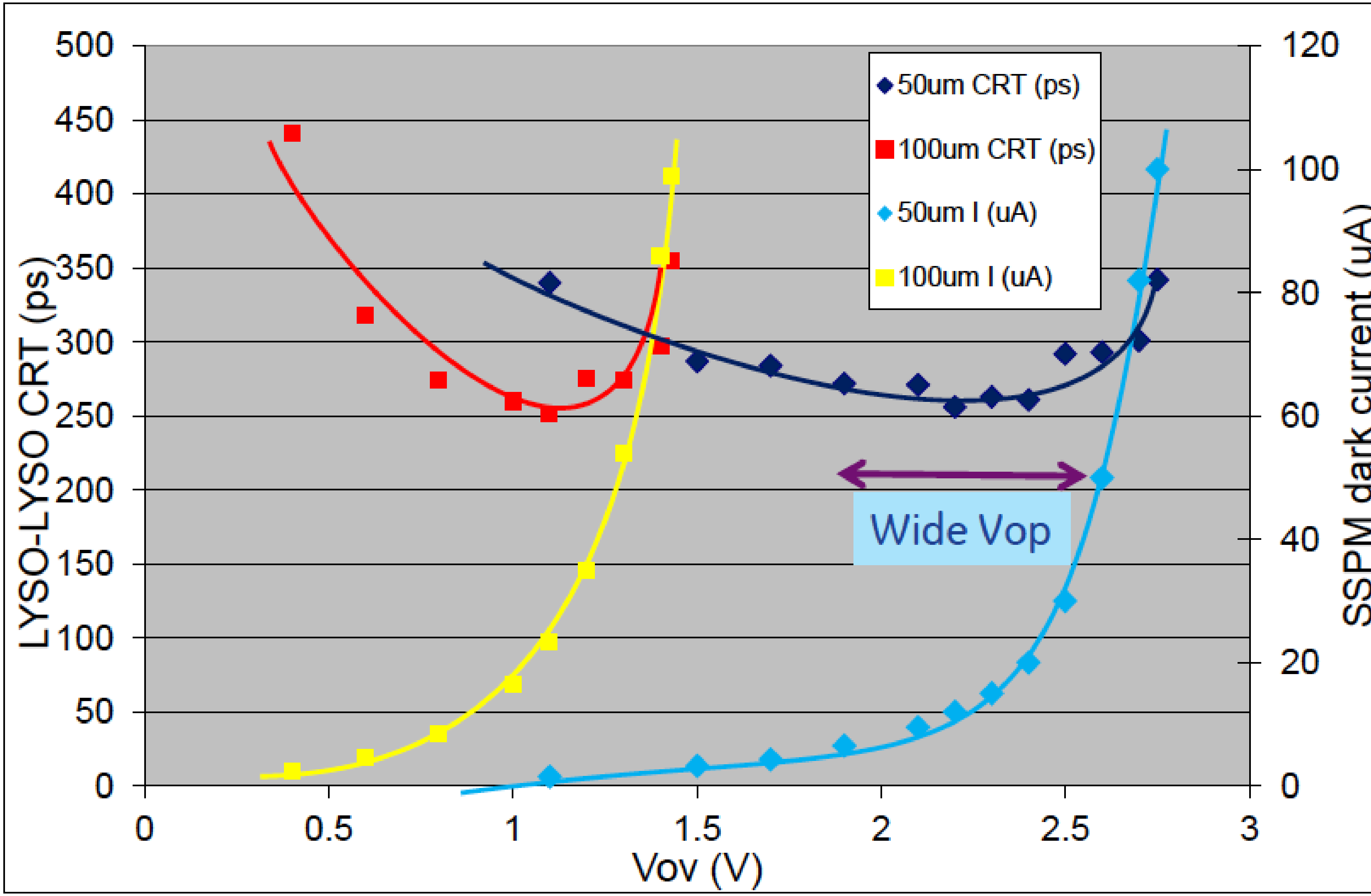

- Wider operational voltage range provided by 50um microcells with similar performance

Design Choice: Hamamatsu MPPC 4x6mm^2

	1	2	3
element size(mmxmm)	3x3	4x4	4x6
microcell pitch (um)	50	50	50
no of microcell/pixel	3600	6400	10375
gain	7.50E+05	7.50E+05	7.50E+05
fill factor	61.50%	61.50%	61.50%
PDE @ 440nm type	50%	50%	50%
capacitance/micro-cell (fF)	89	89	89
total capacitance (pF)	320	570	920
dark counts typ. (Mcps)	6	11	13

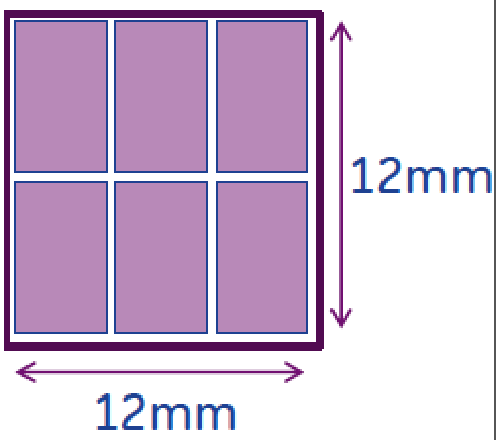

- 4x6mm^2 MPPC with 50μm provides the wider stable operational range
- larger area reduced number of readout channels to be processed

imagination at work

Detector Unit Design

4x3 LYSO array ($4x5.3x25mm^3$)

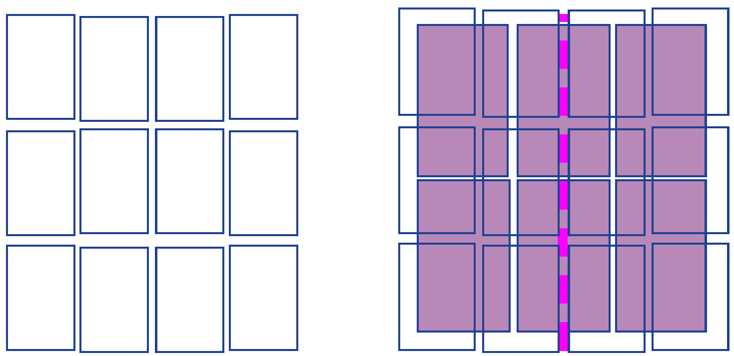

2mm UV plastic

Timing Resolution - 350ps
Walk Correction - 340ps

Energy Resolution 9.7%

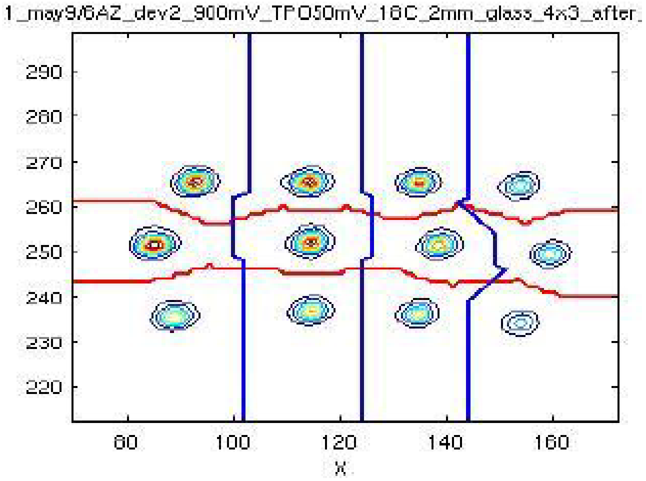

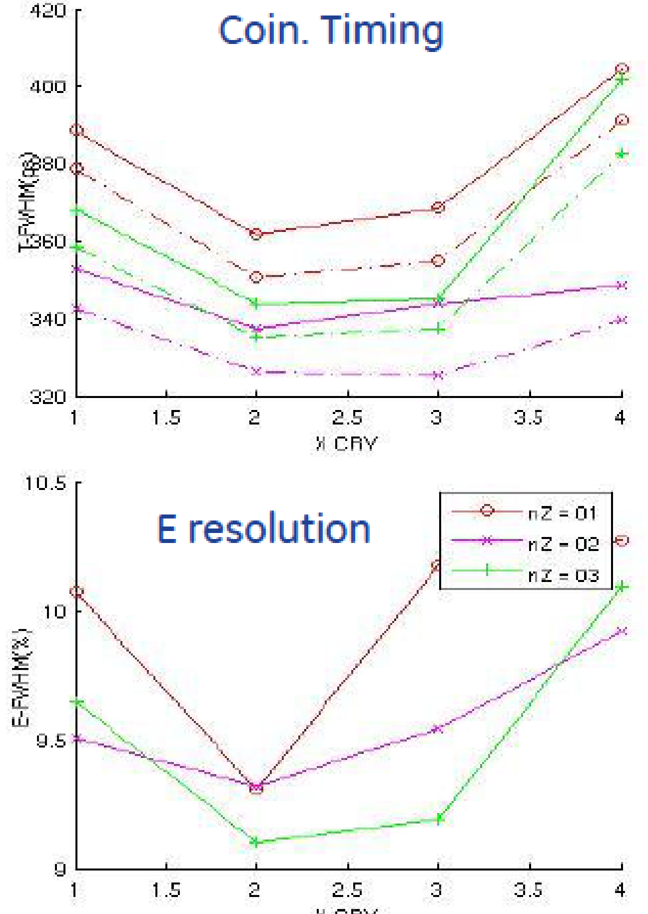

imagination at work

Tapered Light-guide Design

- Transition from crystal block 16x16mm^2 to SiPM 12x12mm^2
- 3x1 array of SiPMs → 3x1 light-guide to cover 48x16mm^2

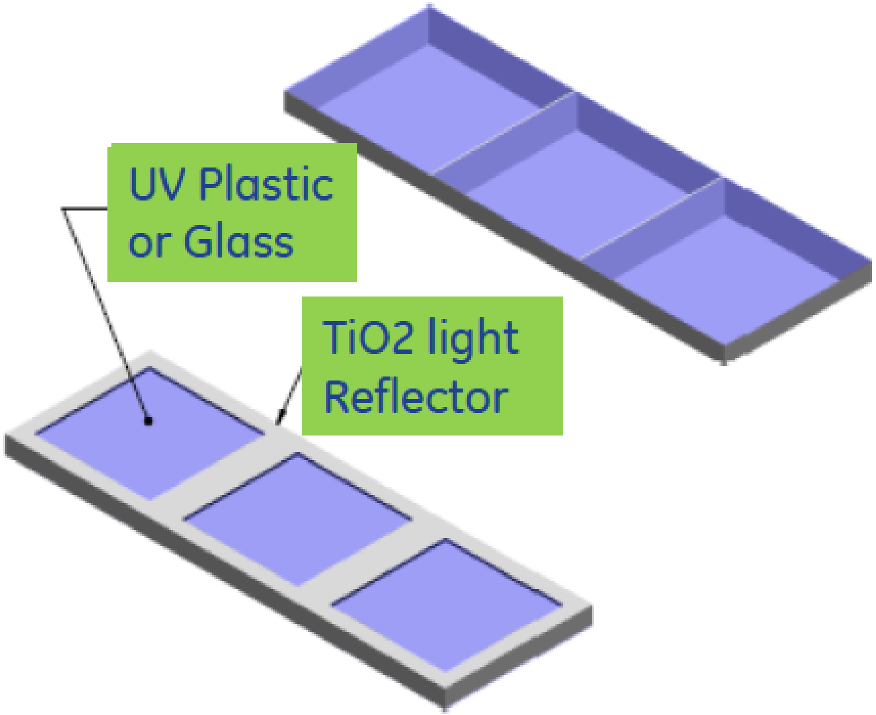

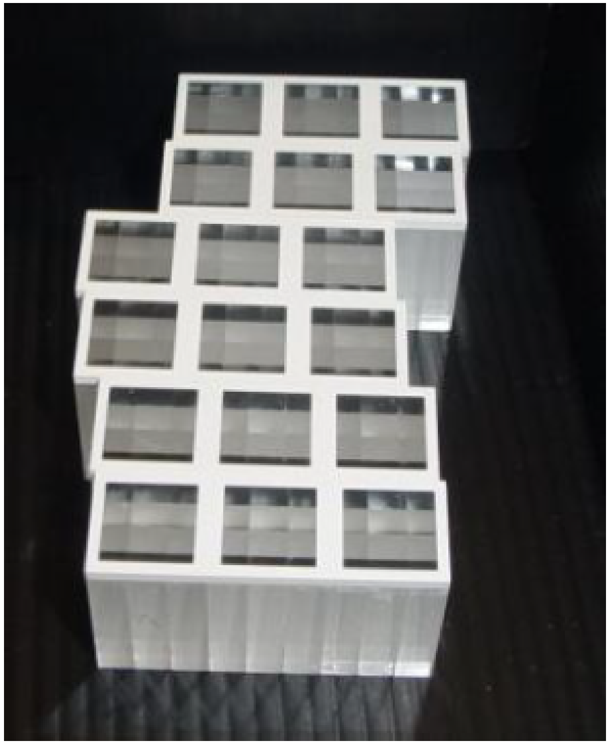

Multiple Blocks Timing Resolution

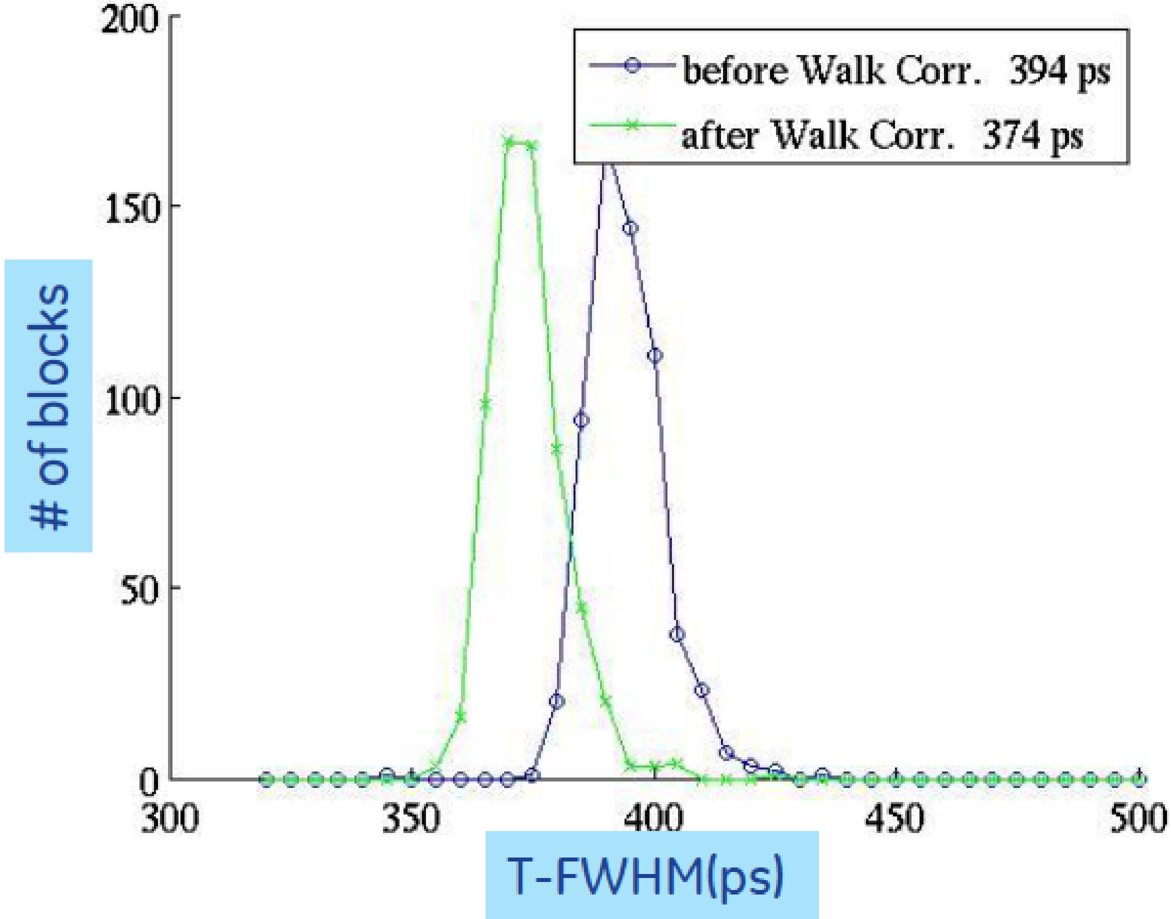

- > 500 blocks were measured: Great consistency in performance among blocks
- Walk correction improves ~20ps in timing resolution

TOF PET-MR Module Design

Detector
4 blocks

SiPM/ASIC
Circuit Board

Light
Guides

LYSO
Scintillator
Crystals

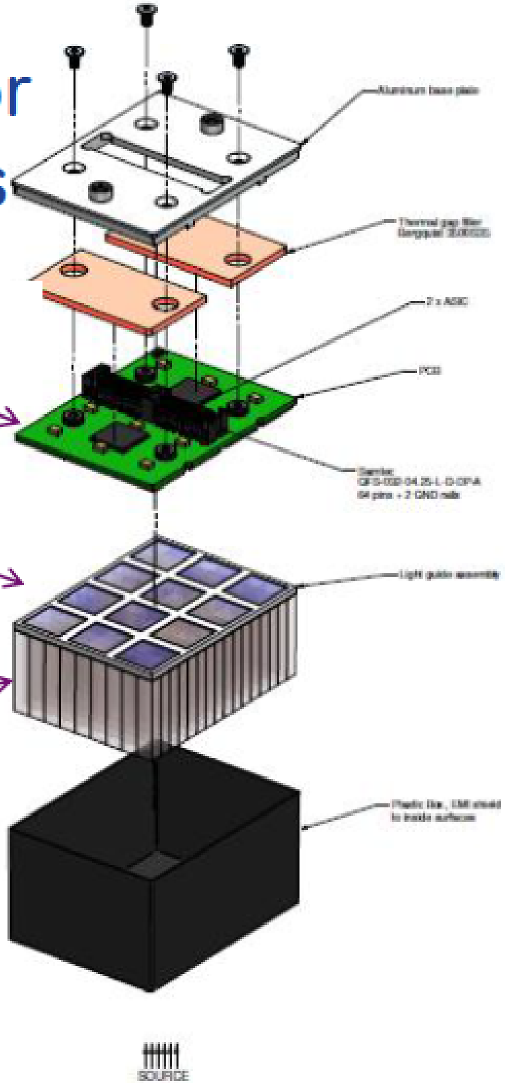

Scalable Detector Module

- 5 detectors per module for 25cm axial extent

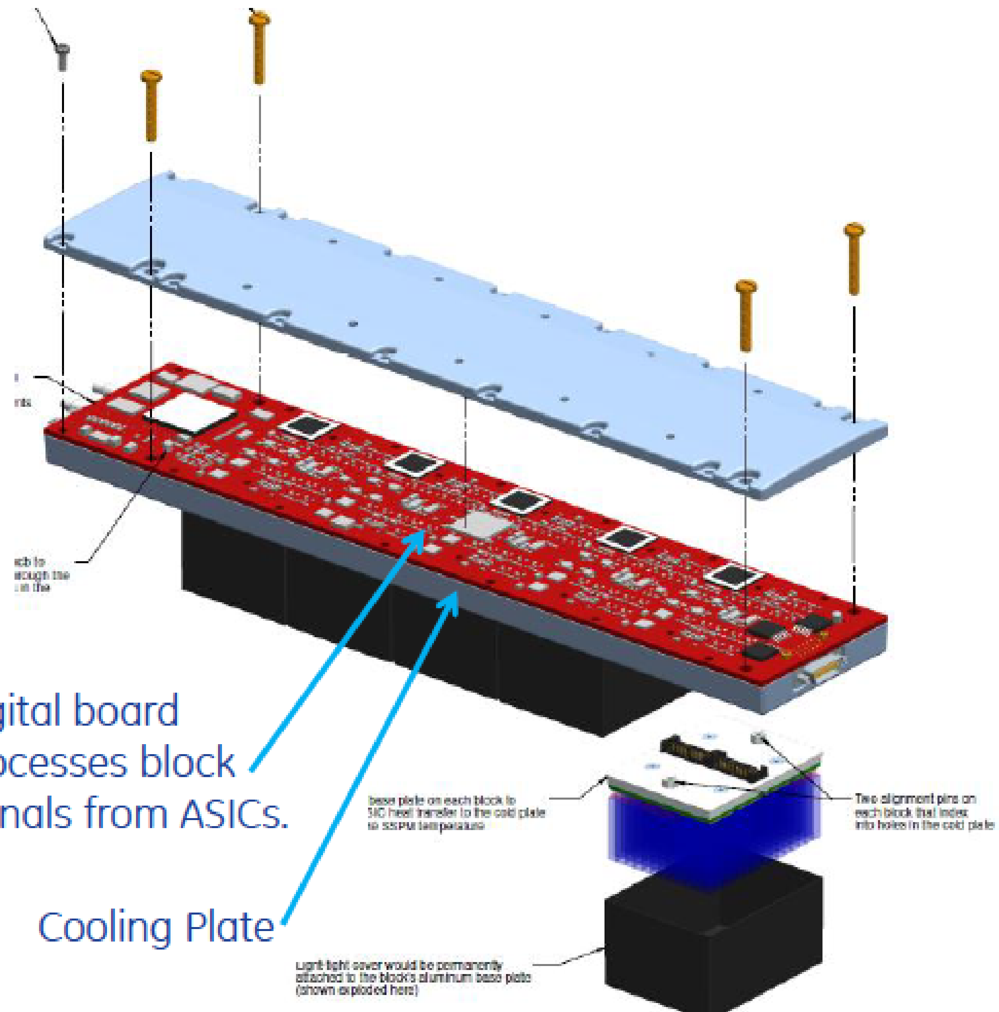

Digital board
processes block
signals from ASICs.

Cooling Plate

imagina...

SiPM Detector Ring Assembly

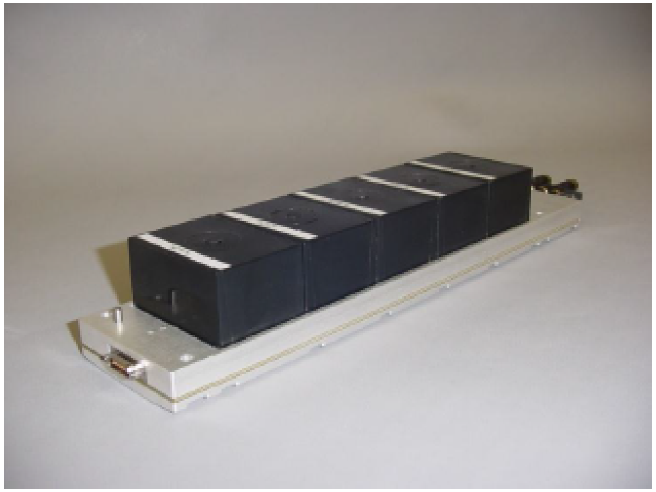

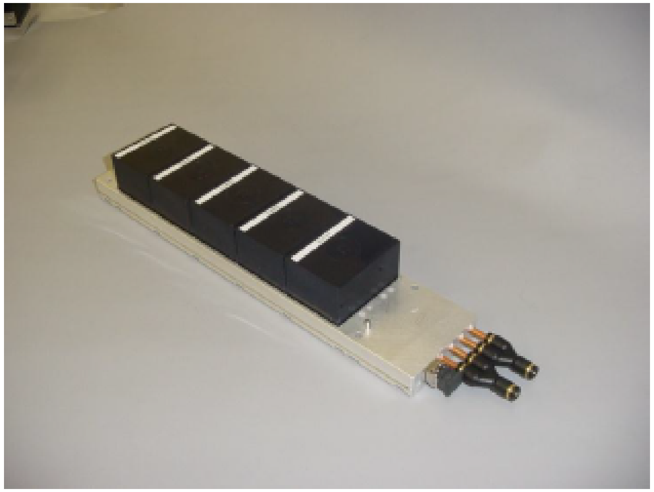

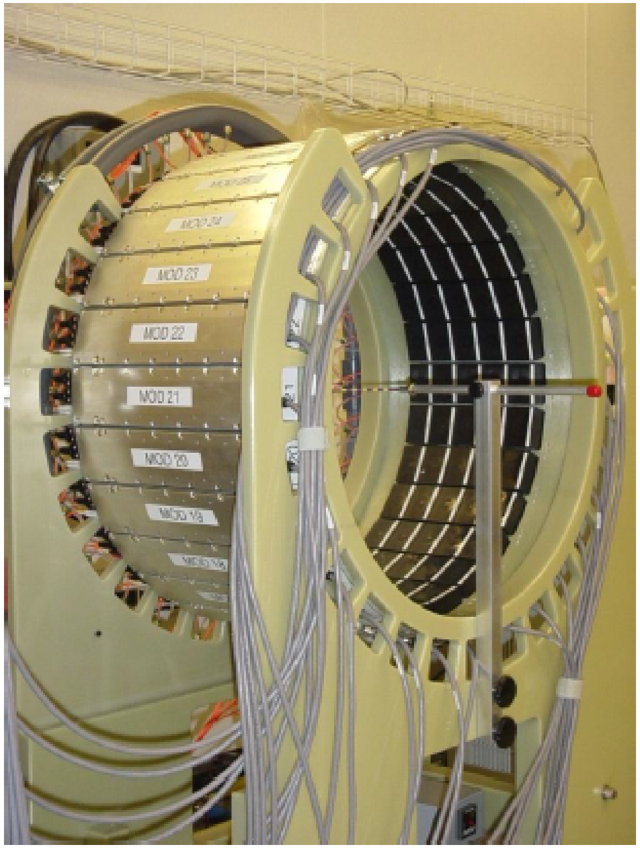

PET Acquisition Performance

- < 400ps FWHM Timing Resolution
- < 11% Energy Resolution
- Successful Crystal Maps, Energy & CTC calibrations

imagination at work

Dedicated Imaging Systems

Motivation for dedicated systems:

- Higher efficiency due to close geometry
- Possibility for low dose scans (repetitive - longitudinal studies, screening ?, children ?)
- Higher resolution (and efficiency via instrumentational Partial Volume Effect)
- Lower cost using small dedicated system as opposed to standard (also occupancy issue of the standard scanner)

Key technical choices:

- Choice of the PET detector technology
- Choice of the on-board readout: functionality, complexity, "compactness", interference with MRI
- DOI or not (always) necessary
- TOF or non-TOF

PET/MRI

Methods to limit the PET-MRI interference: passive and active

- Minimize on-board electronics
- Place active components and photodetectors outiside the MRI imaging volume (scintillation light coupling via optical light guides)
- Shielding of detectors and cabling
- RF noise filtering
- Placement of coils and integration of the PET insert with the RF coil
- Optical electelectronic signals coupling
- Selection of proper MRI sequences
- Sequential imaging

MRI compatible PET technologies:

- APDs
- SiPMs
- Scintillators
- Light guides
- CdTe, CdZnTe,

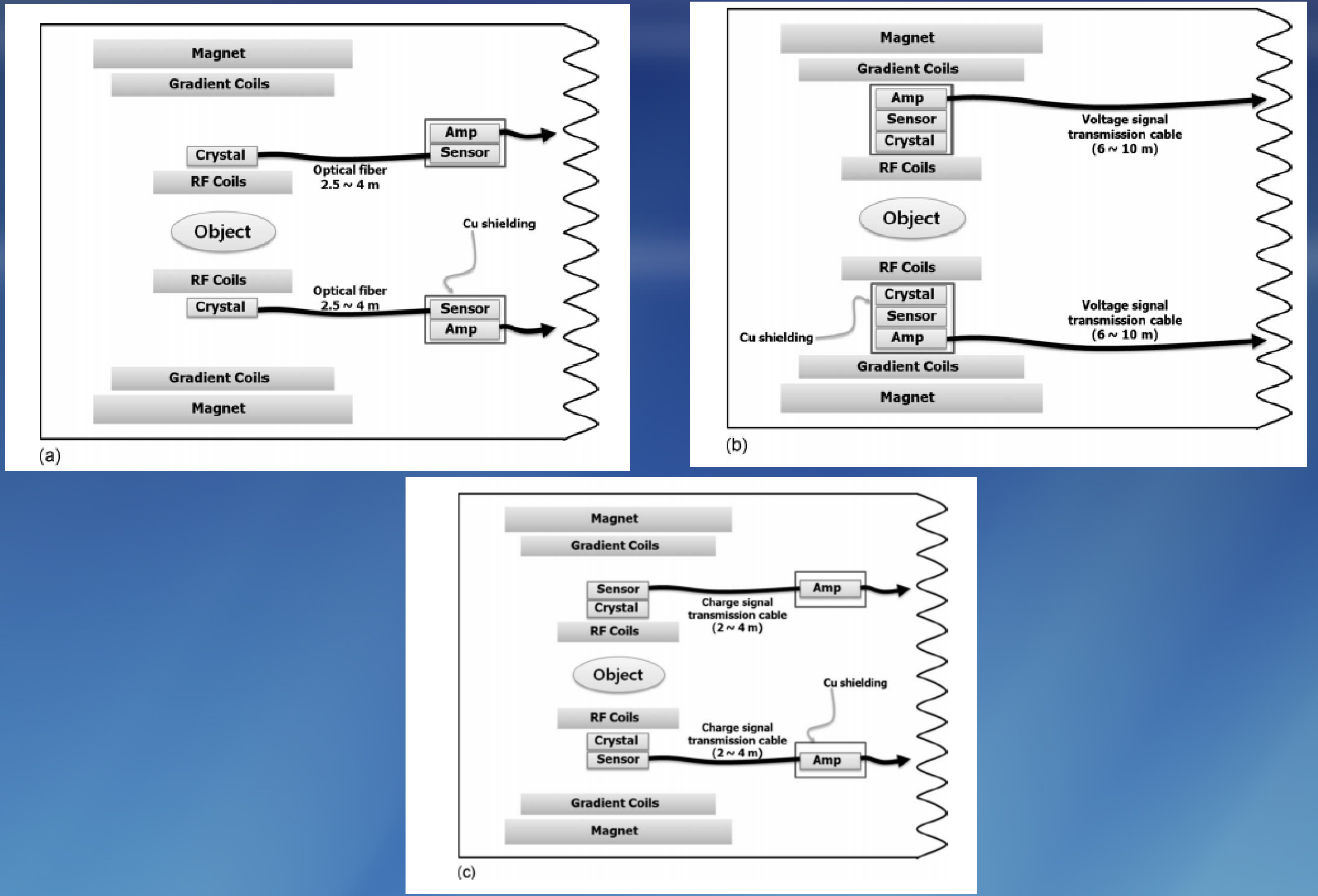

FIG. 1. Several approaches for designing hybrid MR compatible PET. (a) Approach 1: Scintillation light transmission from crystal to photosensor. (b) Approach 2: Voltage signal transmission from amplifier to subsequent electronics. (c) Approach 3: Charge signal transmission from photosensor to preamplifier.

SOGANG UNIVERSITY

iPET/MRI II: MR-compatible PET and MRI

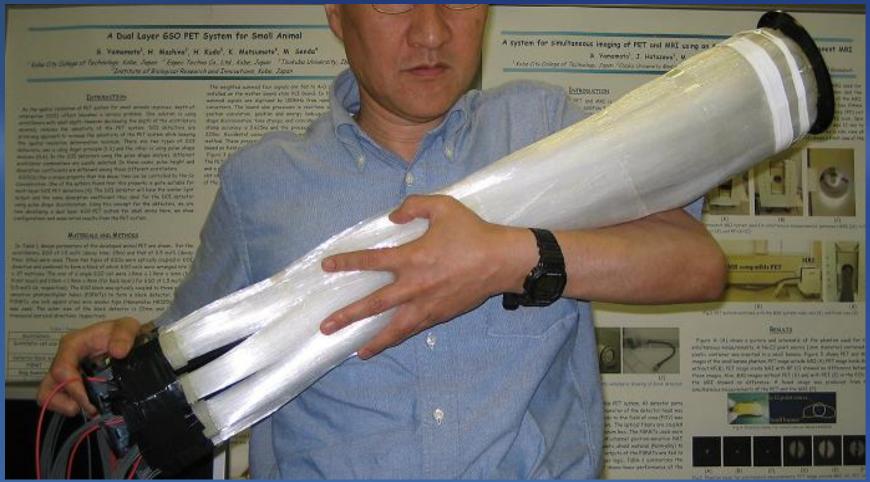

High resolution optical fiber based MR-compatible PET

0.3T MRI with hole in yoke

Combine

2 types of LGSOs (31ns & 46ns) for DOI detector

Pulse shape analysis was used

0.5mm diameter optical fiber bundle (75cm long)

Light loss: ~75%

integrated PET/MRI-II

Electro-optical signal transmission of PET detector signals

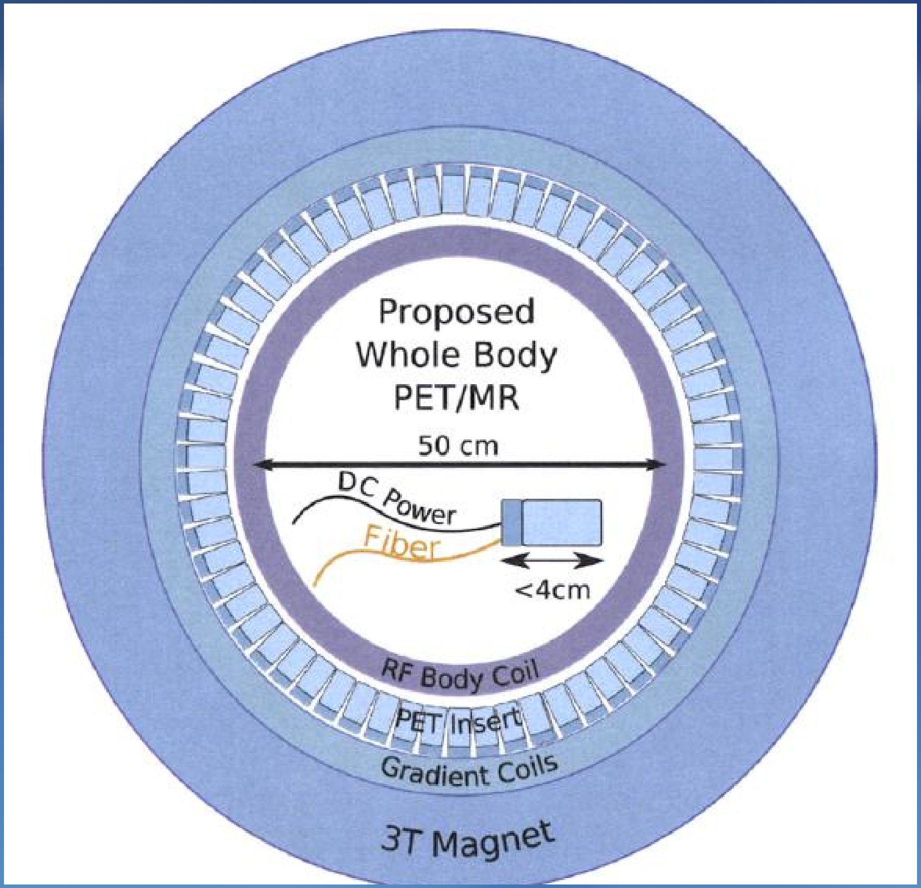

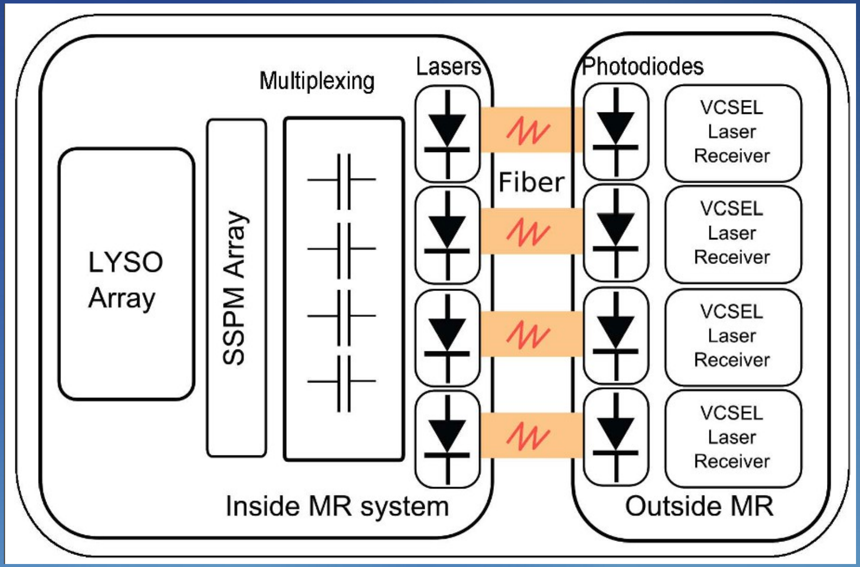

(Craig Levin, Stanford)

Electro-optically coupled PET detectors operated simultaneously with MRI system

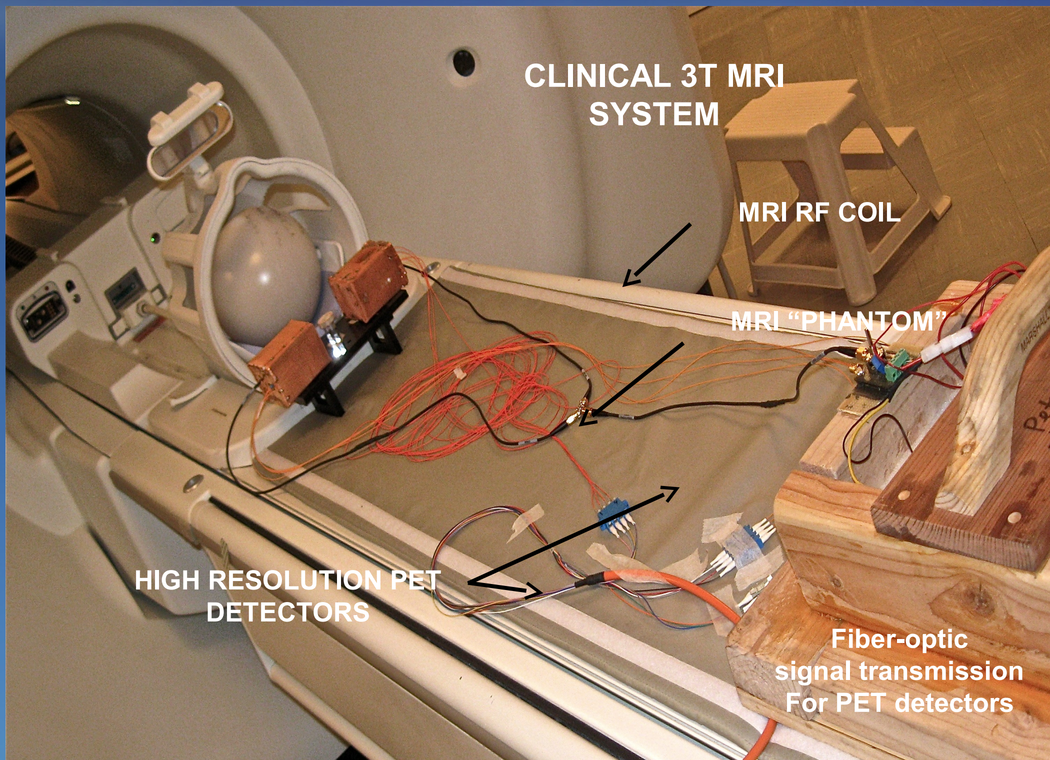

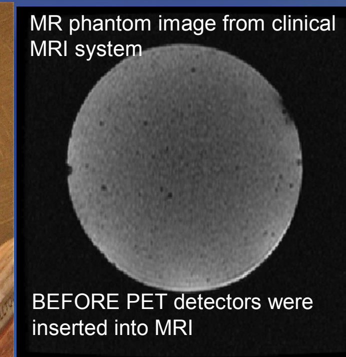

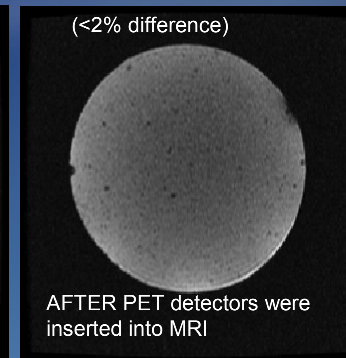

Image of PET detector crystals acquired OUTSIDE clinical MRI

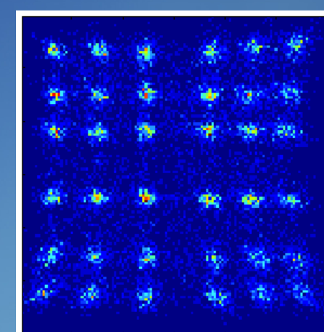

Image of PET detector crystals acquired INSIDE clinical MRI

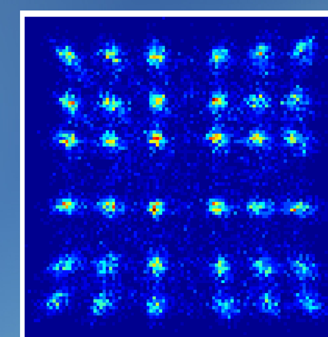

(Craig Levin, Stanford)

The full ring PET brain insert is now under construction…

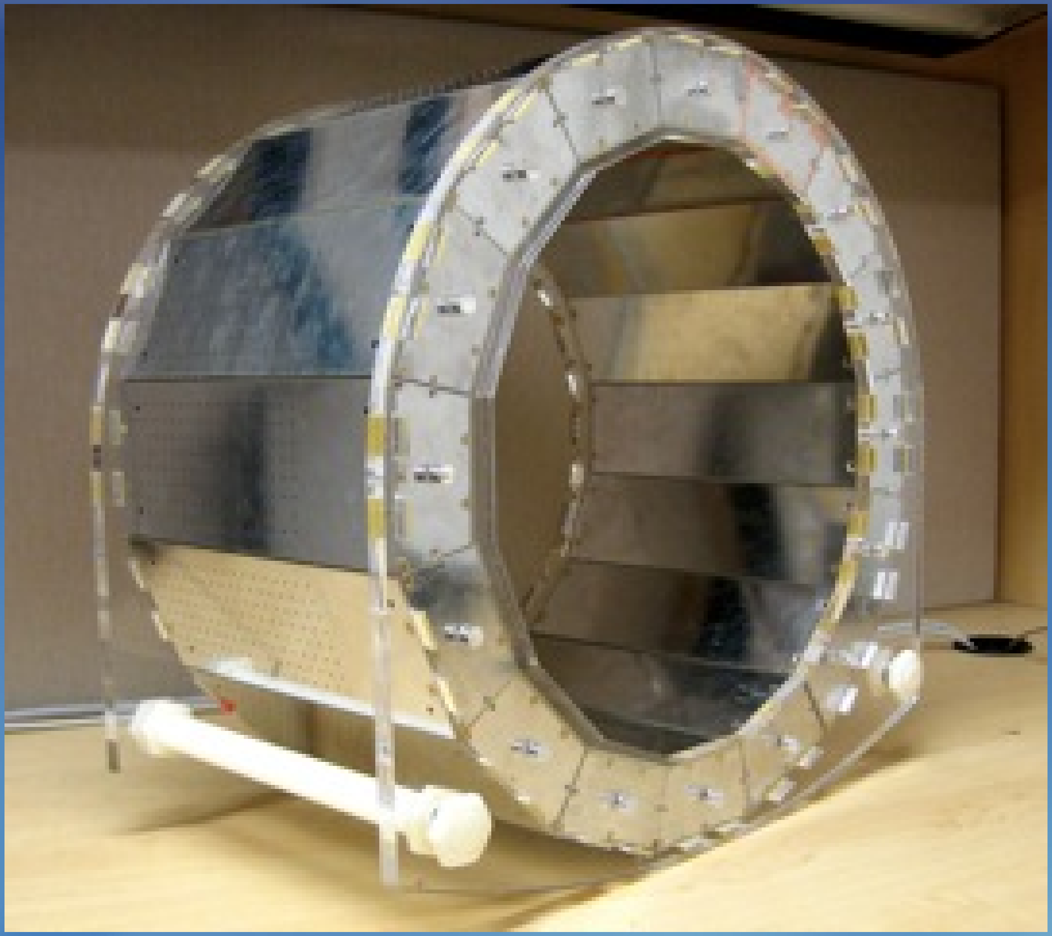

(Craig Levin, Stanford)

Prior art:
Existing mobile brain PET/CT systems

Left: mobile NeuroPET/CT from PhotoDiagnostic Systems. Right: FMI ScintiStarTM Neuro LPX PET/CT.

Mobile but with limited positioning capabilities

HEP spin-off and First use of SiPMs in a human brain imager

PHOTO DIAGNOSTIC Systems

85 Swanson Road, Boxboro MA 01719
Tel. 978 266-0420 Fax 978 266-0425
www.photodiagnostic.com

NeuroPET/CT • The World's First Portable PET/CT

System Characteristics

PET

Crystal Type:	LYSO:Ce
Sensor Type:	Silicon Photomultipliers (SiPM)
Patient Aperture:	34 cm
Crystal Size:	2.3 mm, 20 mm total thickness
Point Sensitivity:	8%
NEMA Sensitivity:	14.5 cps/kBq@350keV (NEMA NU2 2007)
Resolution:	2.5 mm
NEC:	≥40kHz (NEMA NU2 2007)
Transaxial FOV:	≥256 mm
Axial FOV (crystal extent):	up to 22 cm, providing single-step head acquisition

CT

CT Detector:	8x1.25 mm detector
Maximum Technique:	140kV 7mA
Detector Channels:	3264
Max Rotational Speed:	60 RPM
Views/second:	1440
Resolution:	0.65 mm

- *Take scanner to patients: powered wheels, flexible power options and self-shielding.*
- *Patient remains stationary while scanner moves axially, allowing for more flexible patient positioning and minimal interference with patient monitors and equipment.*

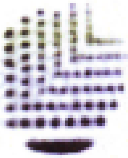

PET

Spot Size: 2.4, 2.7, 3.2, 3.5, 3.9, 4.7 mm

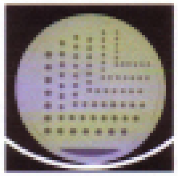

CT

Versatile Power Options
Battery-powered scans
Portable use with 120V, 20A service
Fixed installation uses 240V, 20A service
Input: 100-240V, 50/60Hz

Portability
Fits through a standard door
Powered transport wheels
Self-shielded CT
21 inch laptop console

Rebinning
Single Slice Rebinning (SSRB)
Fourier Rebinning (FORE)

Acquisition
Step-and-shoot PET acquisition
List mode acquisition is standard

Reconstruction
Filtered Back Projection (FBP)
2-D MLEM/OSEM
3-D MLEM/OSEM-MAP

Acquisition/Reconstruction Computer
Processor: 2 x Intel Xeon 6-Core
Memory: up to 144 GB RAM
GPU Enhanced Reconstruction engine
Ethernet Data Receivers

DICOM Compatibility

This device is available for research use only until pre-market clearance from the FDA.

PET detectors integrated with a RF coil for MRI

The design that extracts maximum work from DOI detectors;
closer detector arrangement will enable not only higher sensitivity
but also higher resolution by reducing the angular deviation effect.

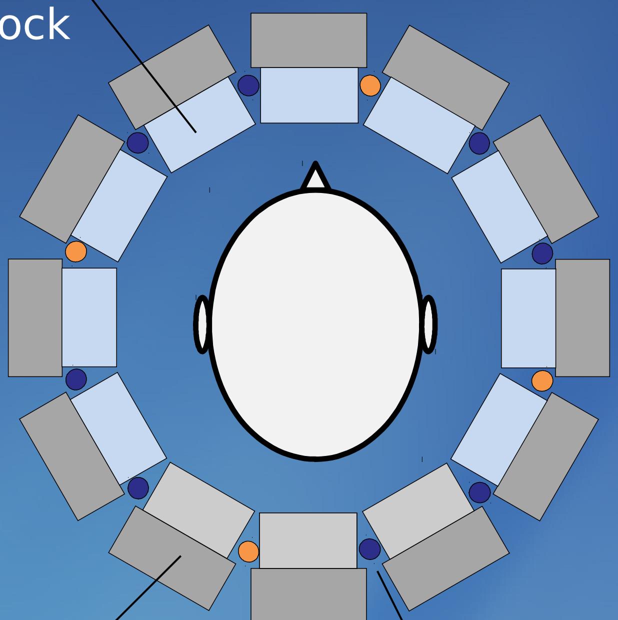

Feasibility experiment

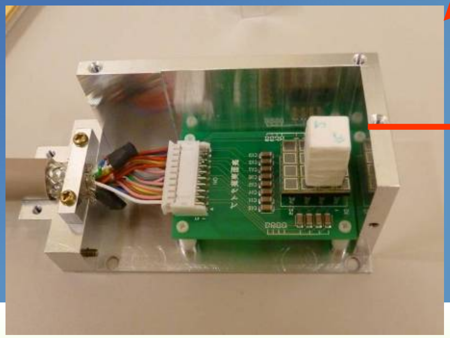

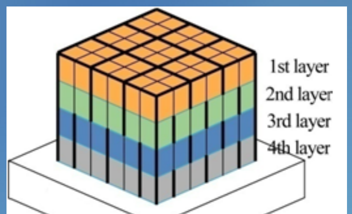

Crystal: 6 x 6 x 4-layer array of LYSO
(1.45 x 1.45 x 4.5 mm3)
MPPC : 4 x 4 array of S11064-050P

PET and MRI did not influence each other.
(F. Nishikido, et al., IEEE MIC2011, MIC13-7)

Depth-of-interaction (DOI) detector

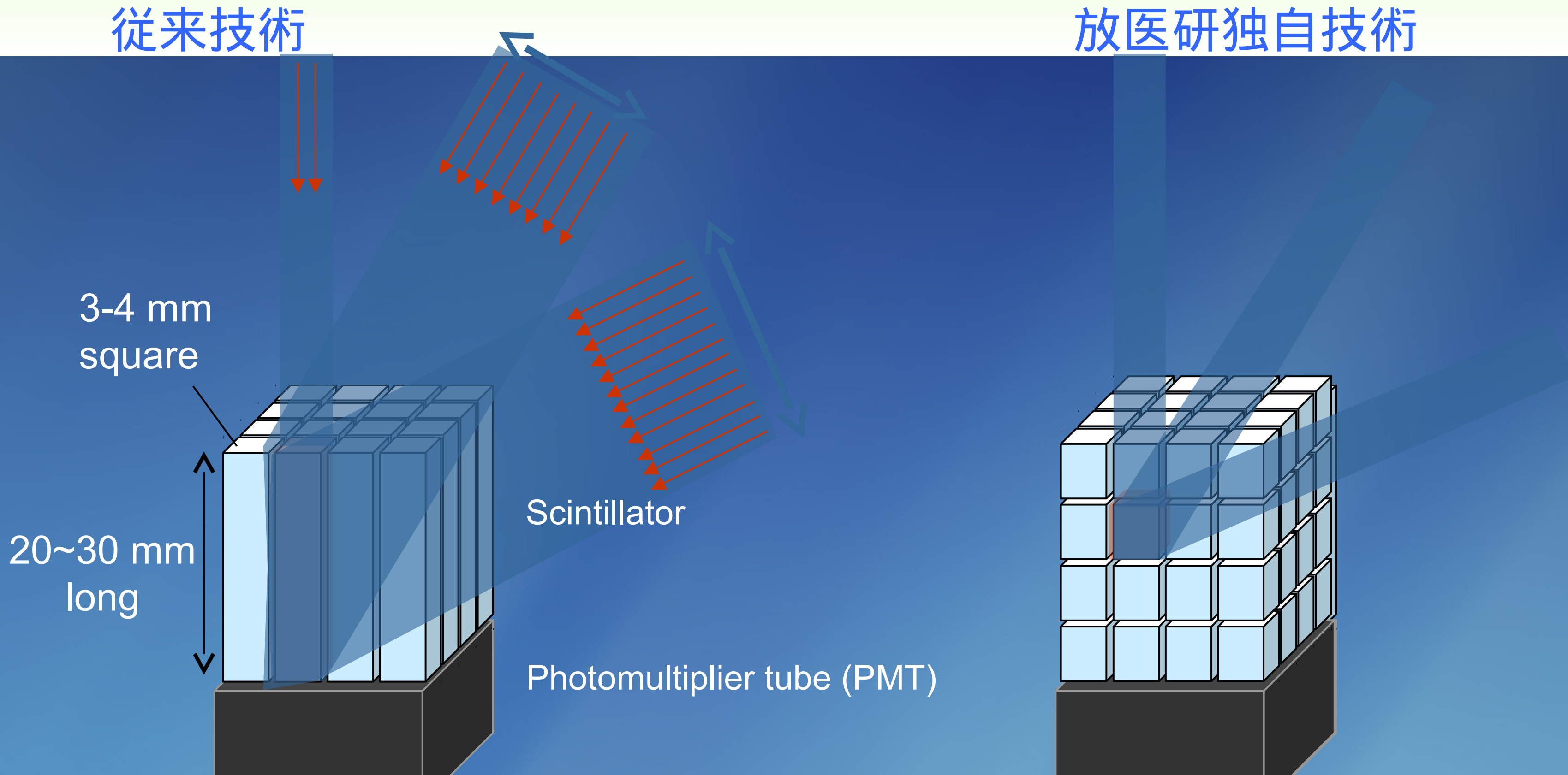

Sensitivity and resolution are incompatible

Both sensitivity and resolution can be improved

"Crystal cube"
A SiPM-based isotropic-3D detector

- Light sharing
  - Higher resolution than photodetector resolution
- A segmented crystal array with no reflector insertion
  - Uniform crystal identification performance for the Anger-type calculation
- Full-face detection of scintillation photons
  - Efficient light detection, thus expecting better spatial, energy and timing resolution.

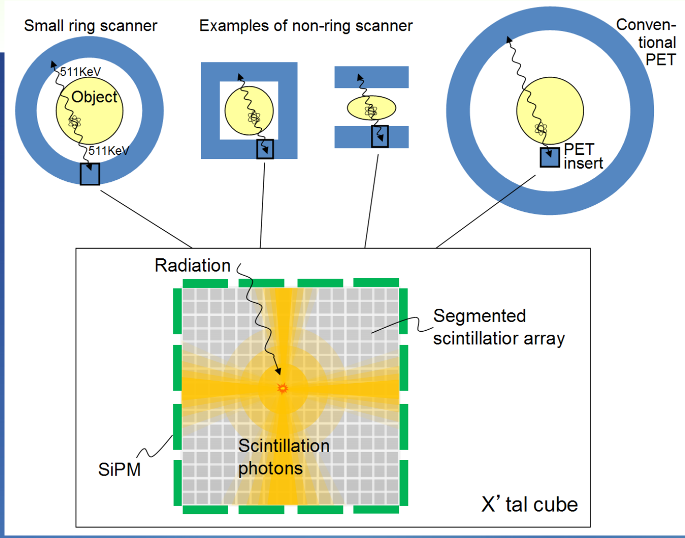

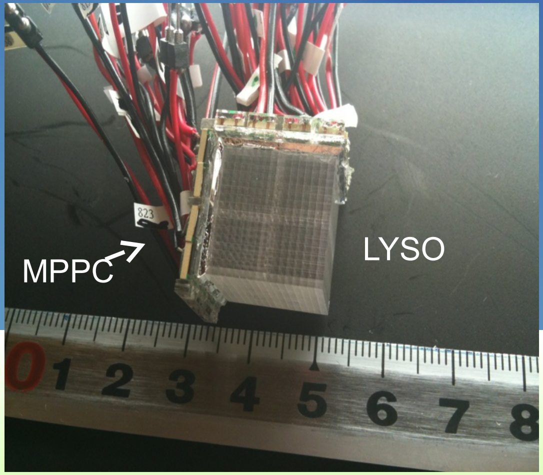

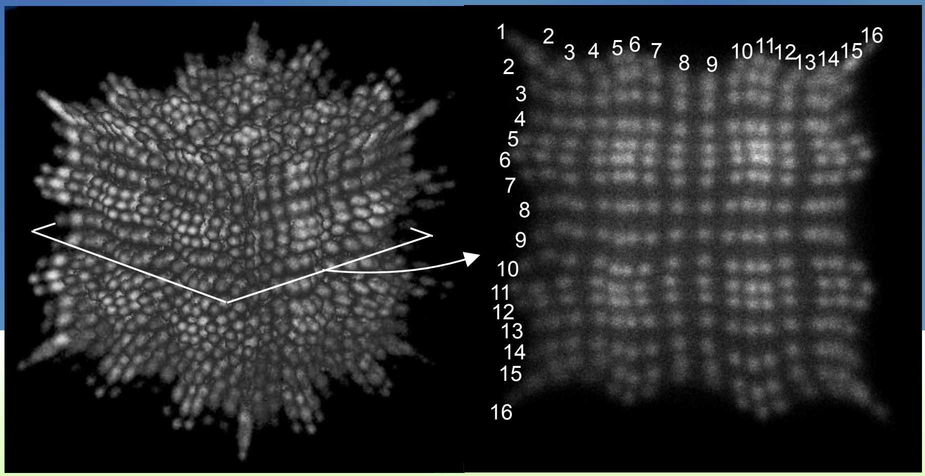

Insertable Brain PET-MRI (Sogang University, Korea)

New design concept

- Use Geiger-mode avalanche photodiode (GAPD) arrays as a PET photo-sensor
- Use charge signal transmission method that transmit the charge signal of the photo-sensor to the preamplifier through charge transmission cables 3 m in length

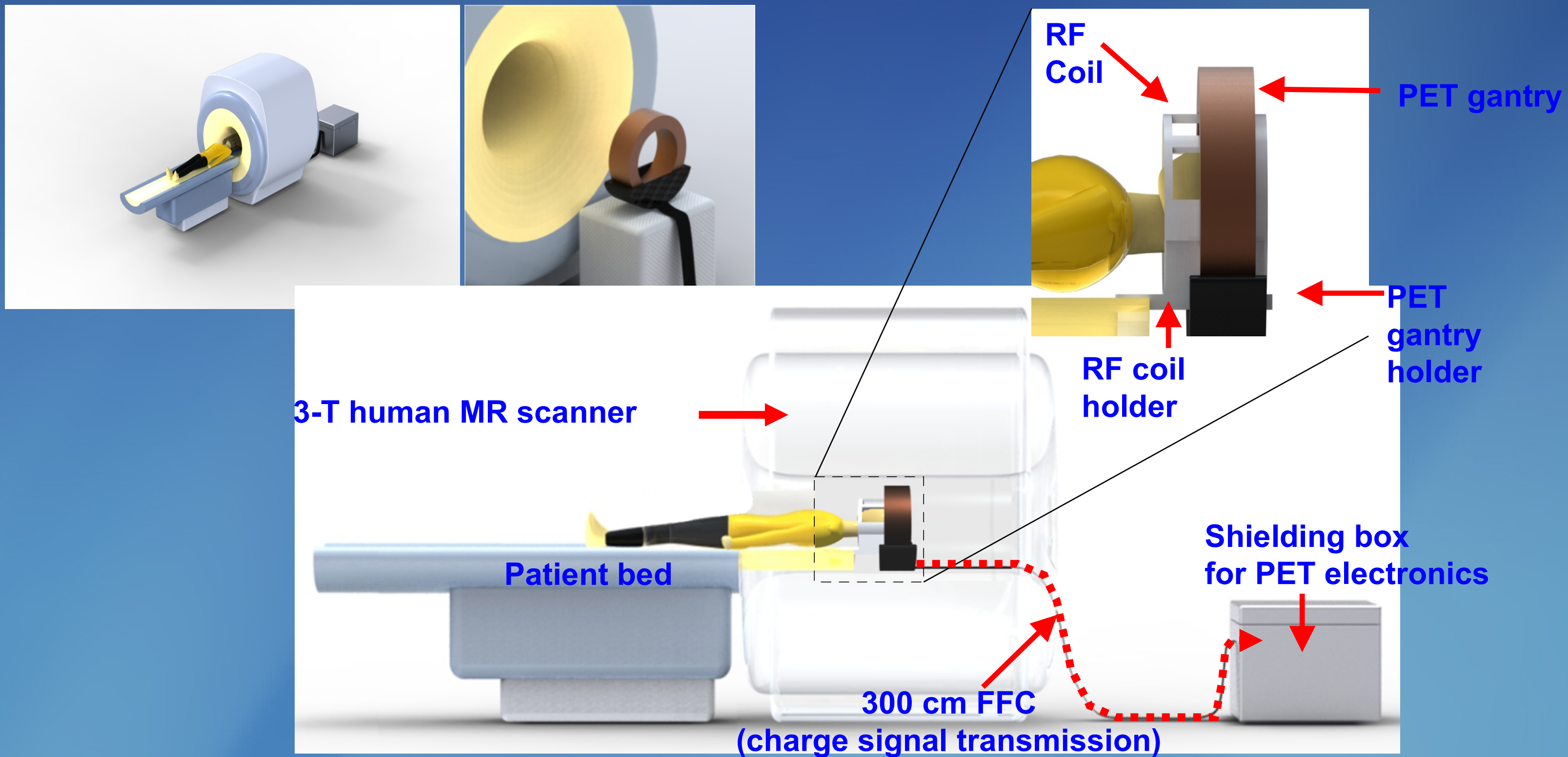

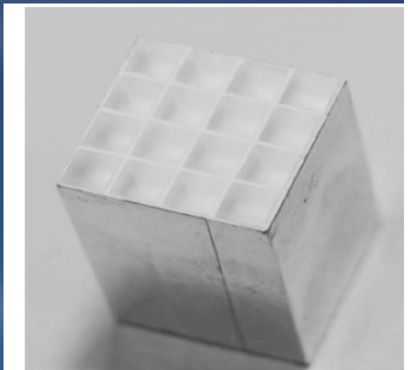

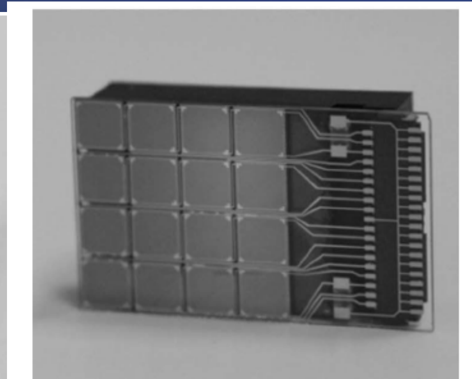

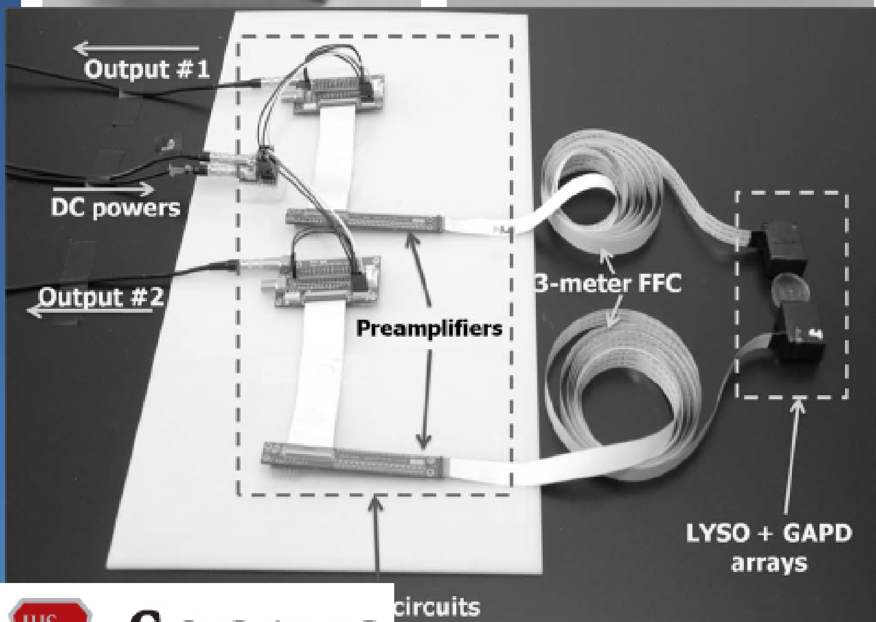

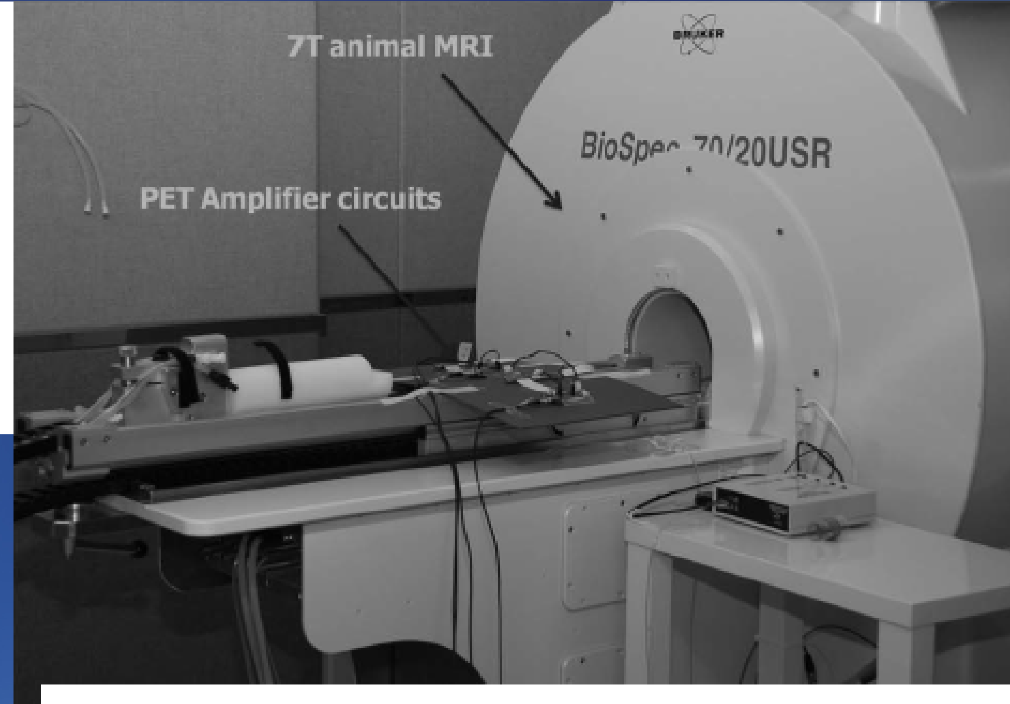

FIG. 3. Experimental setup to examine the effect of the cable length on both PET and MRI. (a) PET detector performance measurement outside MRI. A pair of PET detector modules was exposed by Na-22 point source and PET charge signals were transmitted to the preamplifier using FFC of 300 cm. (b) PET performance measurement inside the MRI. The PET detector modules were inserted into the MR bore between the RF coil and gradient coil (not displayed), while the preamplifier is located outside the MR bore (<5 G line, ~1.5 m away from the magnet isocenter).

SOGANG UNIVERSITY

1) Molecular Imaging Research & Education (MiRe) Laboratory, Department of Electronic Engineering, Sogang University, Korea
2) Sungkyunkwan University School of Medicine, Korea
3) Department of Electrical Engineering, Korea Advanced Institute of Science and Technology (KAIST), Korea

Insertable Brain PET-MRI (Sogang University, Korea)

- Simultaneous imaging of 3D Hoffman brain phantom (inside MR bore)

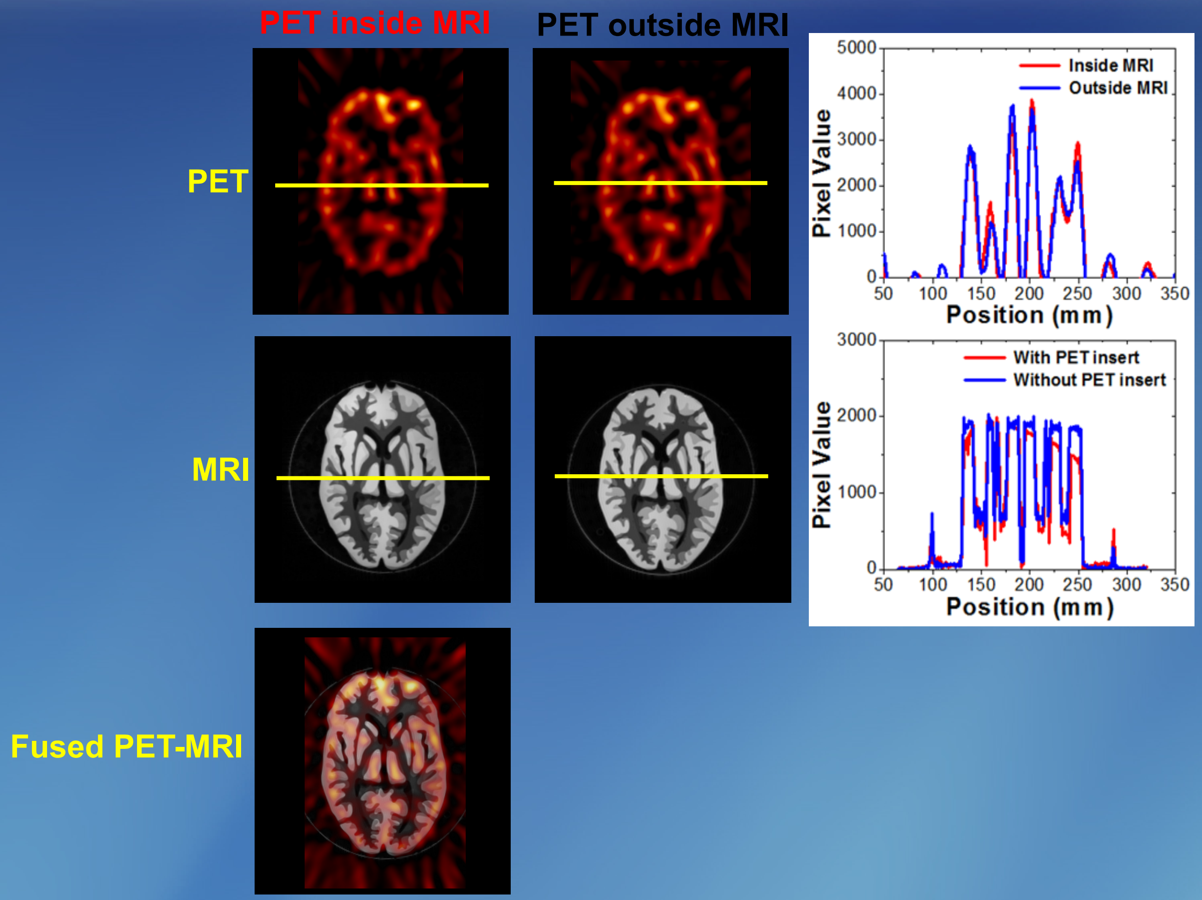

New cancer scanner halves radiation

Particle physicists have developed a new medical technology that combines PET and MRI in one. Benefit: Improved image quality and less radiation.

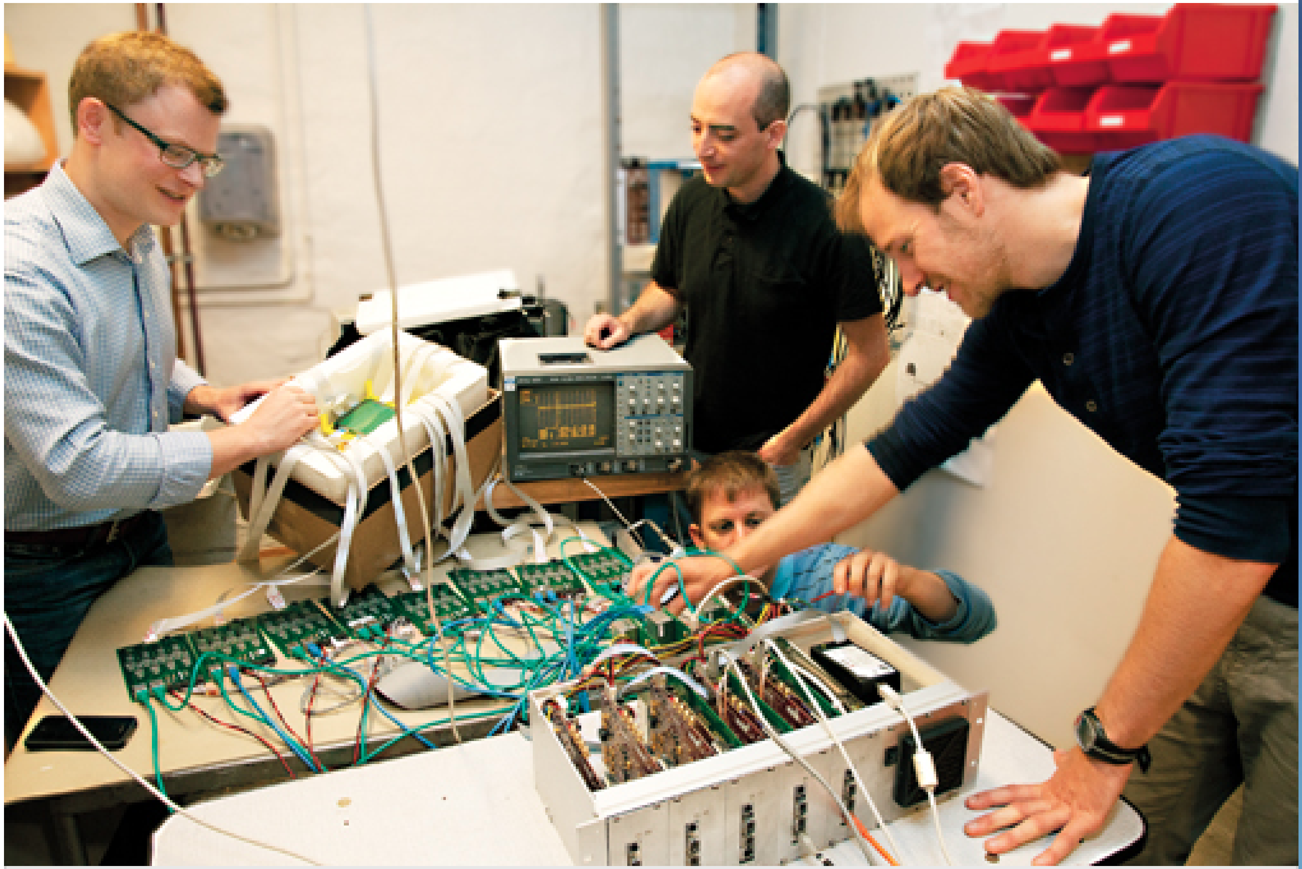

FIFTY PER CENT LESS RADIATION: The particle physicists Erlend Bolle, David Volgyes, Michael Rissi and Kim-Eigard Hines have developed a completely new technology that makes it possible to halve radiation from a PET scanner. The PET scanner is also built at such a small scale that it can be placed inside an MR scanner. This makes it possible to take the MR and PET images at the same time. Photo: Yngve Vogt

From calorimetry to medical imaging: a shining example of successful transfer!

A team at CERN has drawn inspiration from calorimetry methods developed for high-energy physics to create a new positron-emission tomography system for use in medical imaging, which they've dubbed AX-PET. With support from European and American laboratories*, the project is reaching fruition, as initial tests confirm its promise.

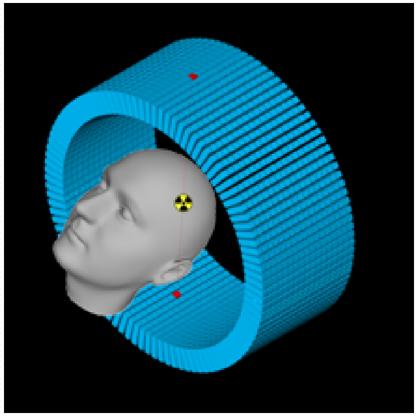

A traditional PET scanner showing the crystal layout.

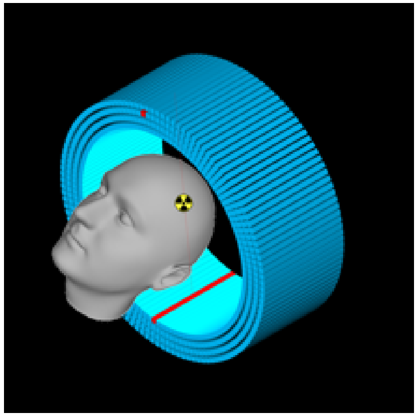

The axial orientation of elongated crystals in AX-PET.

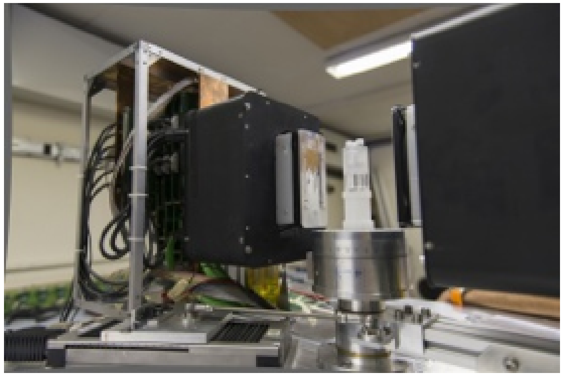

Snapshot of a "phantom", a test object, surrounded by the AX-PET photon detectors.

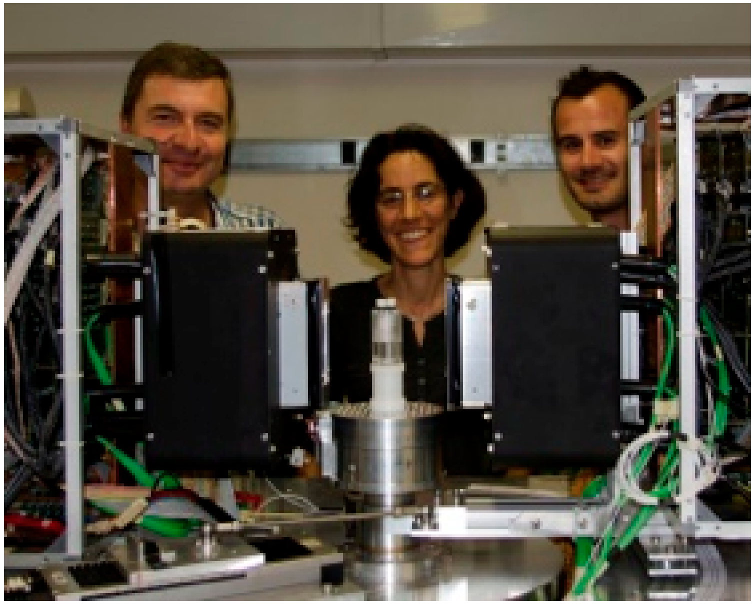

Some members of the project team: Christian Joram (CERN), Chiara Casella (ETH Zürich) and Matthieu Heller (CERN) pose behind AX-PET.

The AX-PET concept

3D measurement of the photon interaction point

- Transaxial coordinate and energy measurement with thin elongated scintillator LYSO crystals
  - The hit crystals gives the transaxial coordinate (x, y)
- Axial coordinates measured with Wave Length Shifter (WLS) strips

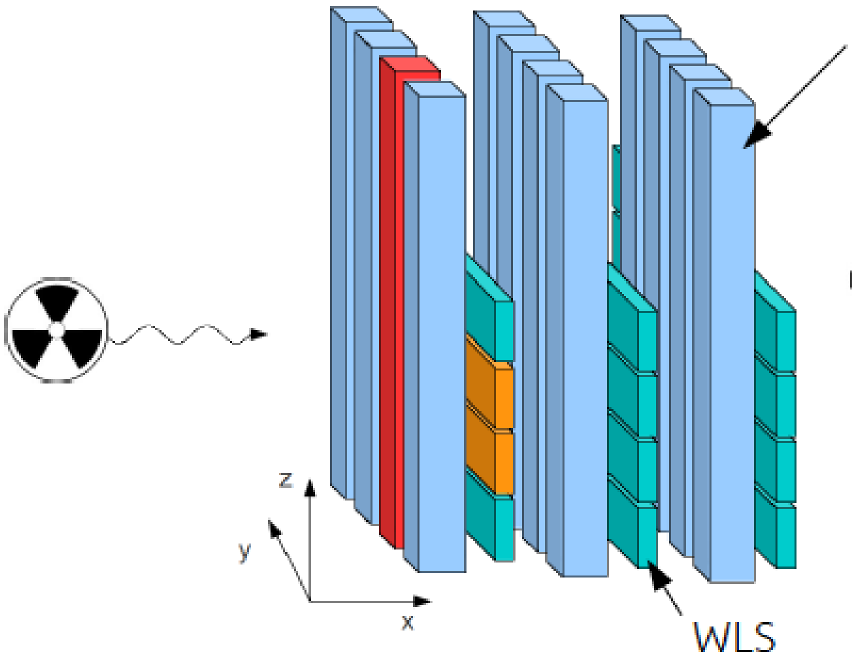

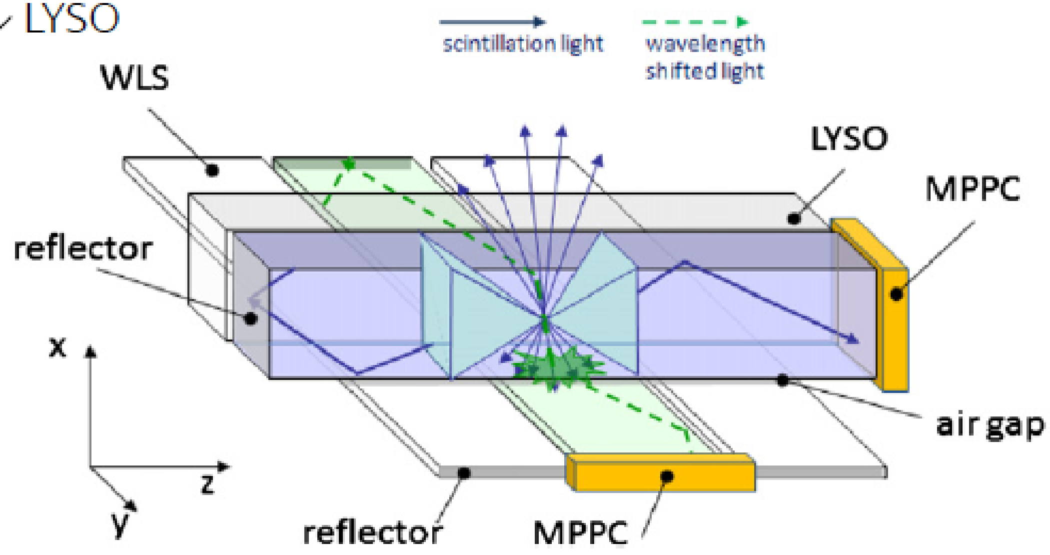

Detector components

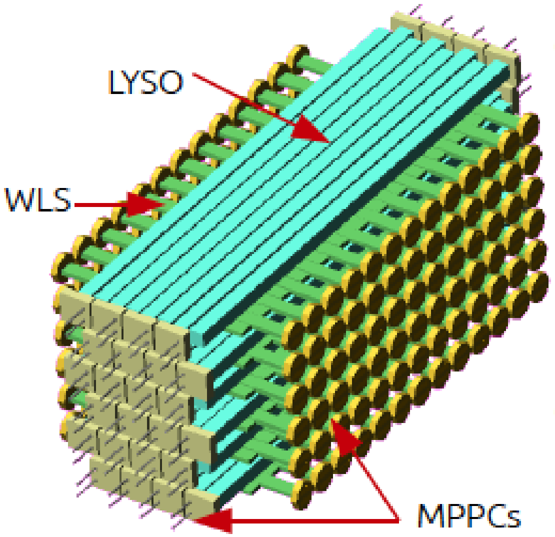

- LYSO ($Lu_{1.8}Y_{0.2}SiO_5$:Ce), Prelude 420 from Saint Gobain
  - 3x3x100 mm^3
  - Light Yield LY=32 photons/keV
  - High density : 7.1 g.cm^{-3}
  - Decay time τ = 41 ns
  - Attenuation length λ_{511}=12 mm @ 511keV

- Wave length shifting strips, ELJEN EJ-280-10x
  - 10 times higher dye concentration for better absorption

Expected LYSO light output@511 keV event : ~ 1000 photons

- 3 x 3 mm^2 area, 3600 cells 50 x 50 um^2
- PDE ~ 40%
- Gain : 5.7 10^5
- Bias voltage ~ 70 V

MPPCs from Hamamastu

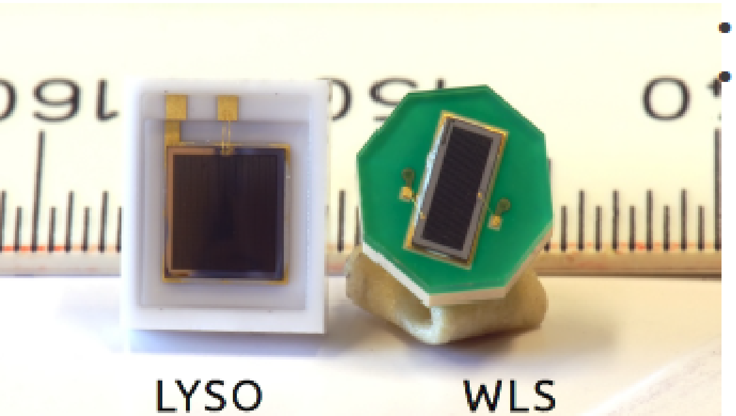

Expected WLS light output : ~ 50 photons

- 3. 22 x 1.19 mm^2 area, 782 cells of 70 x 70 um^2
- PDE ~ 40%
- Gain : 4 10^5
- Bias voltage ~ 70 V

Results from tomographic reconstruction

NEMA NU4

Image Quality
Mouse Phantom

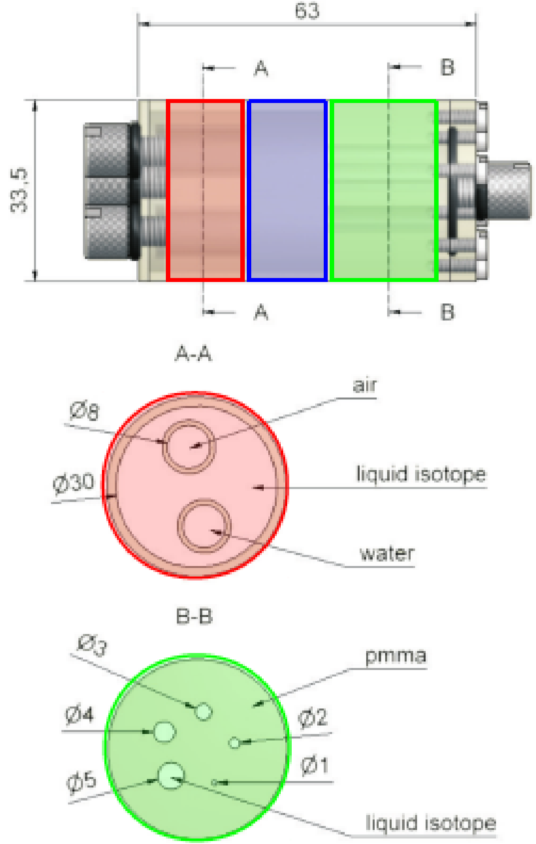

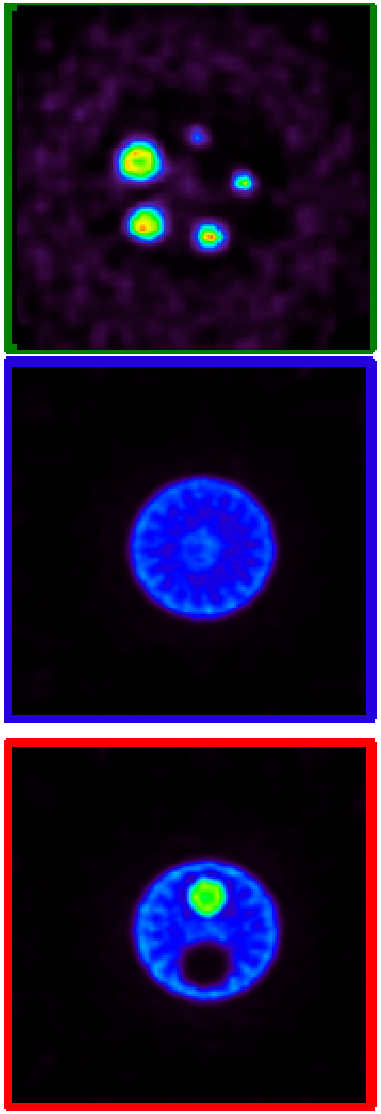

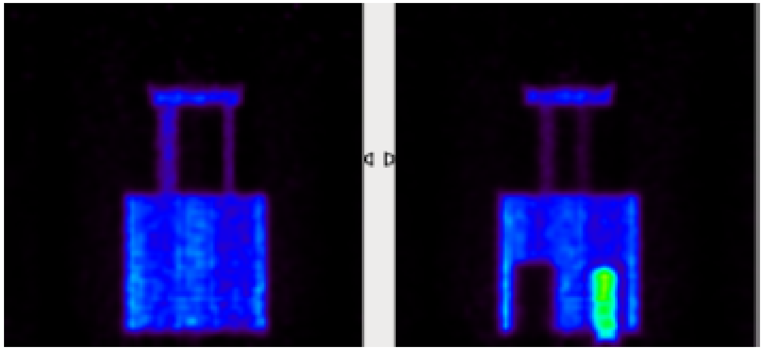

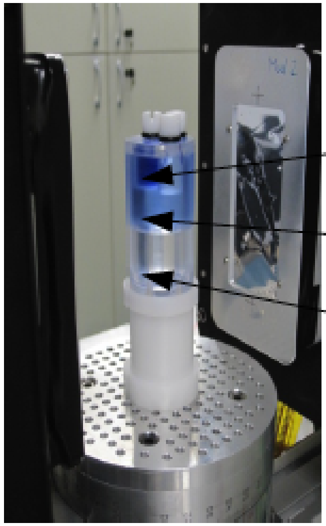

- Contrast region
- Homogenous region
- Spatial resolution region

Resolve 1 mm rod with 1.6 mm FWHM

Prior Art – Upright PET Brain Imager

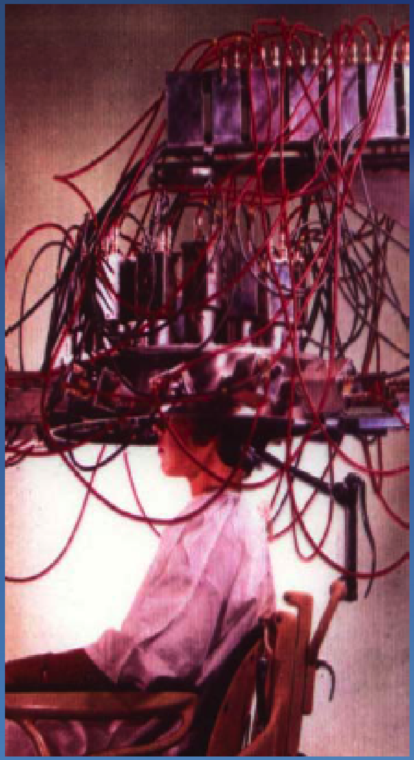

Photograph of one of the first brain PET scanners at Brookhaven National Laboratory, the "Headshrinker" (1961),

Photograph of the developed PET Hat with a subject

Photograph of a novel PET Hat ring imager, permitting imaging a 4.5 cm brain section of a sitting person. The detector modules are built on the basis of the H8500 PMTs. (Yamamoto, Kobe).

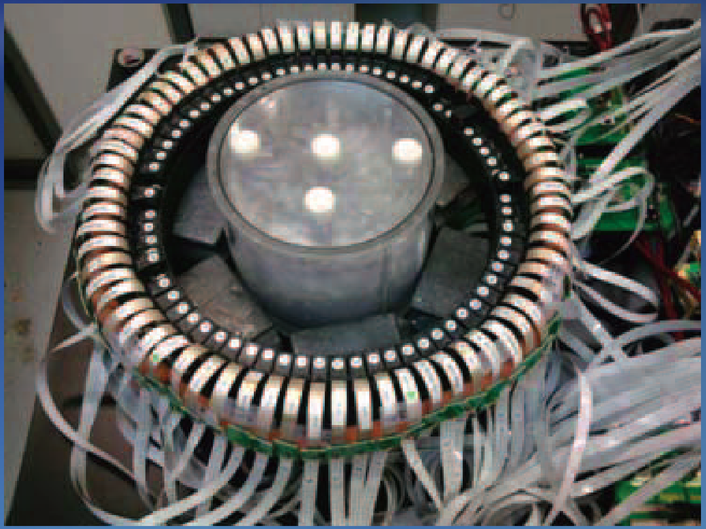

The prototype brain PET consisting of 72 compact detector modules built with SensL SiPMs. This imager covers a narrow 12mm slice of the brain but can operate in an MRI magnet (Korea).

PET-Hat: concept

1) Measurement at sitting position is possible

2) PET can move with subject by wearing the counter-balanced PET

3) Small size and controlled by a Note PC

PET-Hat with subject and phantom images

Front view

Side view

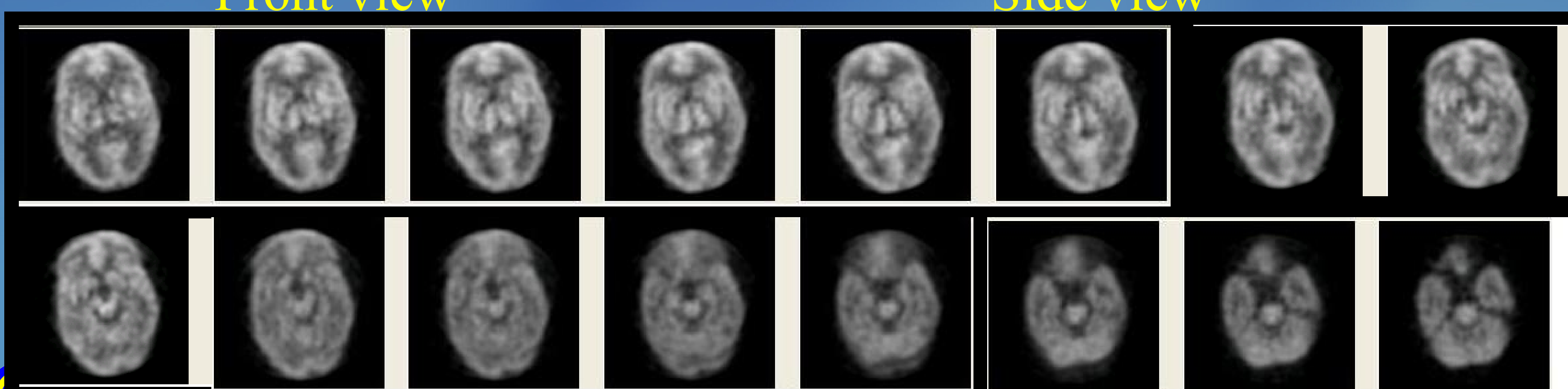

Images of brain phantom

S. Yamamoto et al. IEEE TNS 2011

Short History of IP for the Wearable PET Brain Imagers: From RatCap to HelmetPET

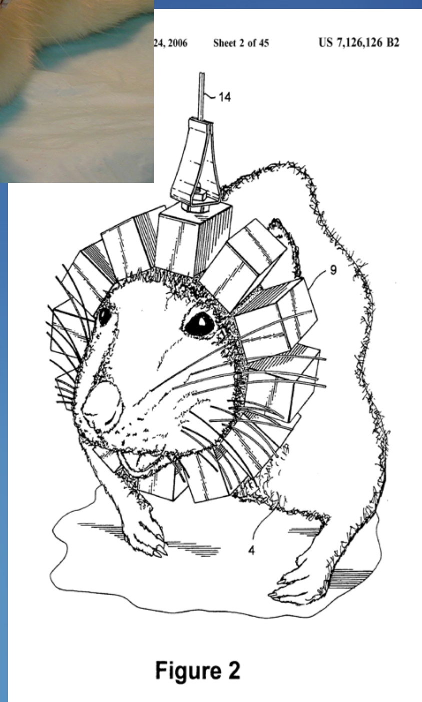

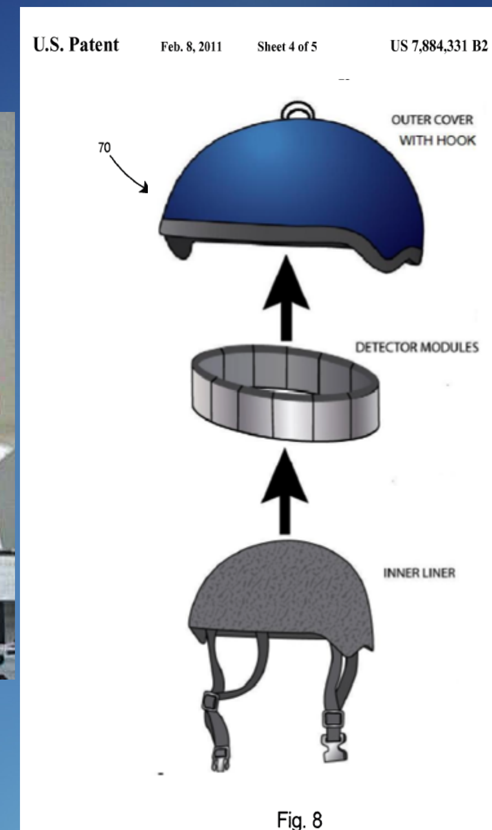

Left: RatCap PET (non-compliant animal); Center: PET Hat and compliant sitting patient; Right: Helmet for a compliant standing, moving etc patient).

Awake Animal Project

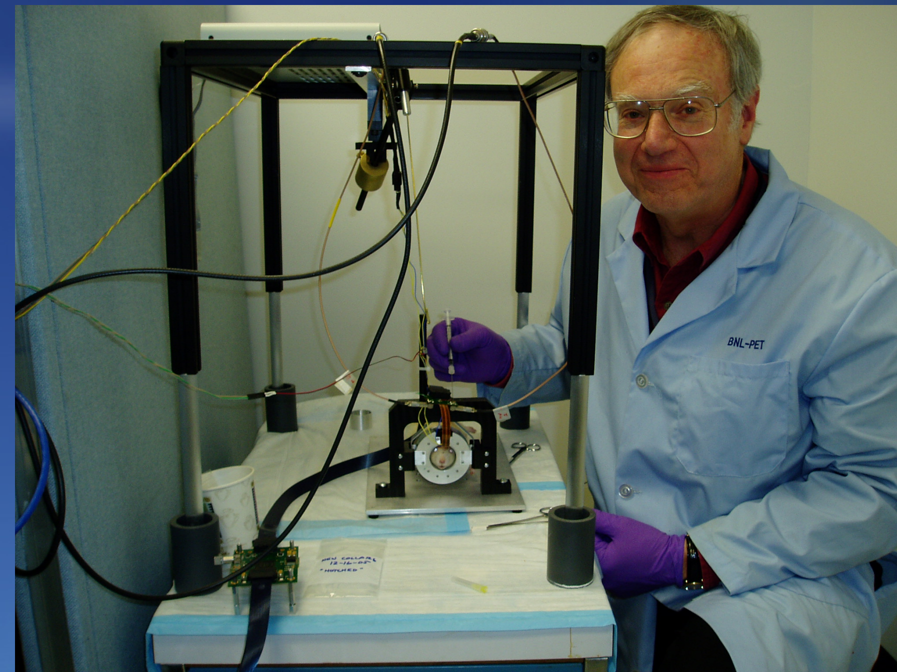

DOE funded research on imaging of the awake rat

For the first time we can watch the brain in action during behavior in small animals

Small Animal (Rat) PET / MRI Camera

ndard Non-Magnetic Components

SO crystals

luminum housing

berglass, kapton, plastic, silicon

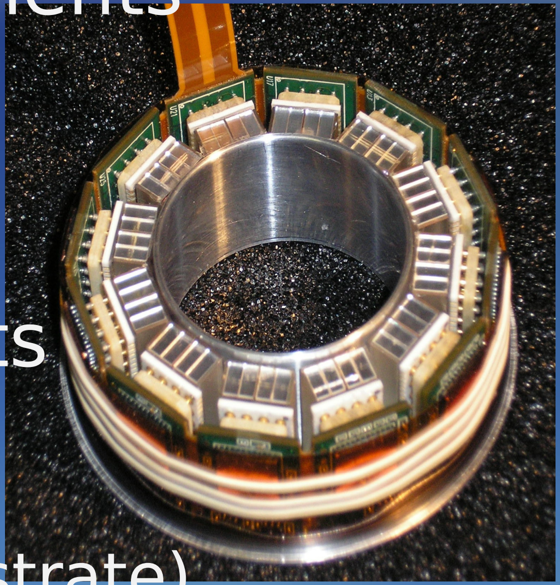

Image courtesy of Craig Woody

Brookhaven National Laborato

ial Non-Magnetic Components

Ds (special pins)

D sockets

n-magnetic flex circuit board (substrate)

n magnetic electronic components (solder leads)

hielding from RF

Aluminum housing

Kapton cable carrying signals

- Non-Magnetic Version of RATCAP
  - Planned to Use for Neurology

U.S. Department of Energy

Office of Science

DOE Imaging Instrumentation

Clinical PET

MicroPET

Mobile PET

JLab Imaging Detector Technology

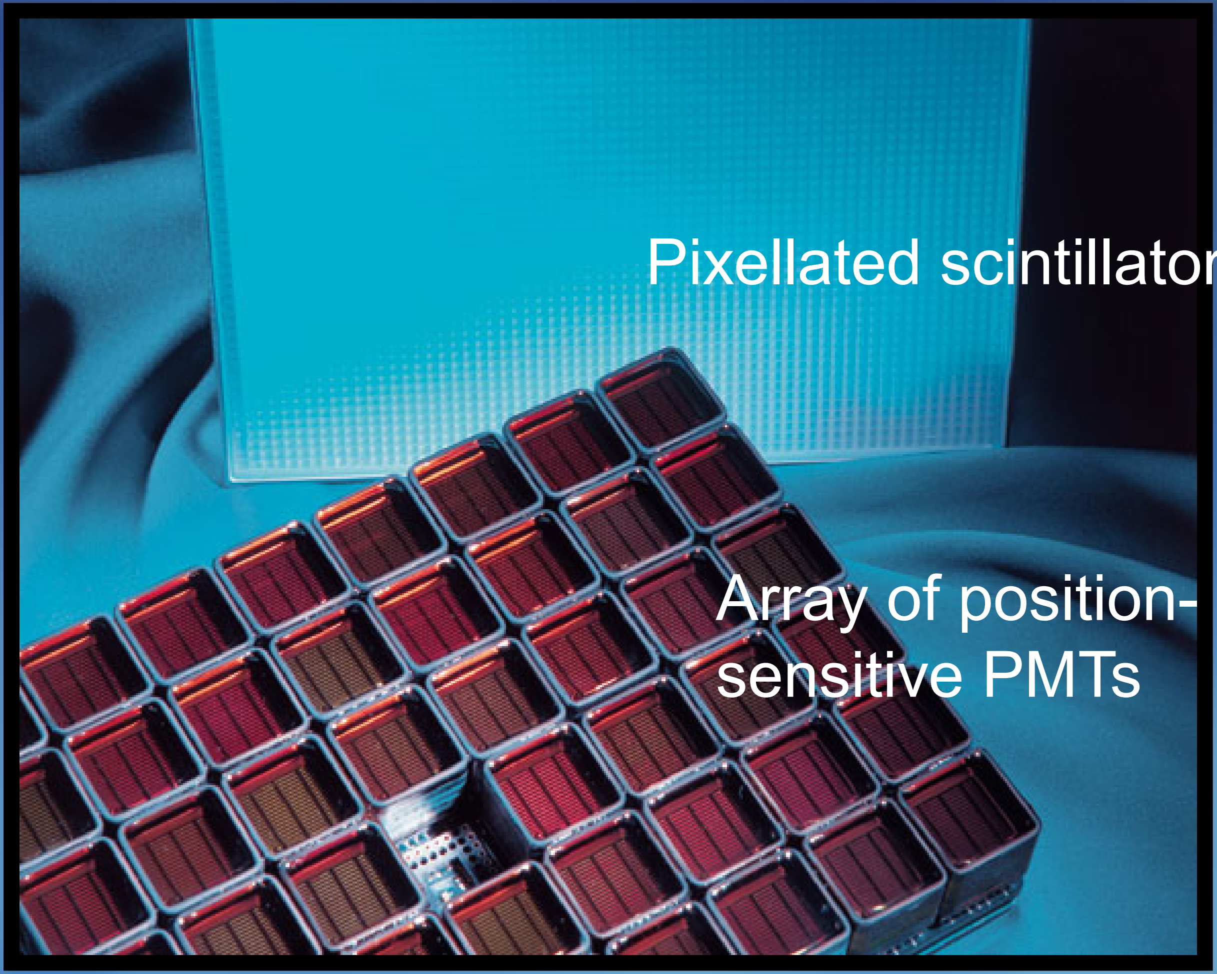

Dilon 6800 Gamma Camera

Removable Smart Shield™ modified to accommodate biopsy hardware.

Removable sliding slant-hole collimator system for stereo viewing.

Microcalcifications with Previous Benign Biopsy

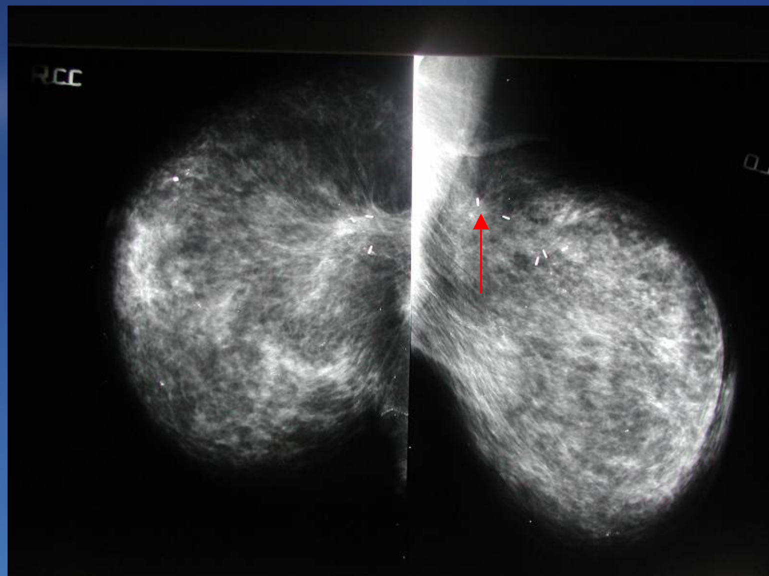

Mammogram: right breast shows area of microcalicifications (see arrow). Previous needle biopsy of this area was negative.

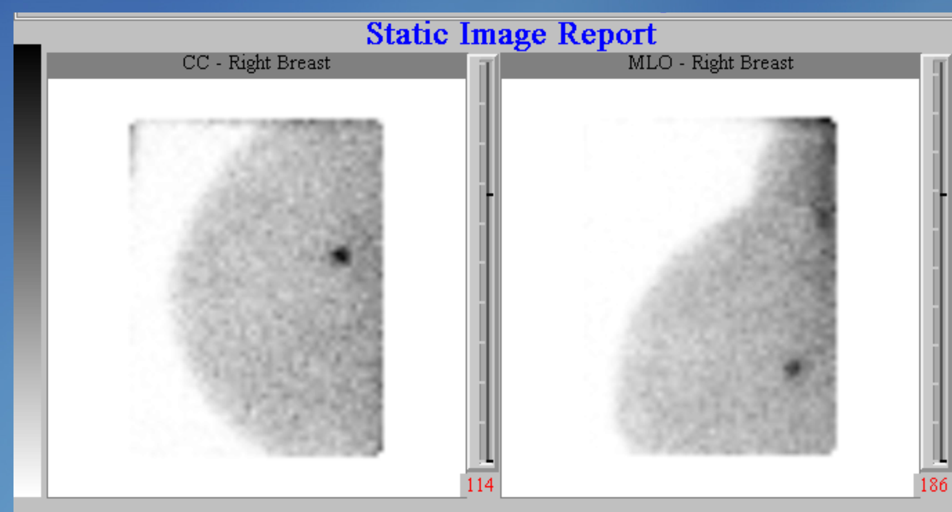

BSGI: demonstrated a high-uptake region highly suspicious and the patient was sent for open biopsy. Ductal

Courtesy of West Valley Imaging

Predicting the survival of patients with breast carcinoma using tumor size, JS Michaelson, M Silverstein, J Wyatt, et. al. *Cancer* 2002; 95: 713-723

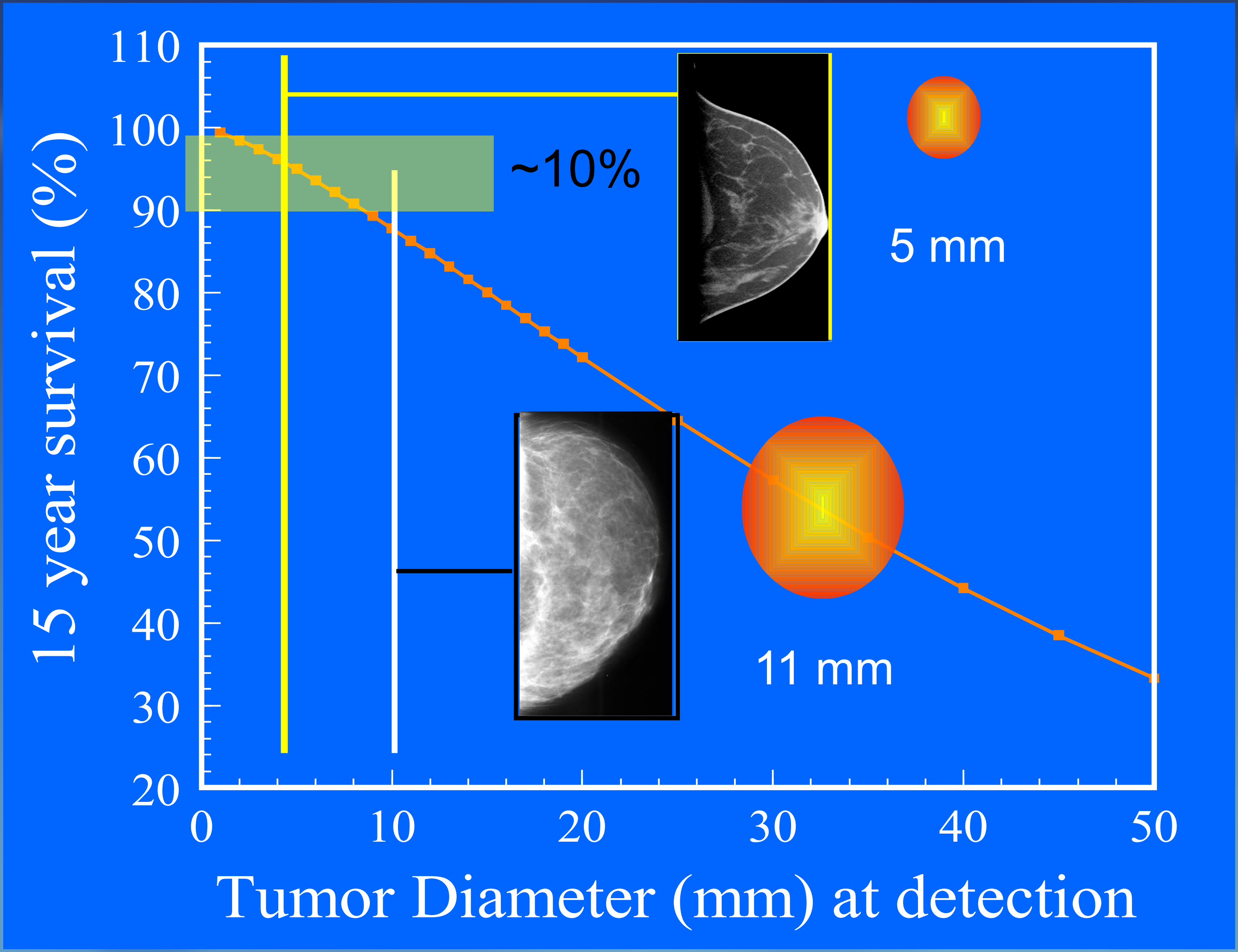

(slide provided by Dr Simon Cherry, UC Davis)

Interesting Activity

=

Meeting Important People

Simultaneous PET-MRI Breast Imaging

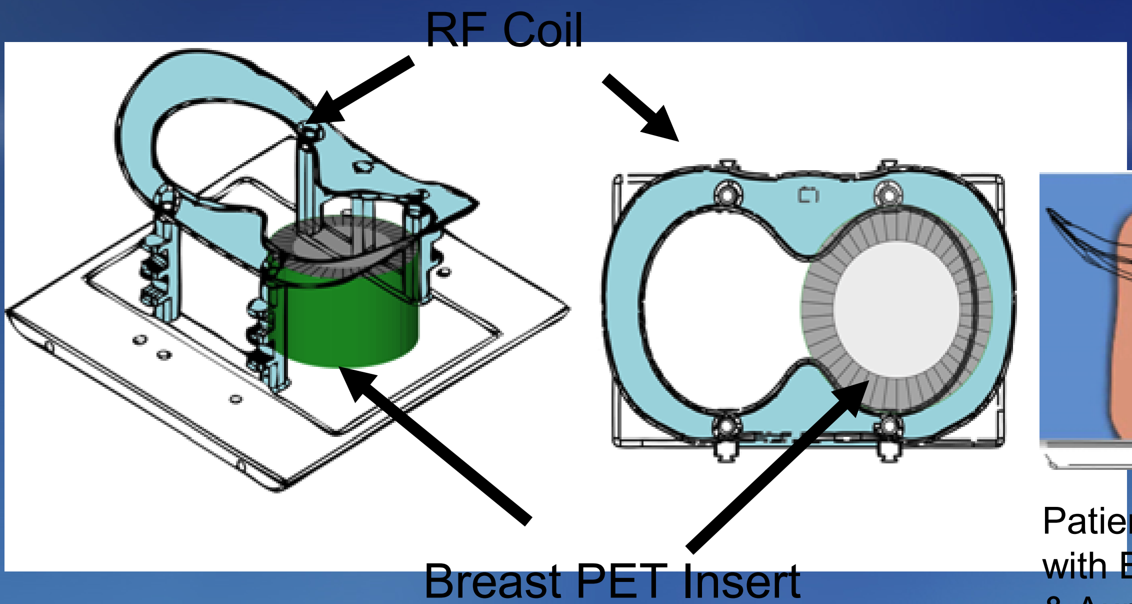

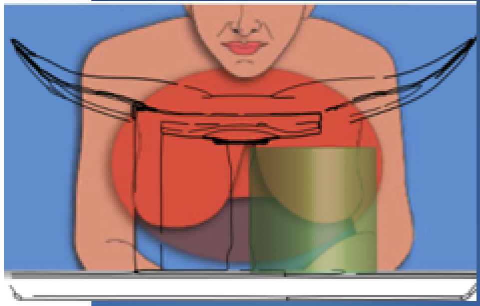

Patient positioned
with Breast PET insert
& Aurora Breast RF coil

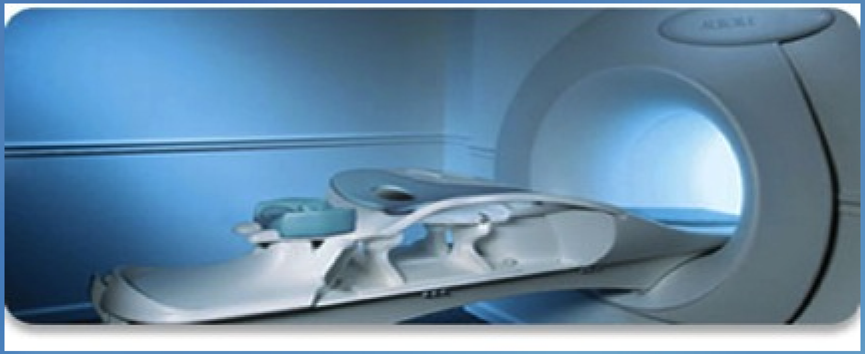

Aurora Dedicated 1.5 T Breast MRI

Clinical Prototype

Need larger ID and flexibility in axial coverage

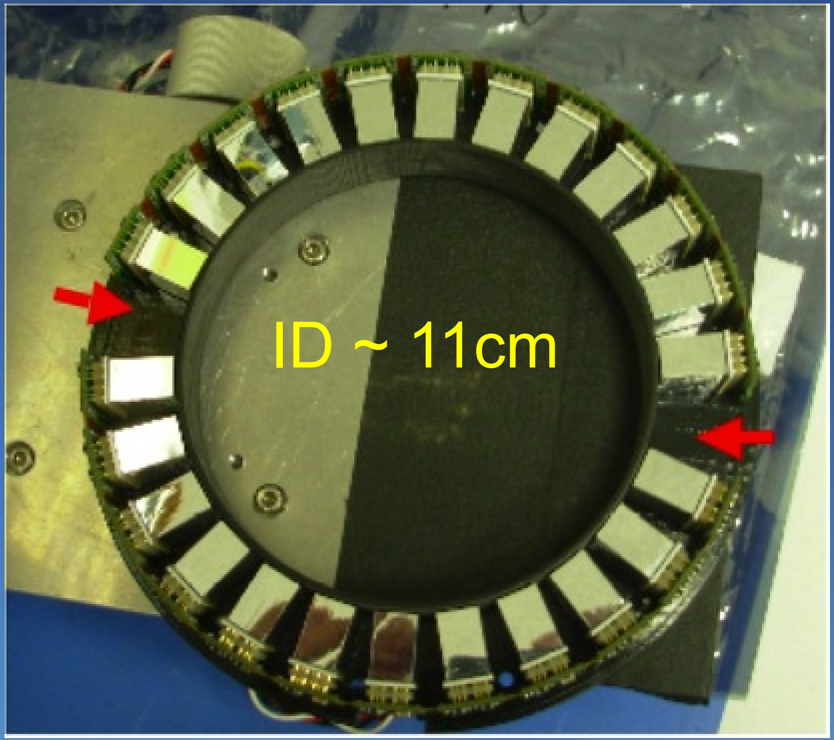

24 detector PET ring with a crystal wide gap on either side

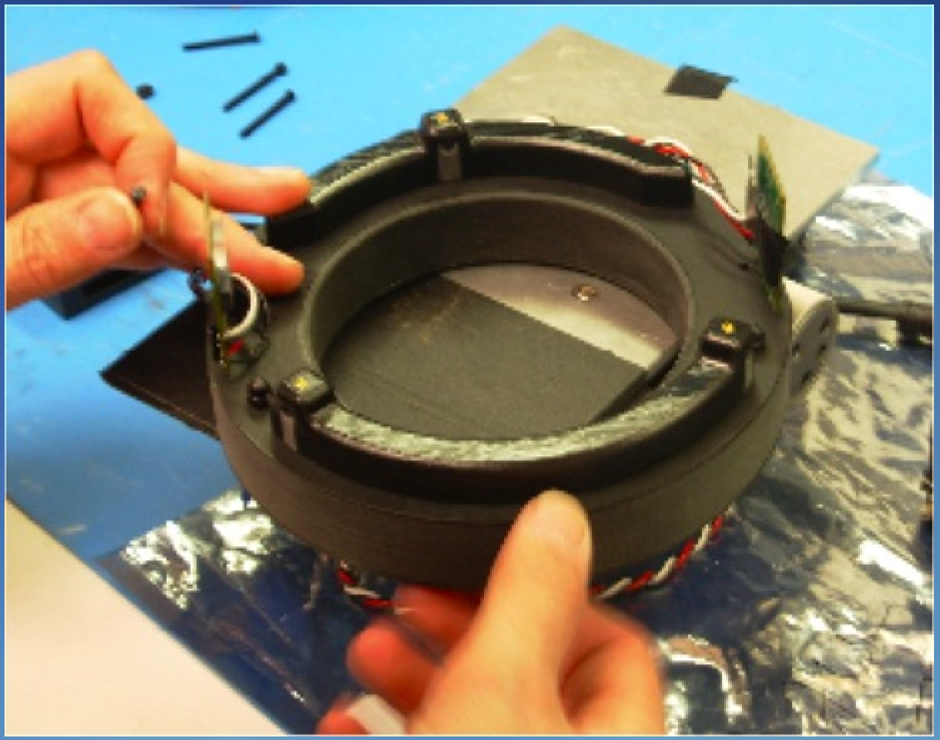

PET ring is assembled in a plastic housing

Clinical Protocol - Taipei Medical University Hospital

Routine Breast MRI to find any lesions

↓

18F-FDG Whole Body Scan*
(supine position)

↓

Chest PET scan*
(prone position)

↓

Simultaneous PET/MRI

↓

Delay phase prone PET*

↓

Biopsy

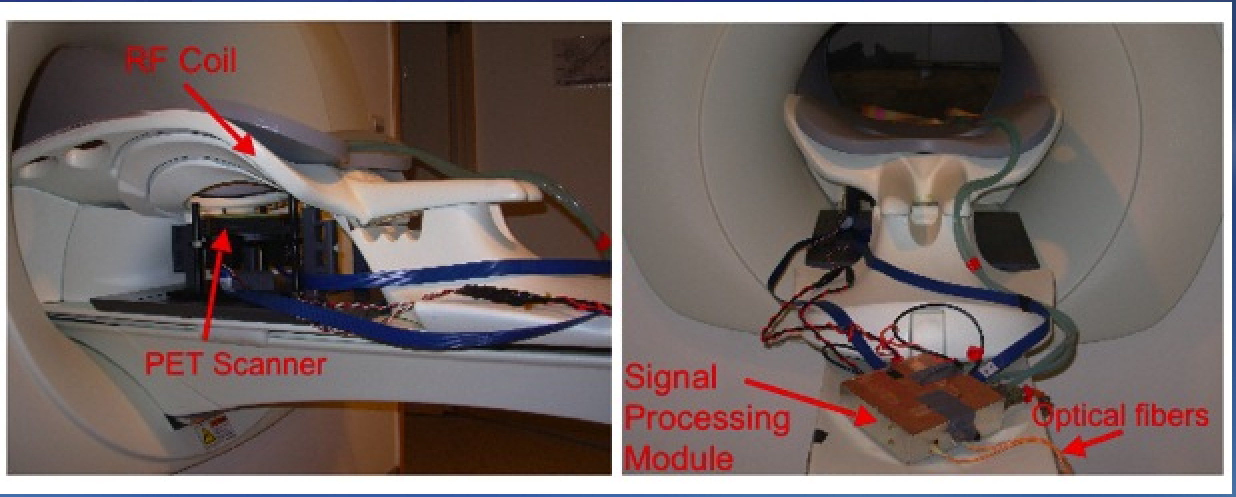

* Scans done on Siemens Accel

Patient 1 - Simultaneous PET-MRI

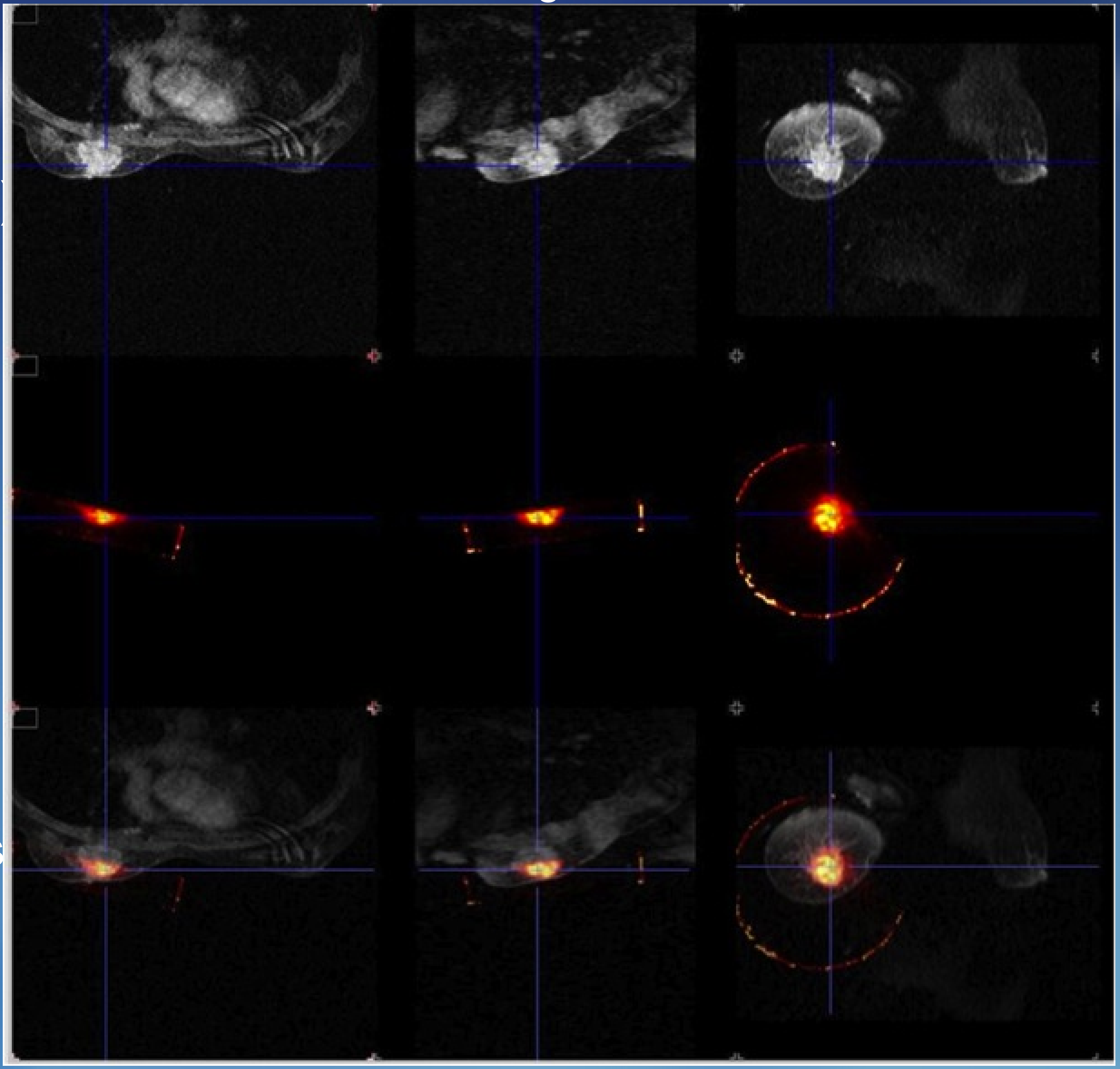

Future Directions

- Next generation is considerably larger both in radius and in length increasing our field of view
- This new deign has only three cables coming out 1 power and 2 optical fibers

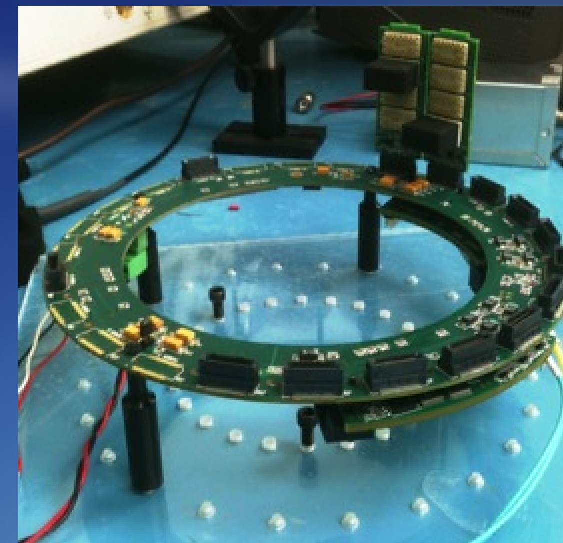

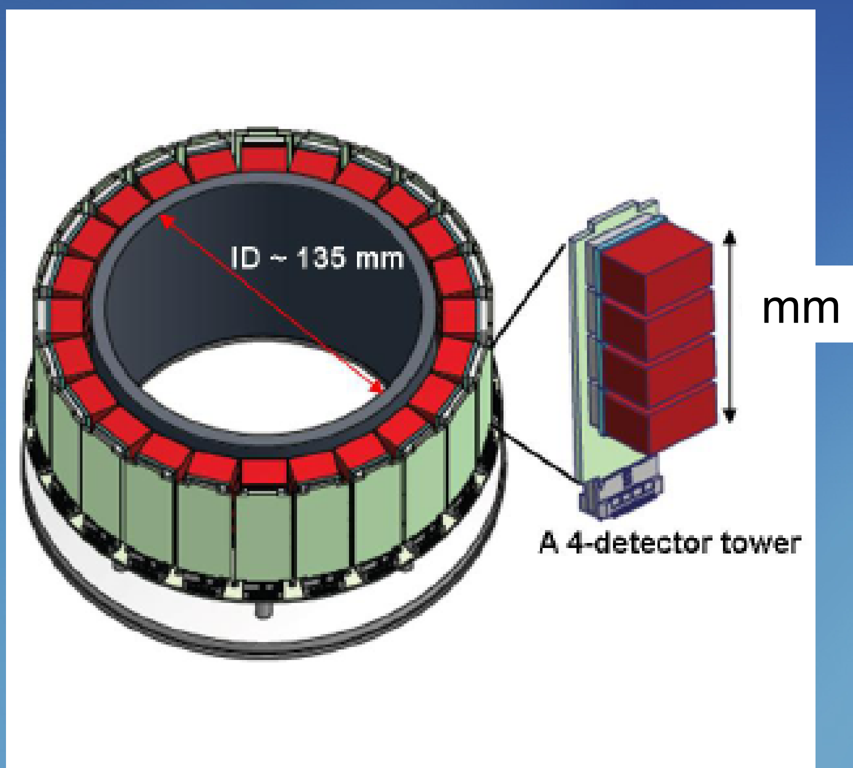

Things to Remember

- The power of PET and MRI lies in the ability to analyze the images, not in making nice pictures
- Think about kinetics as a way to better utilize PET and MRI data
- Think about ways to retrofit the 30,000 MR scanners in the world to make PET/MR available for the clinic

WVU HELMET PET BRAIN IMAGER

xamples of some possible situations with patients wearing the imager helmet: sitting in a chair *eft)*, exercising *(center)*, and laying down on a bed *(right)*. Another option with a (helium) balloon upporting the weight of the helmet, allowing for even more movement freedom during imaging ession, is not shown here. Except for the case of a patient on a bed, the helmet is suspended by a lexible harness /suspension attached to a hook on the helmet.

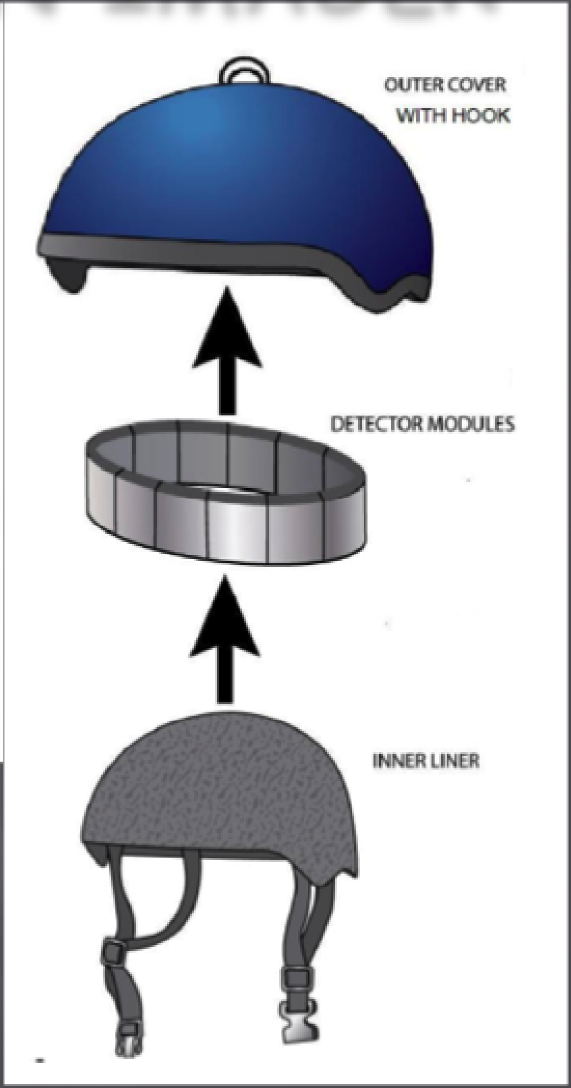

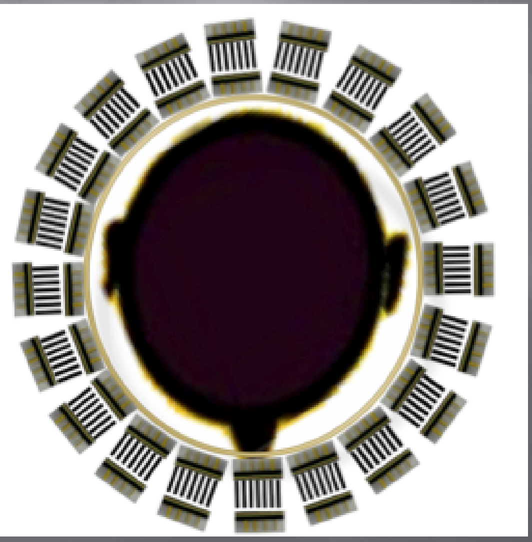

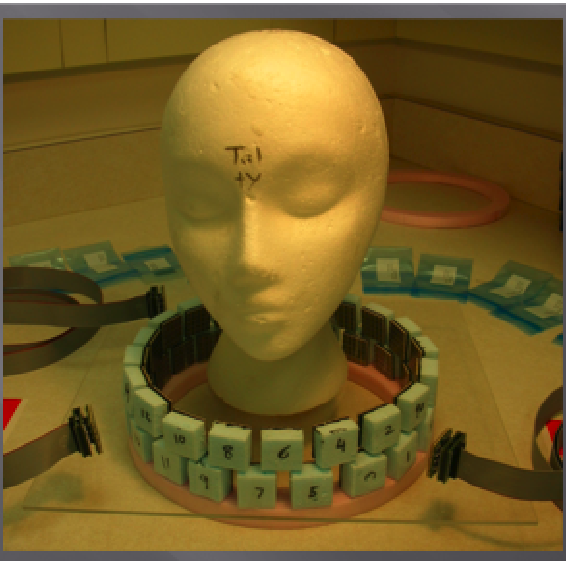

Each detector module is based on two 1"x1" Silicon Photomultiplier modules and a 1.0-1.5mm LYSO scintillation array (not shown). Status (5/2010): under construction, WVU.

Anticipated Applications Of The Helmet_PET Scanner

1. Stroke Patients – Diagnosis and recovery
2. Epilepsy Patients – Treatment
3. Dementia Patients

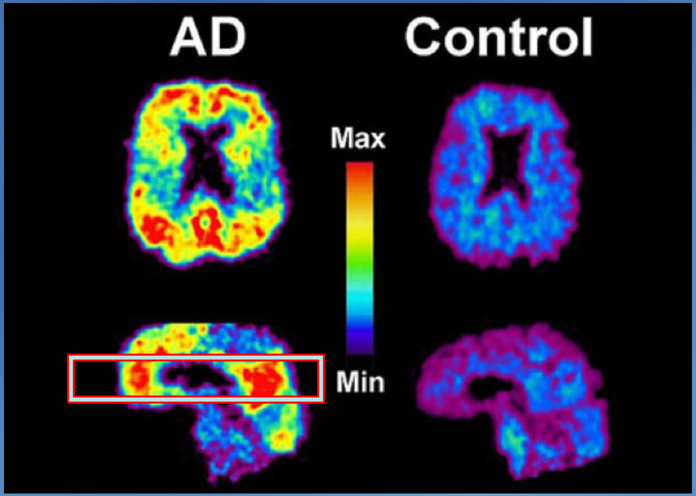

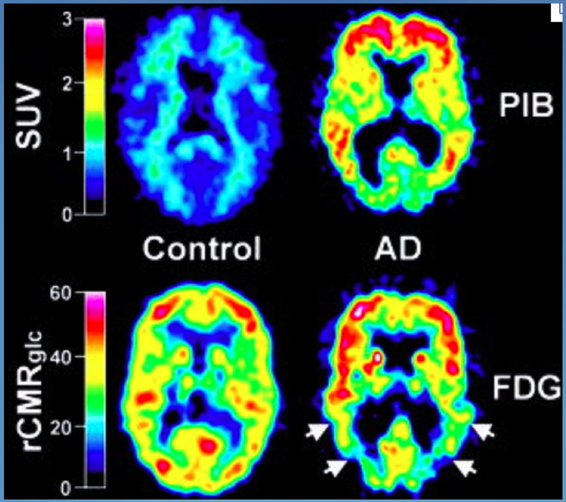

Examples of planned uses. Left: balancing patient tests using the computer controlled platform system. Center and Right: F18-PIB and F18-FDG PET images in Alzheimers.

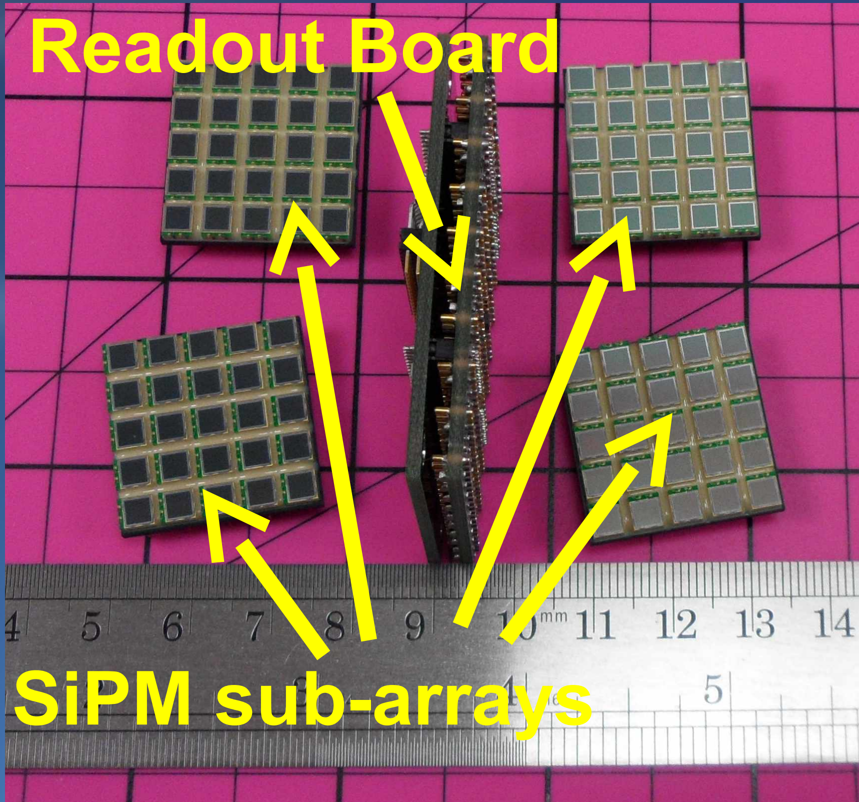
Readout Board
SiPM sub-arrays

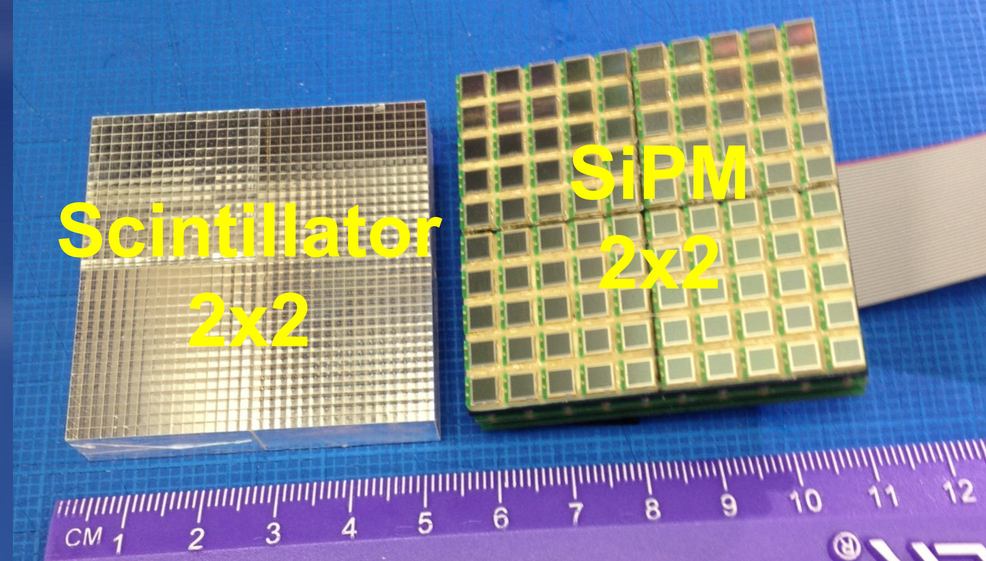
Scintillator
2x2
SiPM
2x2


SiPM
SiPM
SiPM
Scintillator
SiPM
Scintillator
Readout Board

New design: 100 MPPC Modules

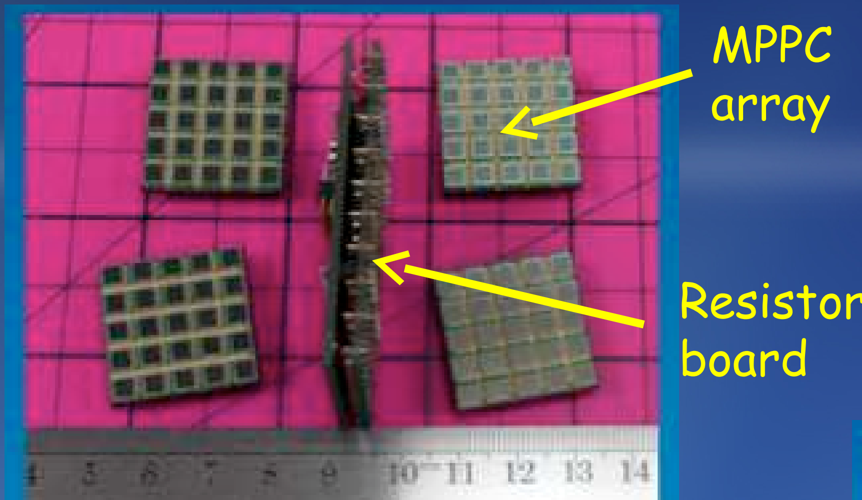

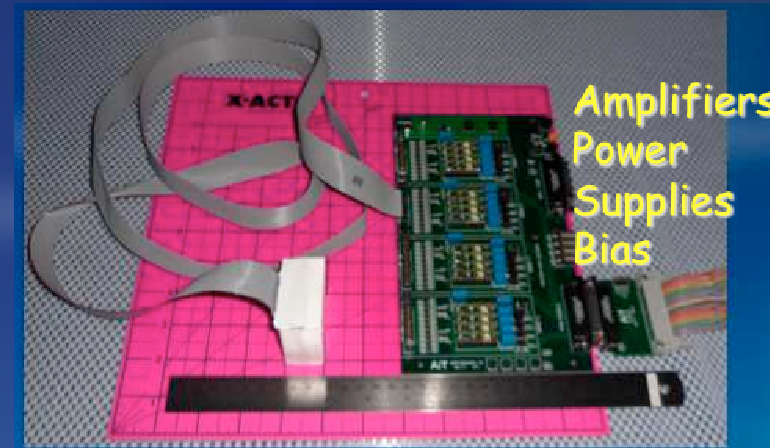

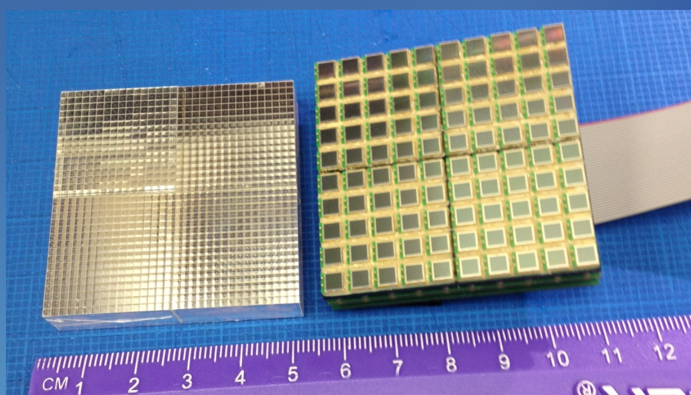

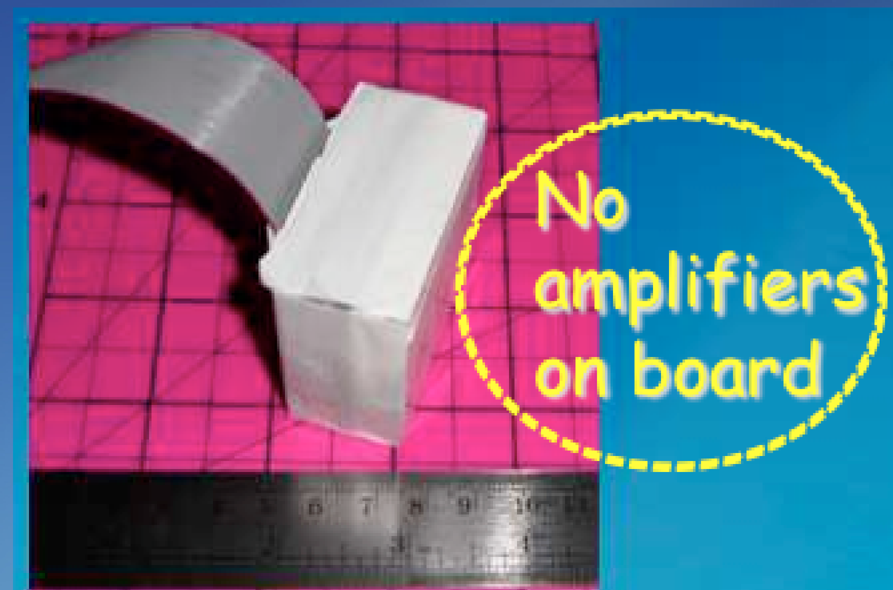

Left: Assembly of one ~5cm square compact module of the first Helmet PET prototype. Four Hamamatsu 25 MPPC arrays assembled on one resistive readout base from AiT Instruments. Four 1.5mm step 10mm thick LYSO arrays from Proteus coupled to form one compact module. There are no amplifiers or other active components on board the detector module, but in the distant (at the other end of the 2m cable) electronics board. There are 4 output channels per module.

WVU 12-Module Brain PET

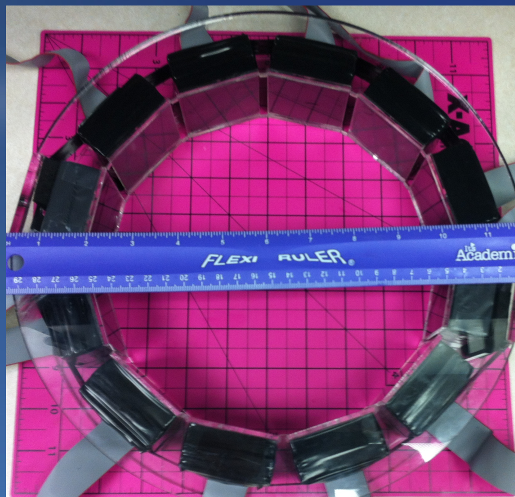

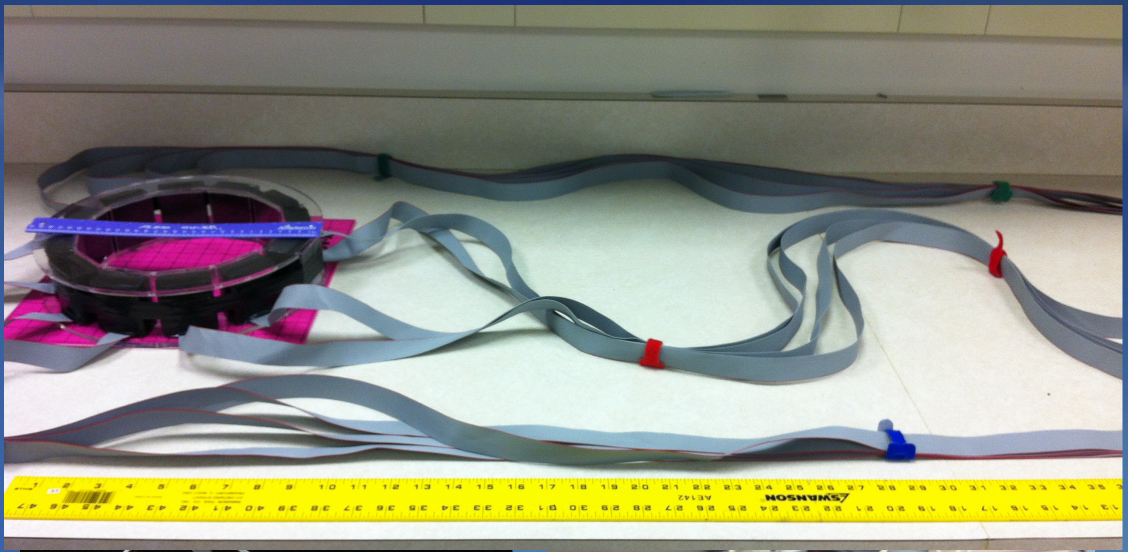

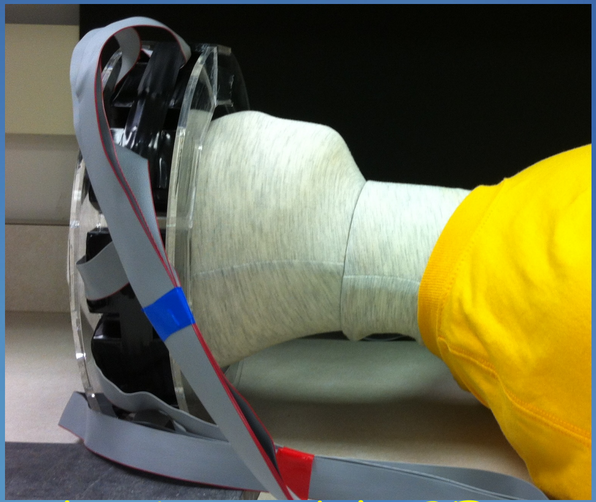

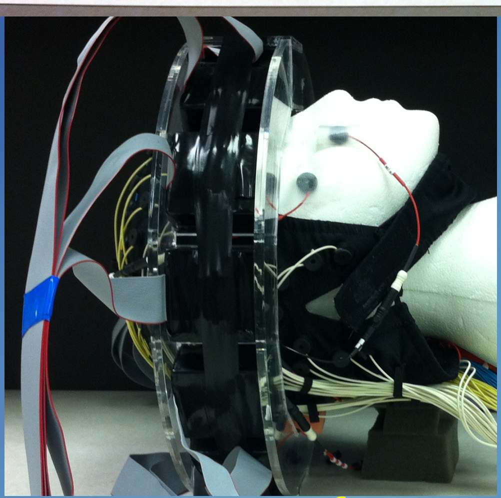

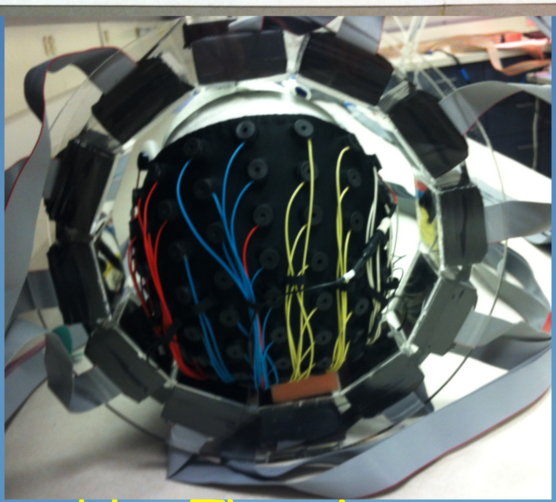

The 12-module PET ring prototype after assembly. The ring can also fit outside the EEG cap in a PET/EEG hybrid configuration. PET/MRI/EEG is also possible.

Brain Phantom Images

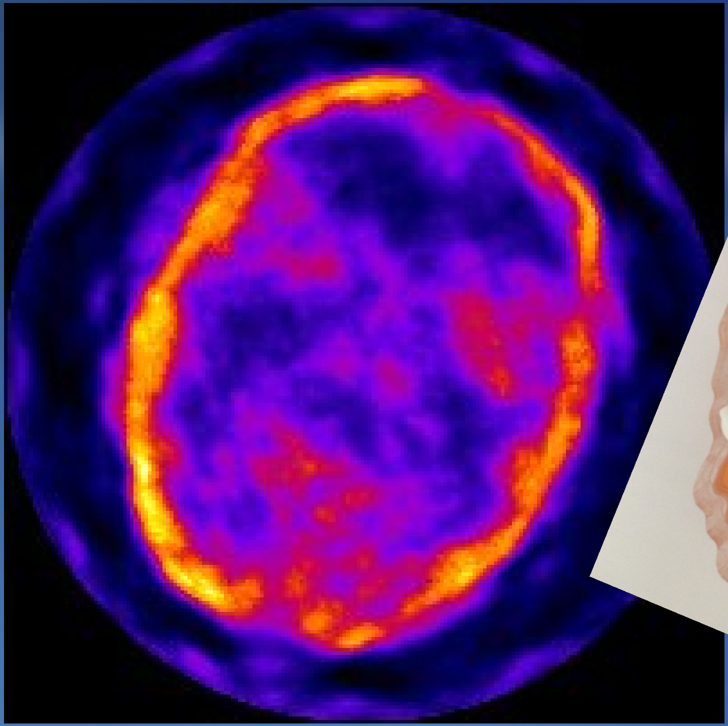

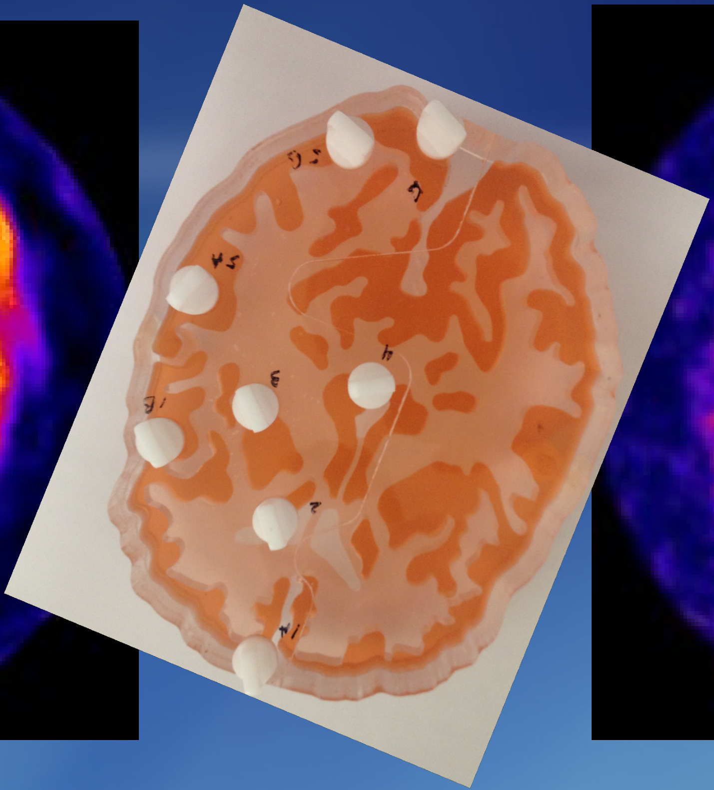

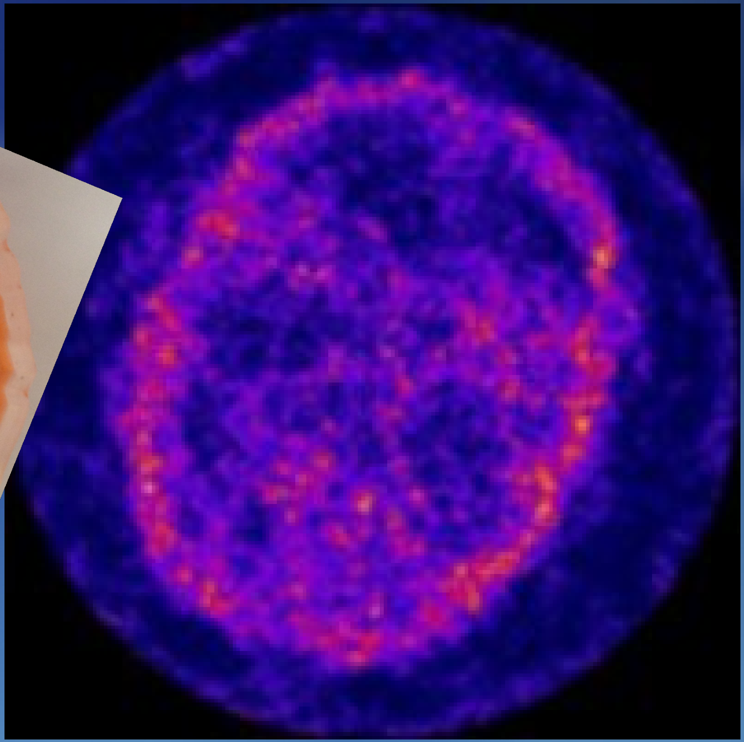

Reconstructed images of a set of 10 1mm slices from a multi-layer multi-compartmental brain phantom (center) filled with 450 microCurie F18 activity. Left: from the 30 minute run. Right; 30 second run. The short run image showed basically the same overall distribution pattern.

Brain Phantom Images

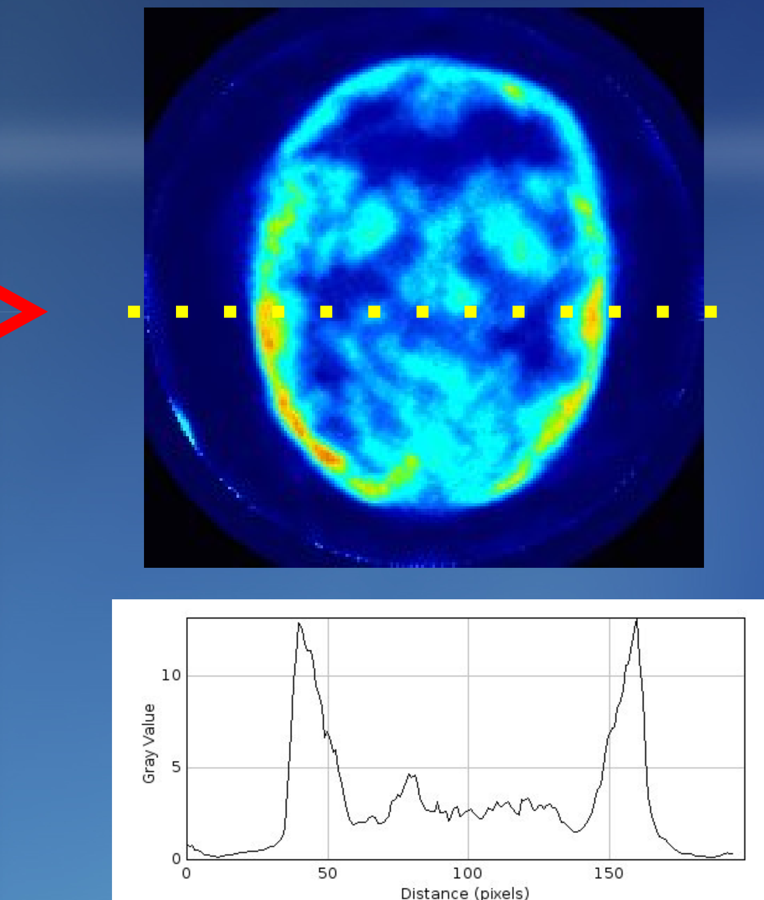

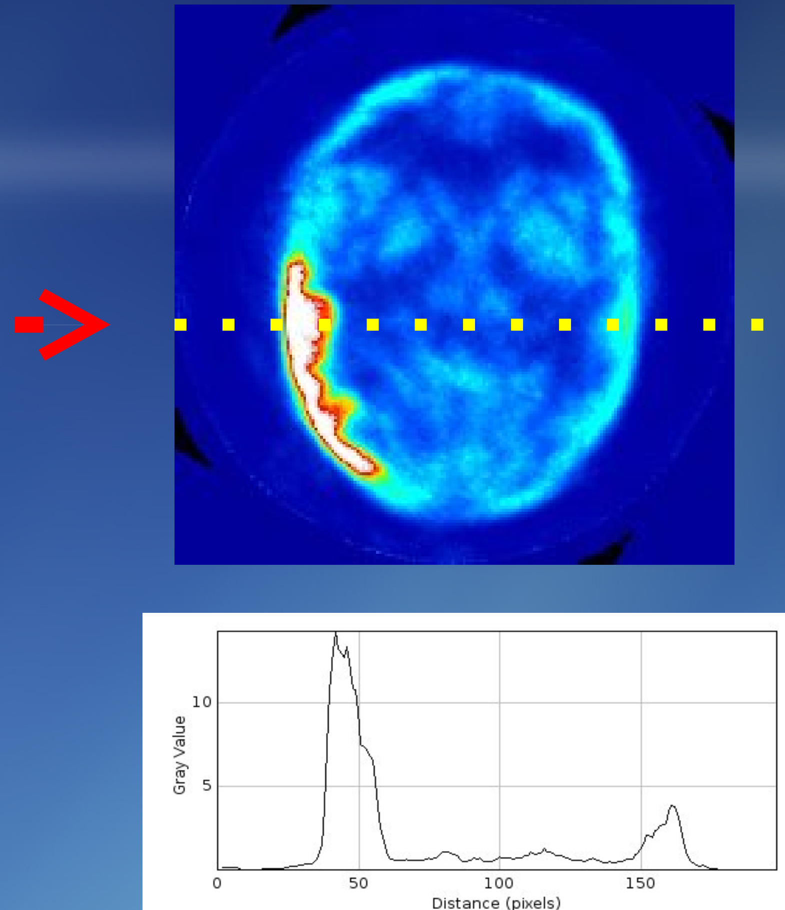

Selected images of a 1mm slice of a brain phantom, left: with uniform activity, right: with increased activity in a section of the brain.

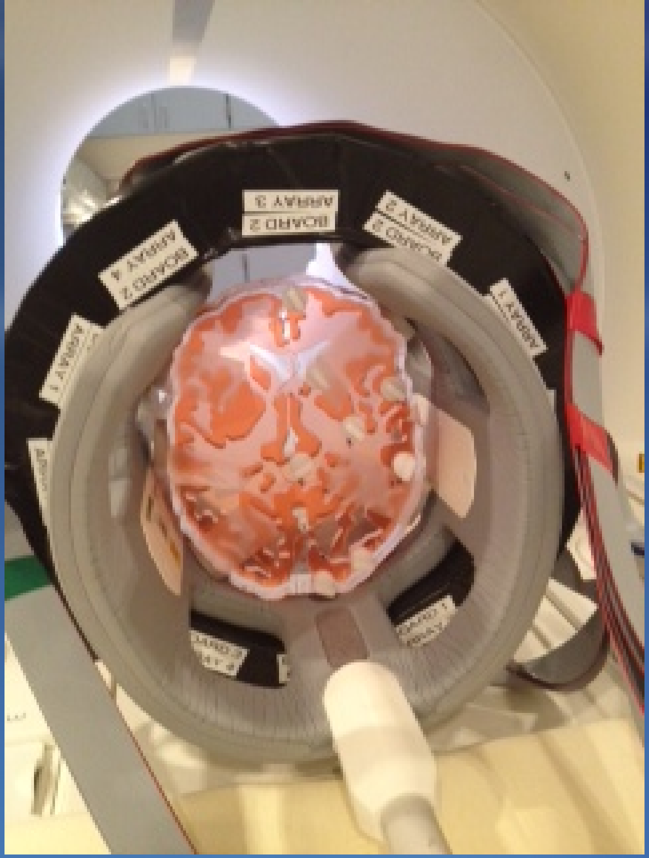

Left: Brain phantom inside the PET ring with a standard flexible MRI coil before insertion into the bore of a 3T MRI Siemens scanner. Right: MRI images of the phantom using MPRAGE sequencing and with the PET ring fully powered.

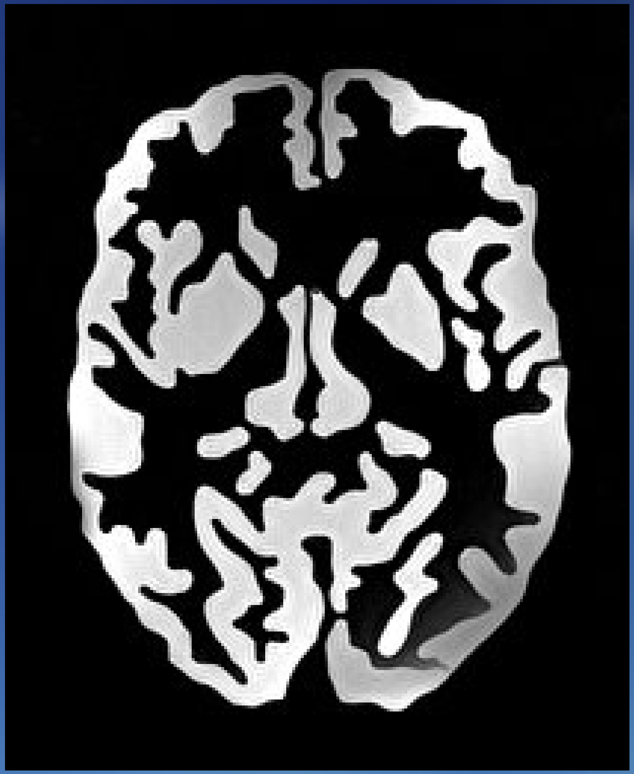

MRI images (2mm slices) of the brain phantom using T2 sequence. Left: obtained for comparison with the RF body coil only. Right: when using 3T Flex Large RF coil. In both cases the PET ring and PET DAQ/computer system was fully powered.

Upright Implementation

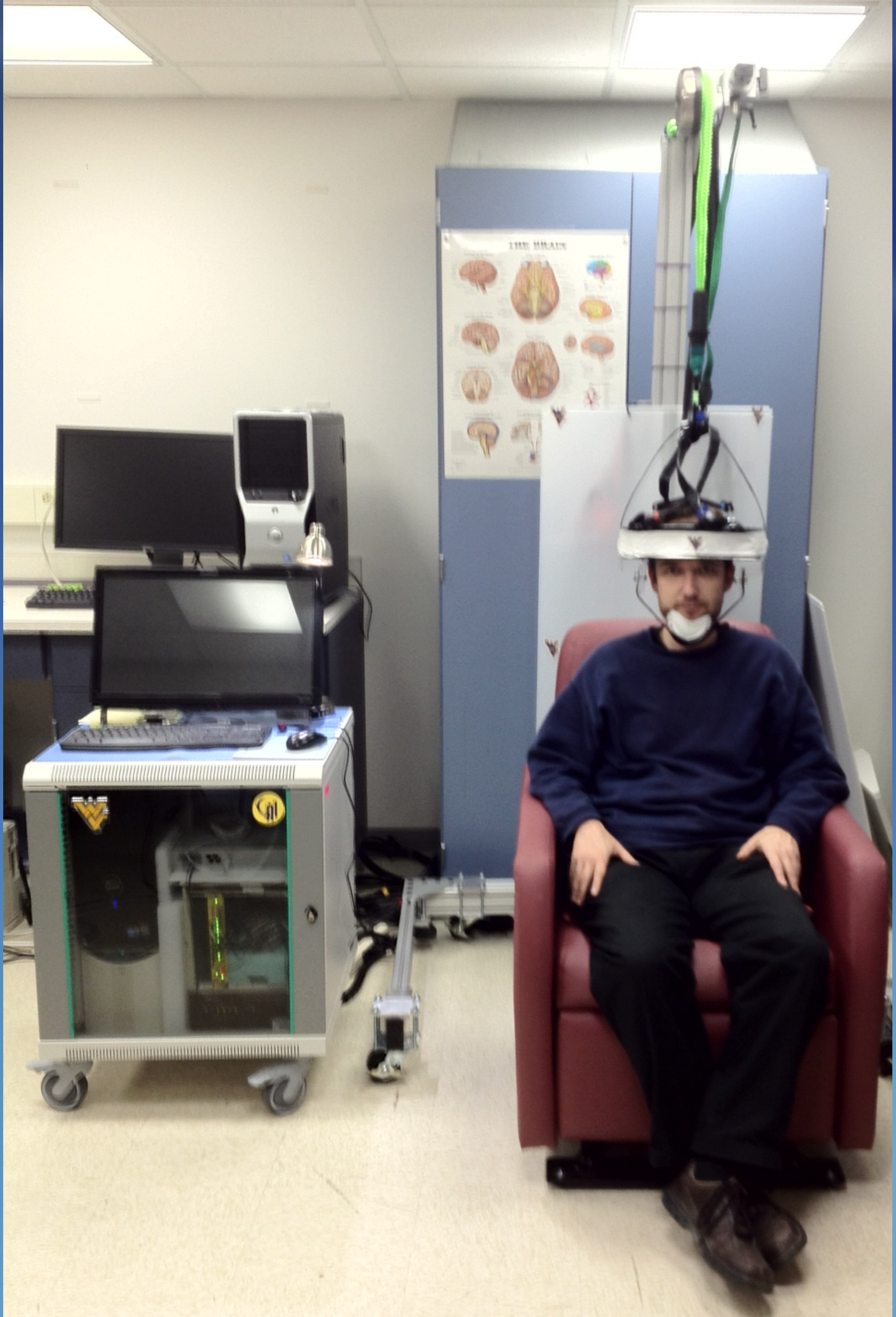

Setting of the upright system in preparation for pilot clinical trials.

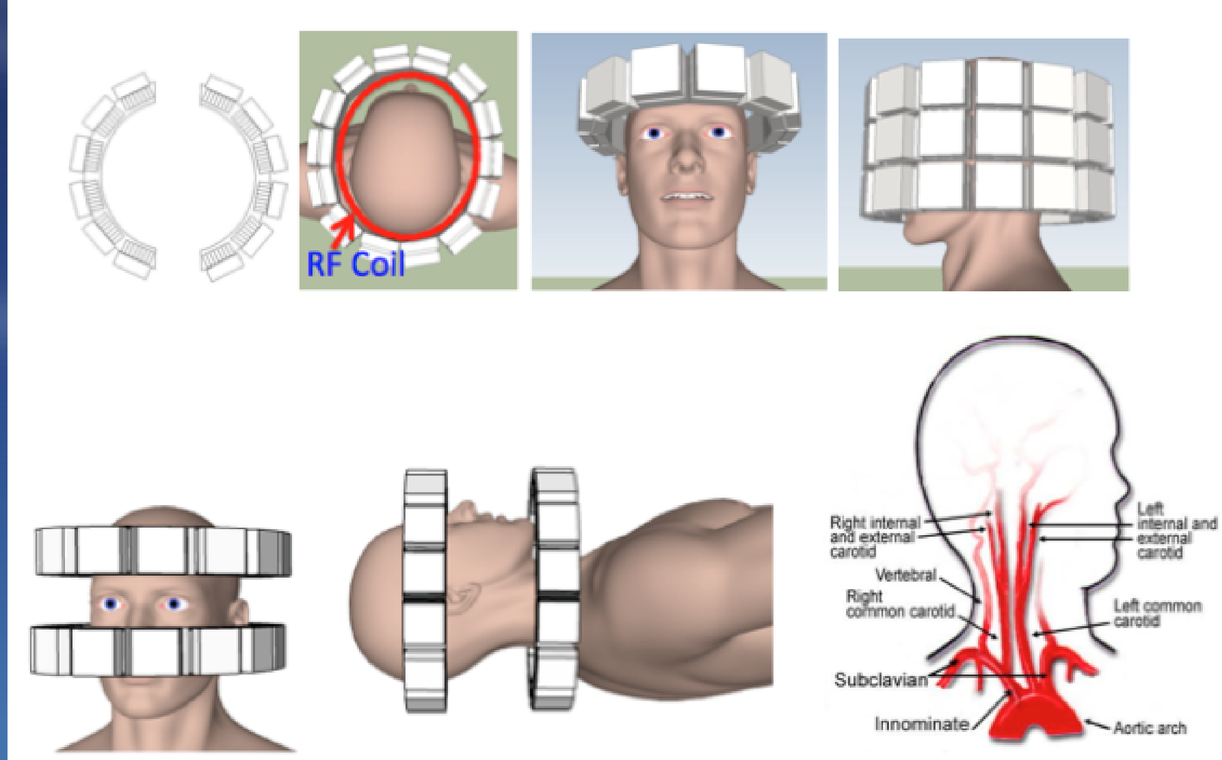

Top: Left: An example of a schematic of a single imager PET ring, shown here with 12 individual MRI-compatible PET modules, divided into two parts, for easy placement and adjustment on the patient's head/brain/neck. Each of the modules is made from a matrix of pixellated LYSO crystals coupled to an array of solid-state Silicon Photo-Multipliers (SiPM). Center: example of an elongated ring – here built with 14 modules, better adapted to the shape of the human head. In the simplest variant only a single ring of modules is built. However, ultimately a three-ring system that will cover the whole brain in one position will be built as shown at right. Bottom: The two-ring variant with two rings spaced apart with an adjustable spacing, is the intermediate - so called "Open PET" type arrangement [Yamaya et al – Ref 5], that provides larger field of view at a reduced complexity and cost. In a special case one of the rings can be placed at the neck level, for example during first path dynamic blood flow imaging with the neck ring measuring the so called input function in the carotid artery. The MRI RF coils - not shown here - are placed inside all the rings.

Dual-sided SiPM readout for “high resolution” PET

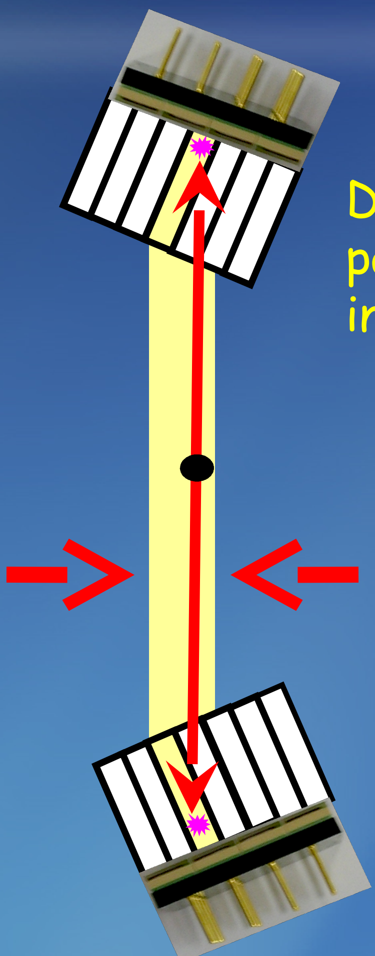

Dual-sided readout reduces the parallax error related to the depth of interaction effect

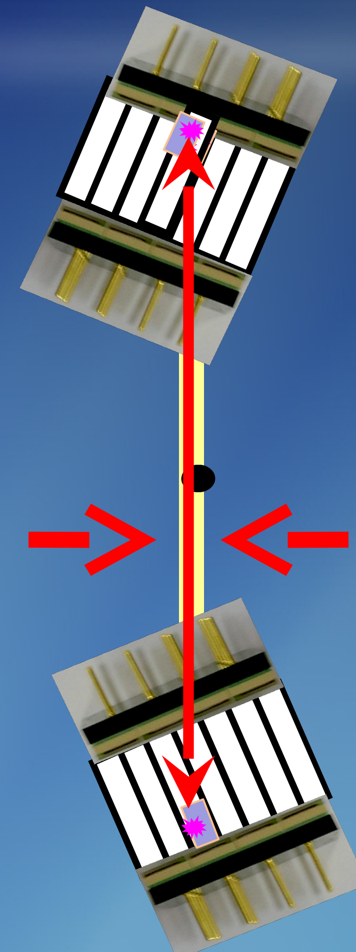

PET DOI Module Structure

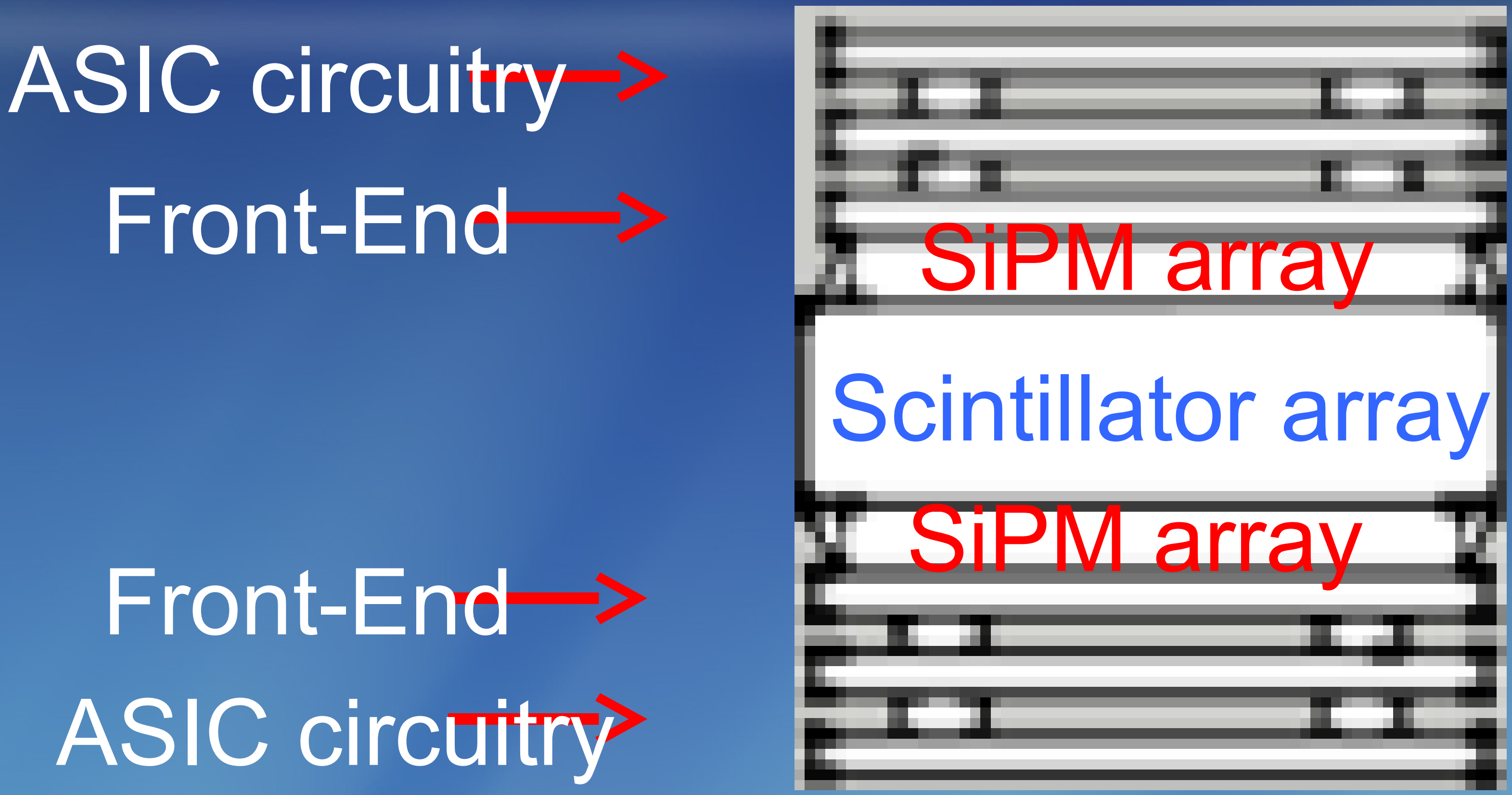

DOI prototype

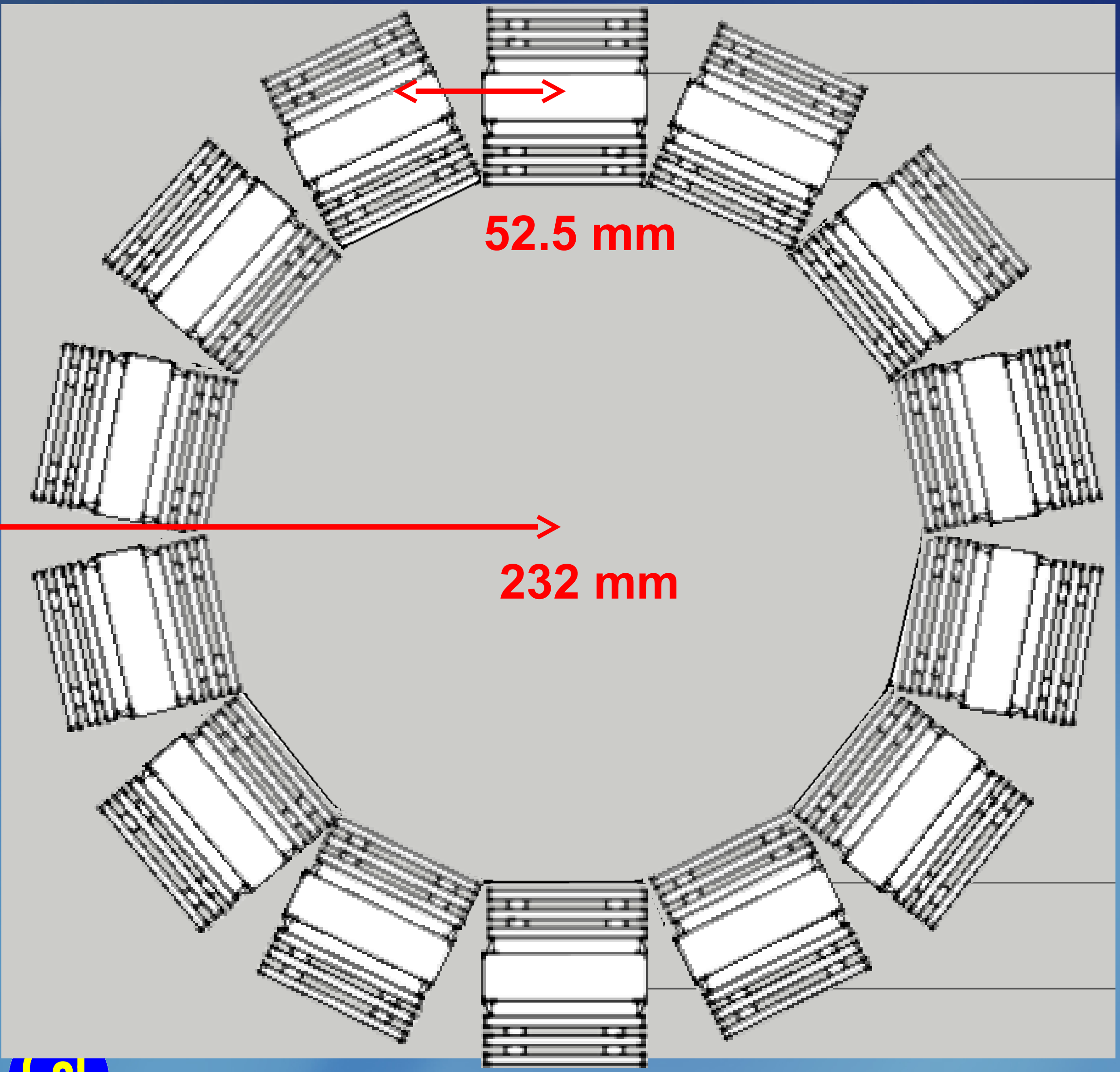

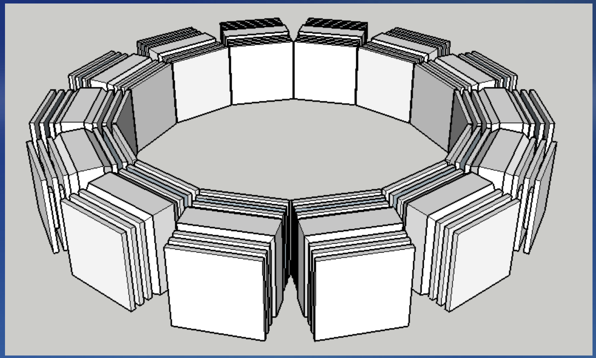

Single ring of 14 modules, 23.2 cm diameter, each module consists of 35 x 35 LYSO 1.5 mm*1.5 mm*10 mm pixels.

Next Upgrade of Upright Implementation !

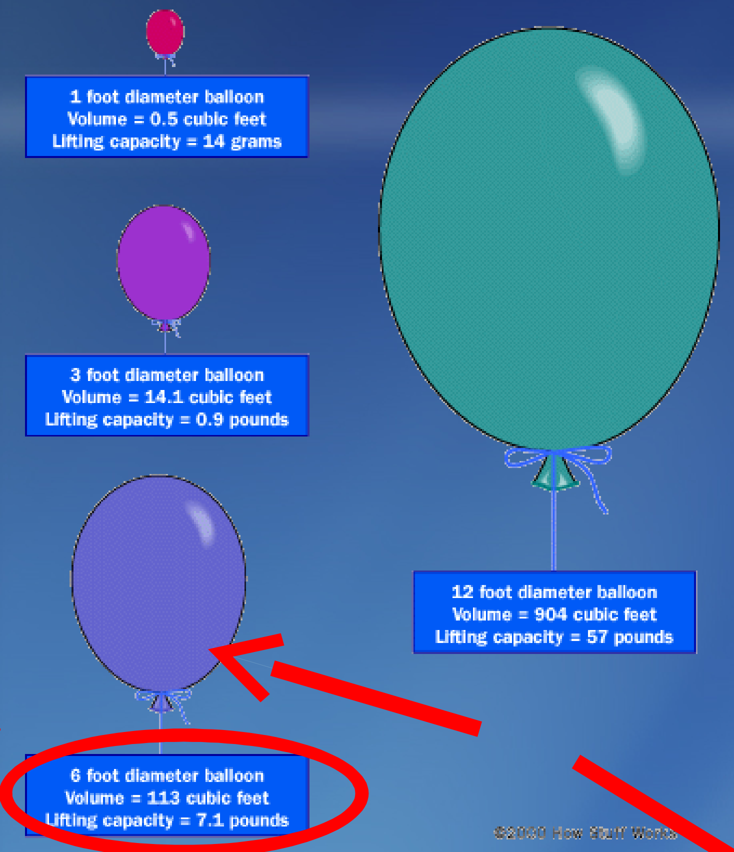

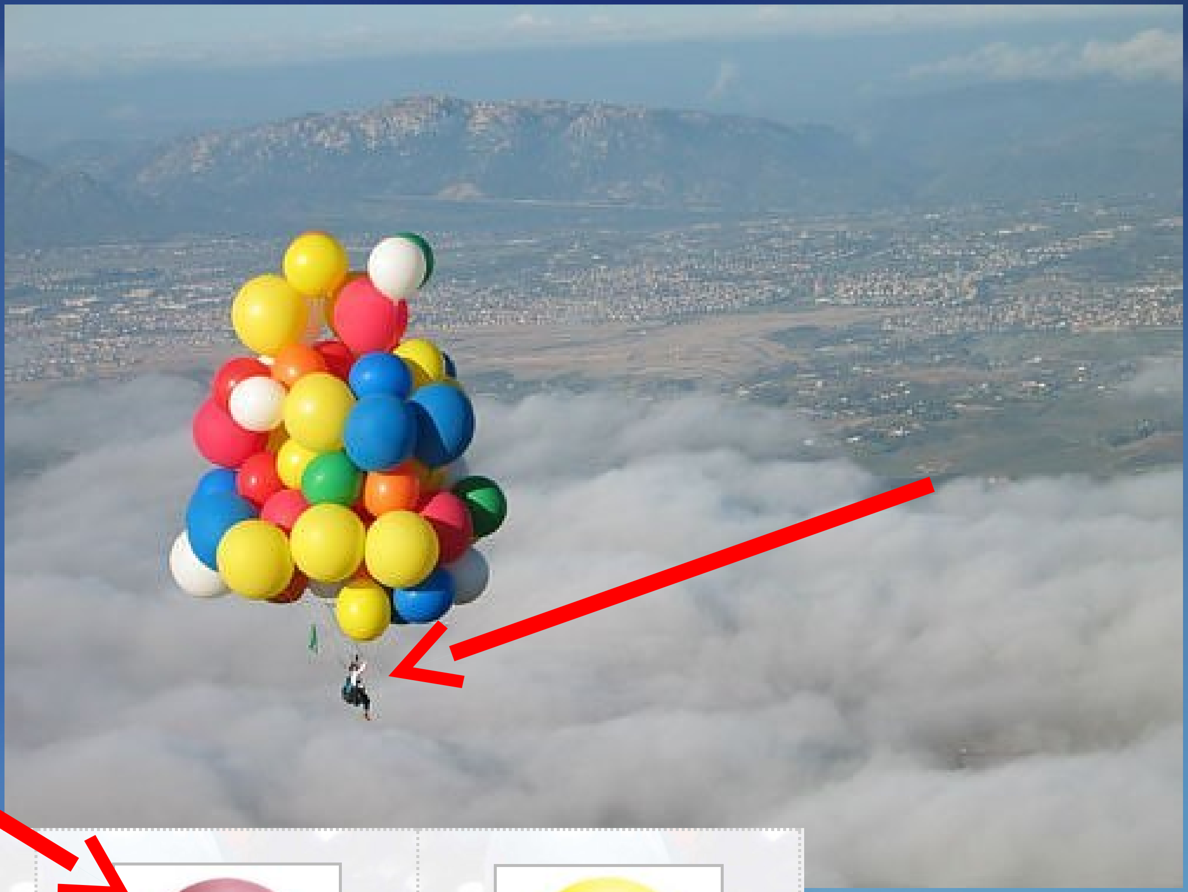

Partial ring TOF PET for breast imaging

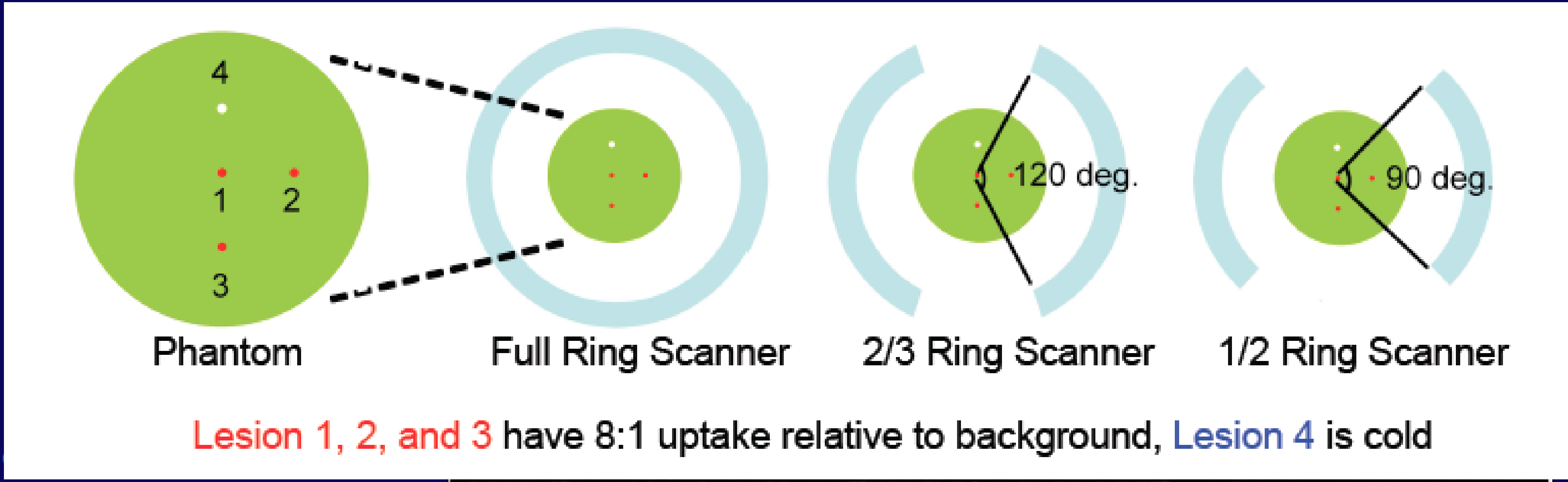

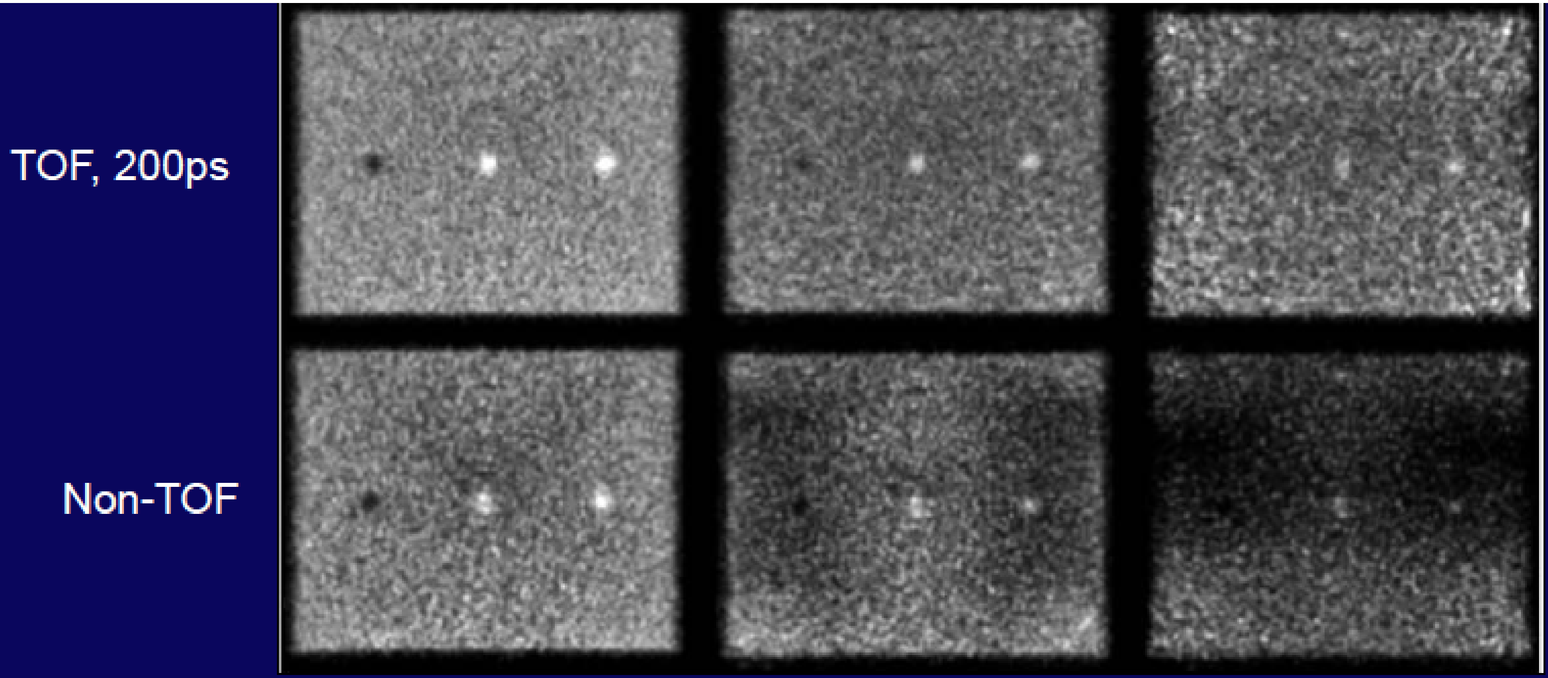

In-situ dose verification for proton beam therapy

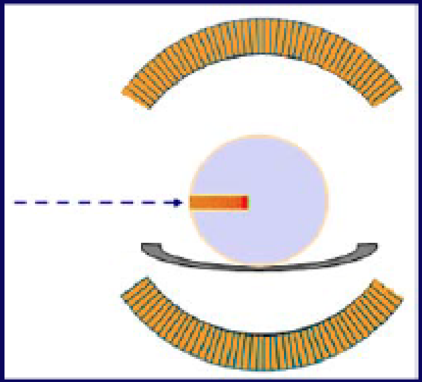

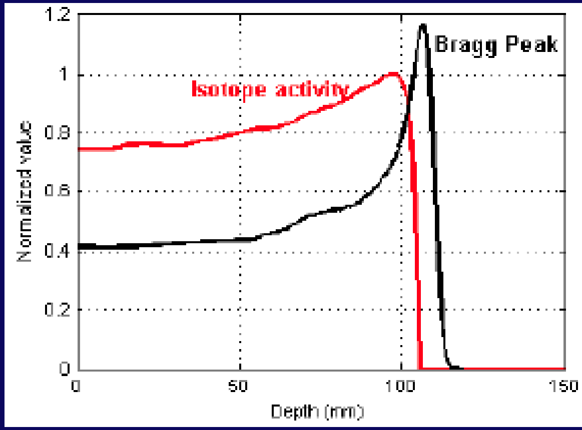

Full ring | Two-third ring

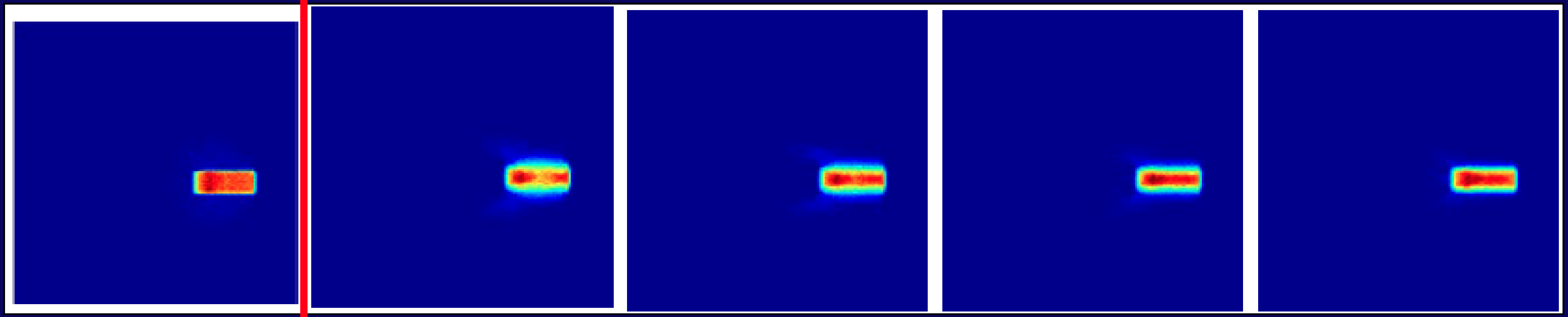

- 30-cm diameter cylinder irradiated by 4x4-cm^2 125-MeV proton beam
- Isotope profile from GEANT4 simulation in skeleton muscle
- PET simulation performed in EGS4 and data written out in list-mode

Timing Resolution Measurement

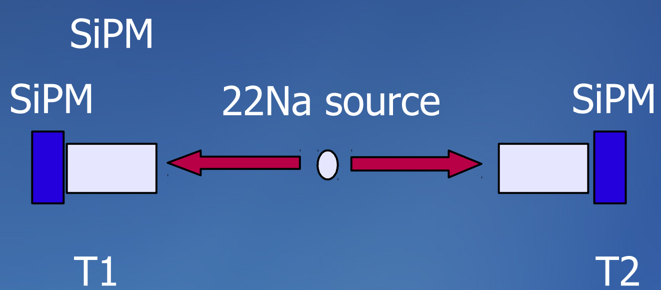

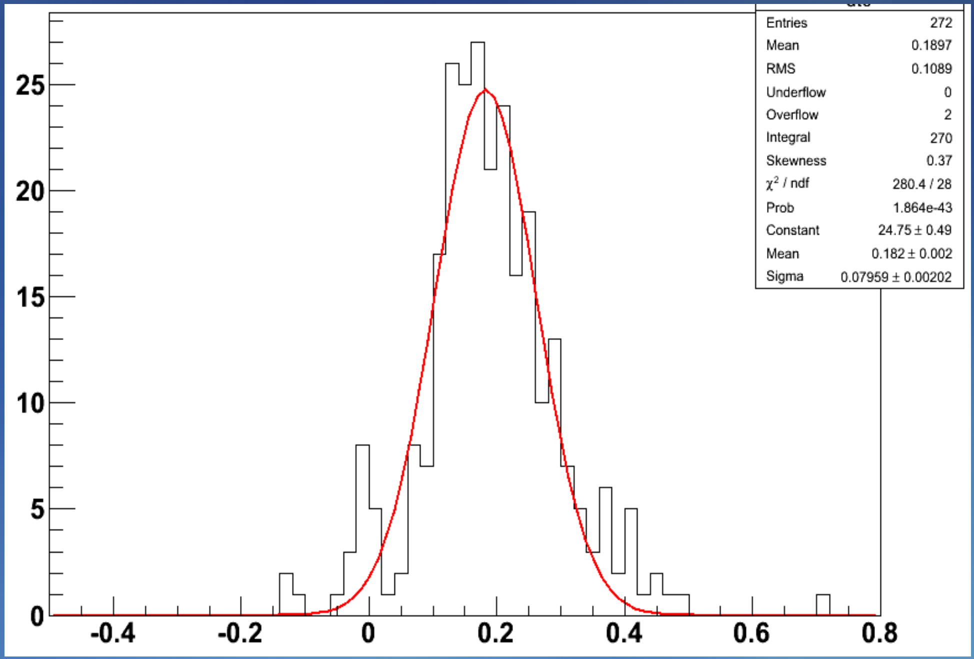

- Setup: 3x3x15 mm3 LYSO crystals read out by Hamamatsu S10362 SiPMs
- coinsidence timing resolution Δ T1-T2 = 188 ps FWHM
- coordinate resolution Δ x=c*Δ T1-T2/2 better than 3cm FWHM

Recovery of the Compton

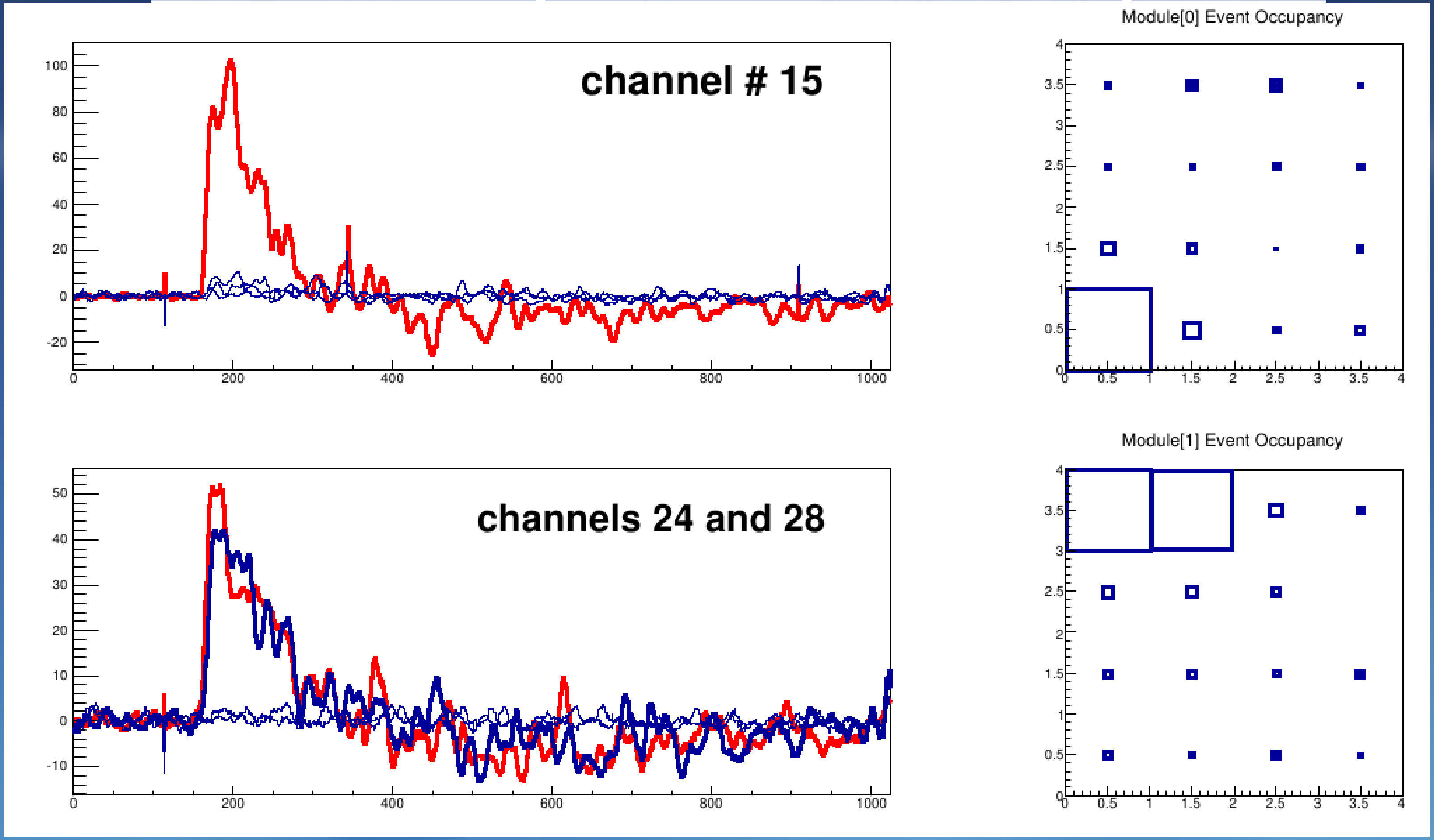

- Read out 2 4x4 LYSO arrays with 4x4.5x15 mm LYSO crystals
- Select events with two hit pixels on one side, sum up the two charges

Recovery of the Compton

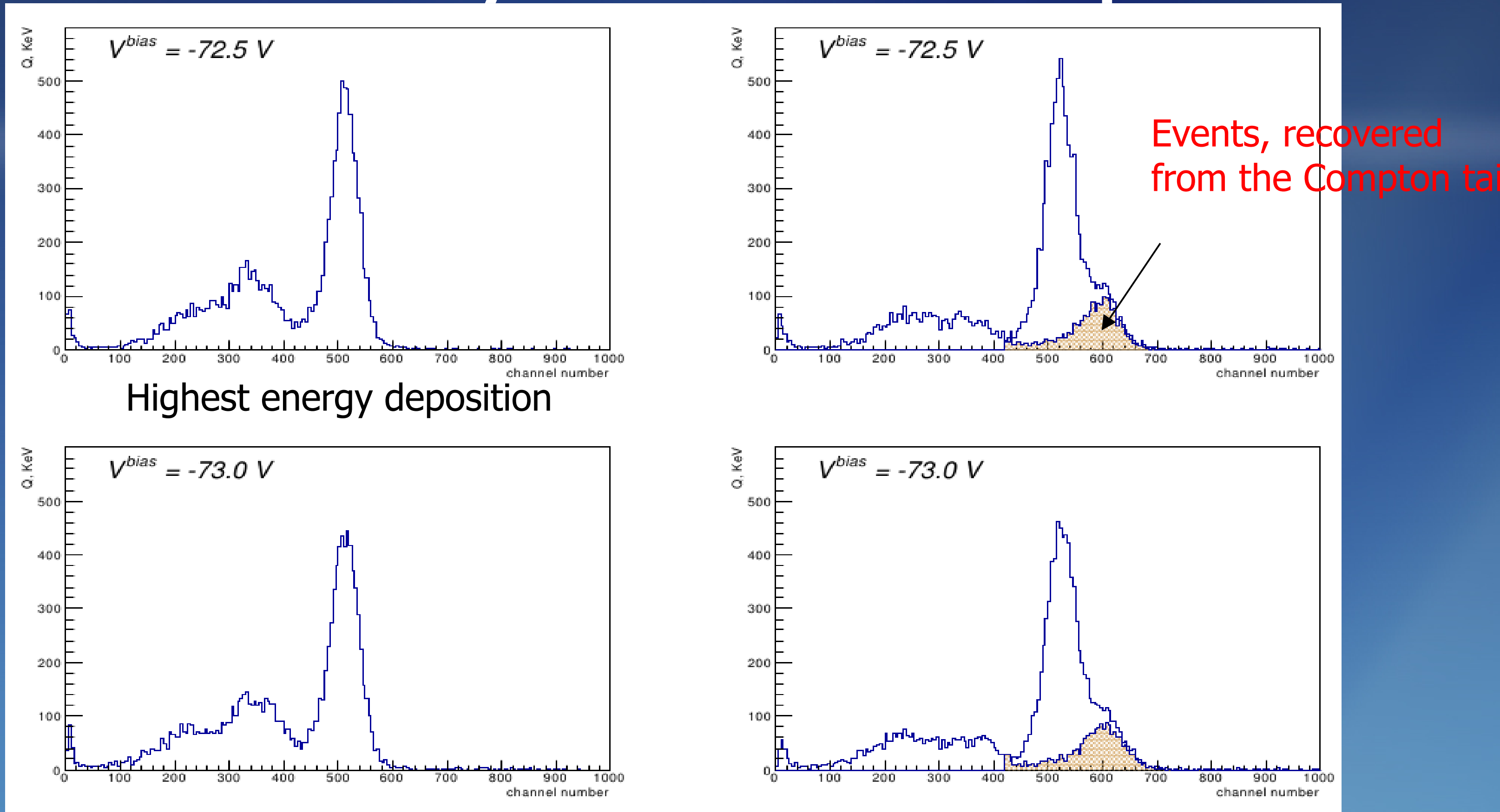

- Photopeak selection: number of events increases by ~40%
- Observe SiPM saturation at a level of 15%
  - <N photons> about 1000, N cells = 3600

Multiplexed Readout to Reduce the Number of Channels

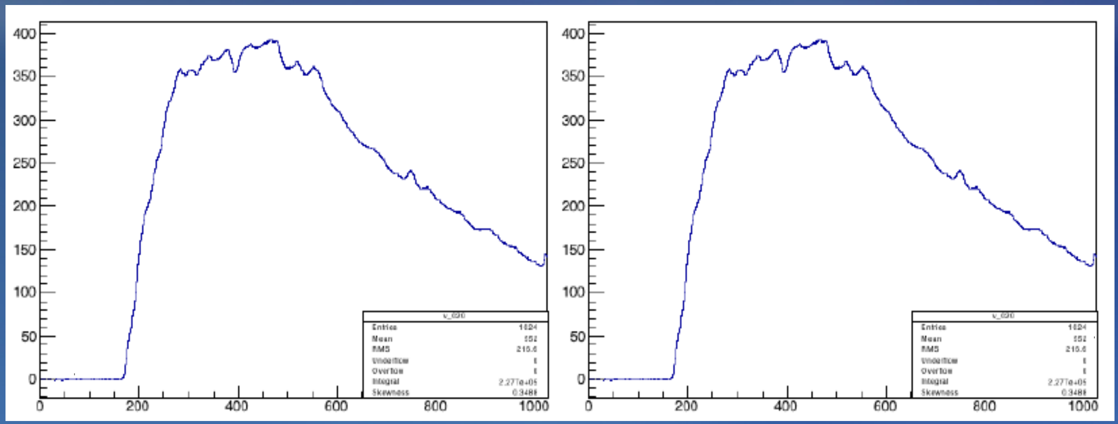

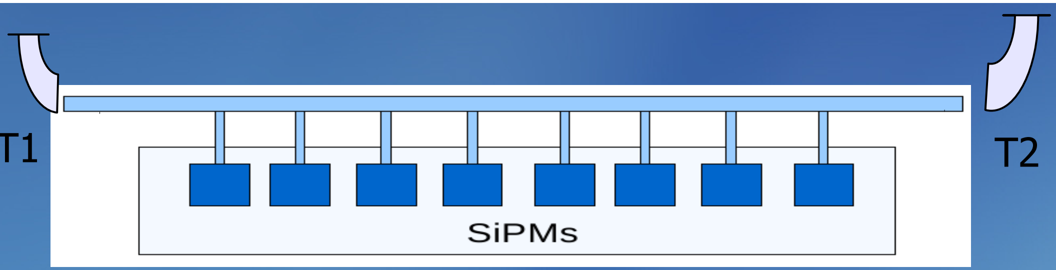

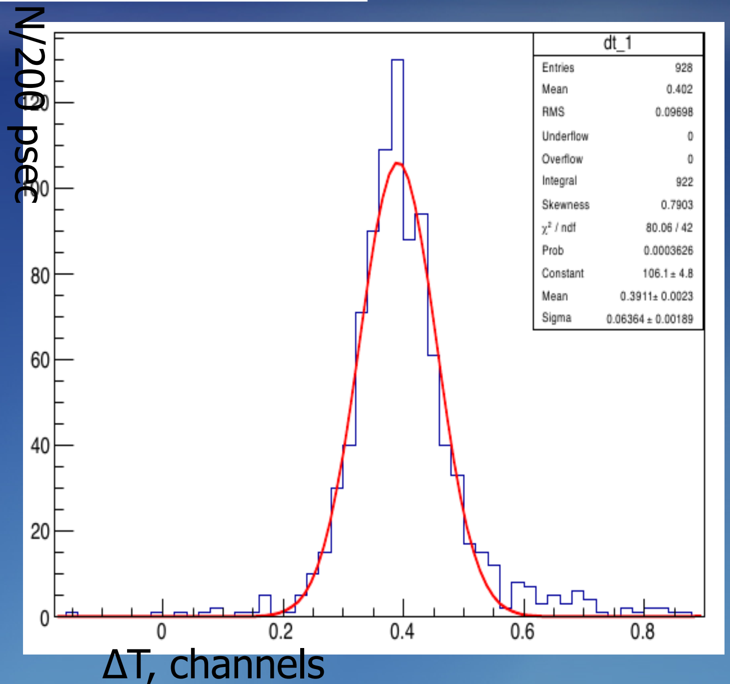

- Use the delay line with 8 SiPMs read out by 2 channels
- Reconstruct hit channel from the time difference ΔT = T1-T2
- Reduce the total number of readout channels by a factor of 4
- σT1-T2 ~ 30 ps FWHM, or ~2.2 mm FWHM along the delay line
- For readout pitch of 4-5mm, individual crystals are well resolved

PET-TOF Strip Line Status

- **Next SL prototype has 4 strings of 8xSiPMs**
  - **Design is for STM 10-contact 5.1x5.1 mm2 package**
  - **Diode pitch is 5.2 mm**
- **Boards should arrive any time now, full component kit exists**
  - **First I plan to assemble 2 boards with a single line of diodes (solder)**
  - **Second step is to assemble a complete board, using anisotropic conductive film (will need 4x8 scintillator blocks for that – to push diodes against the board)**
  - **If conductive film does not work – will solder everything, and we have to learn how to ensure a good optical contact between scintillator and diodes**

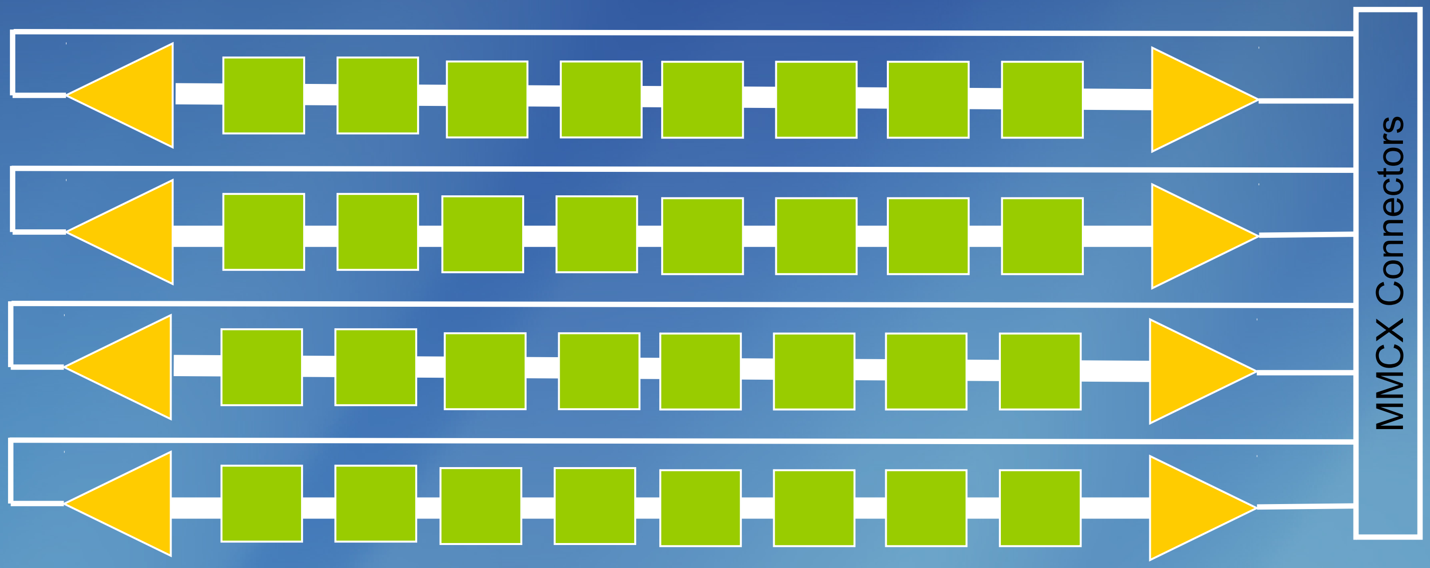

Strip Line Details

- Next SL prototype will have 4 strings of 8xSiPMs
  - Design is for STM 10-contact 5.1x5.1 mm2 package (that is a rather challenging package for board layout)
  - Diode pitch is 5.2 mm
- I have a layout of an elementary cell, note two strip lines per row, the second one returns far end signal to the "digital end" of the board
  - GALI-S66+ amplifier from MiniCircuits (not an ideal package, but layout is possible) relatively low power consumption 16mA@6V, gain of x10@1GHz / x6.6@3GHz)

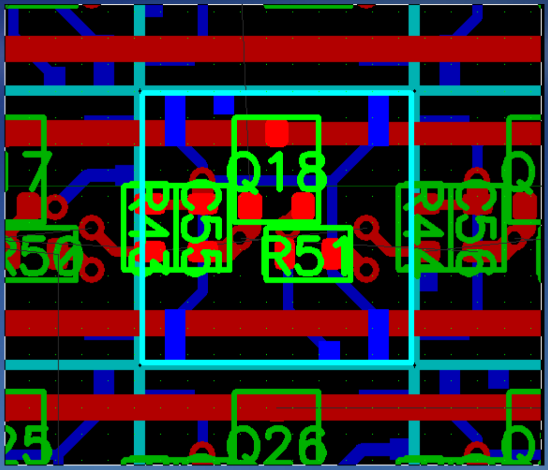

Diode cell layout

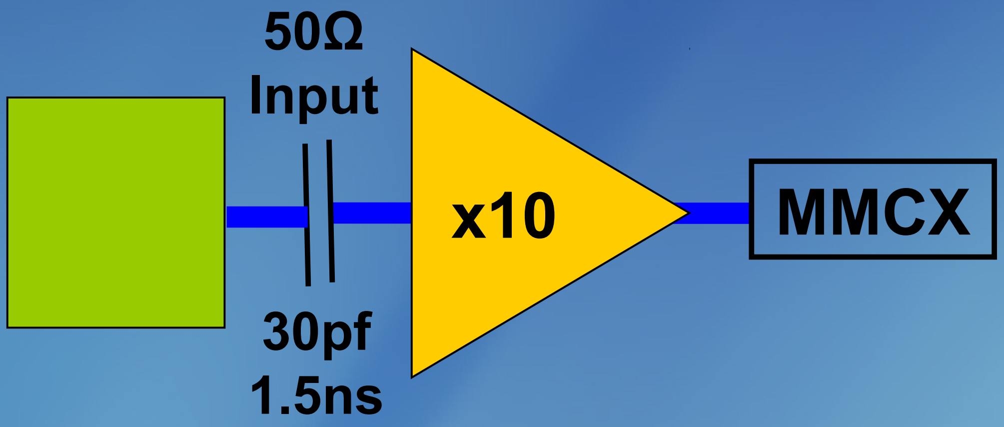

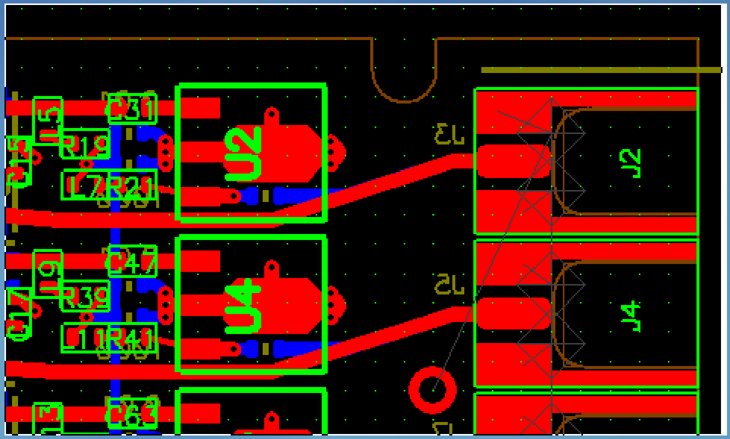

Amplifier cell layout

Signal Shape Simulations

- I have run a series of Spice simulations to get an idea of the pulse shape, and amplitude for various scenarios of diode interfacing, and pulse shaping
  - Light pulse shape:
  - 0.3ns rise time
  - 40ns fall time (LYSO time constant) -
  - Assumed 20ns of SiPM recovery timeLYSO light yield is 500 pe, and SiPM gain of x106 (easy to scale if different)
  - For shaping a simple C-R differentiating ("clipping") circuit is used with time constant of the order of 1ns

SiPM output pulse shape for different pixel stray capacitance:

0.1%(green) 10%(red) 20%(blue)

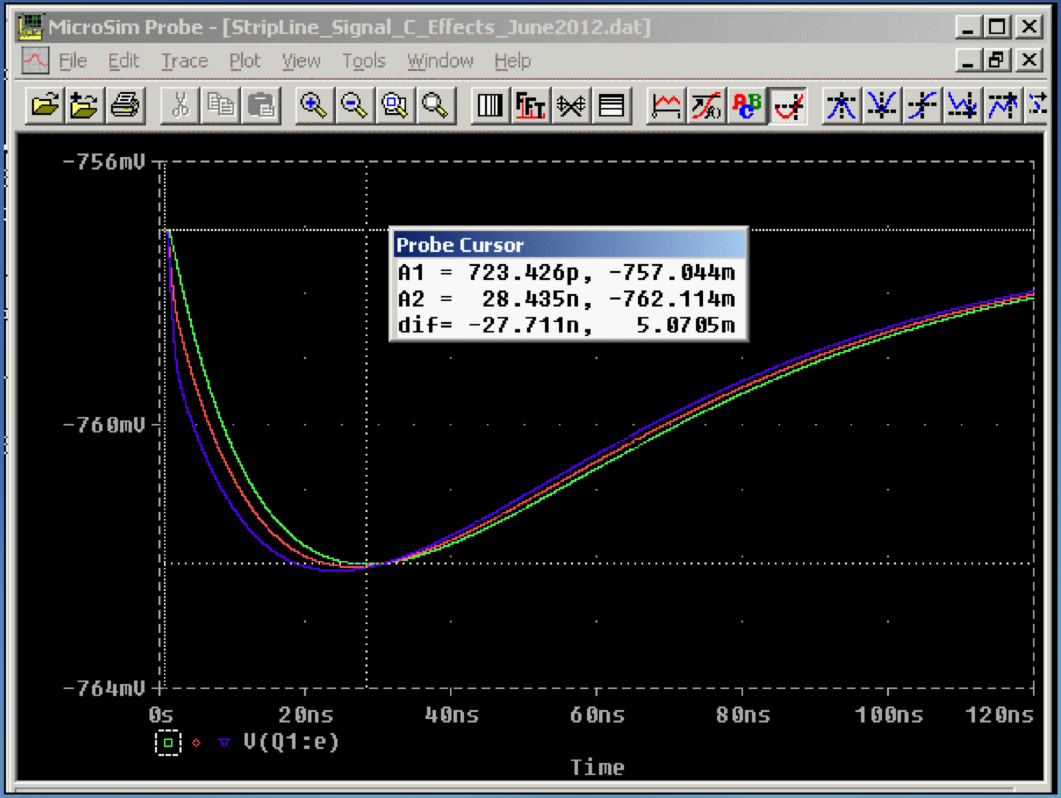

Output Signals (after x10 amplifier and shaping)

- Signals shown at the two ends of the same transmission line (aligned in time):
  - Output 1 – near end
  - Output 2 – far end (lower peak amplitude)
- Pulse shapes are shown for different output capacitances of the SiPM buffer transistors:
  - Left - 0.5pf (previous SL board)
  - Right – 0.1pf (new SL board)

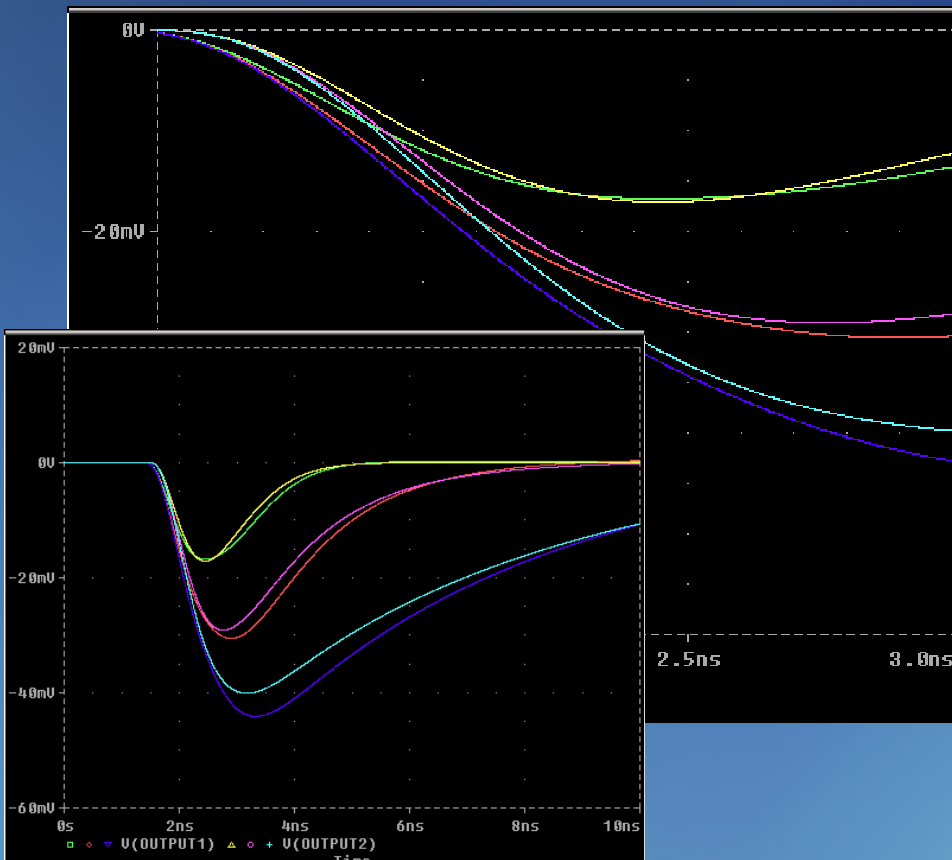

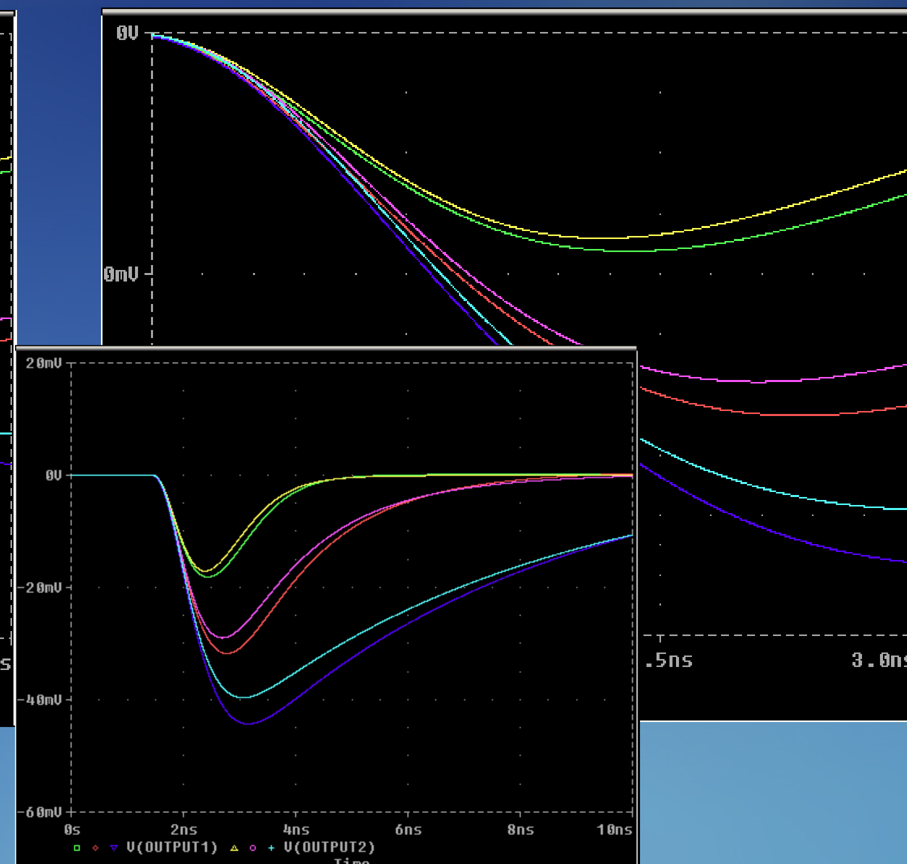

SiPM output pulse shape for different shaping capacitors: 10/30/100pf

Ring Designs – version 0

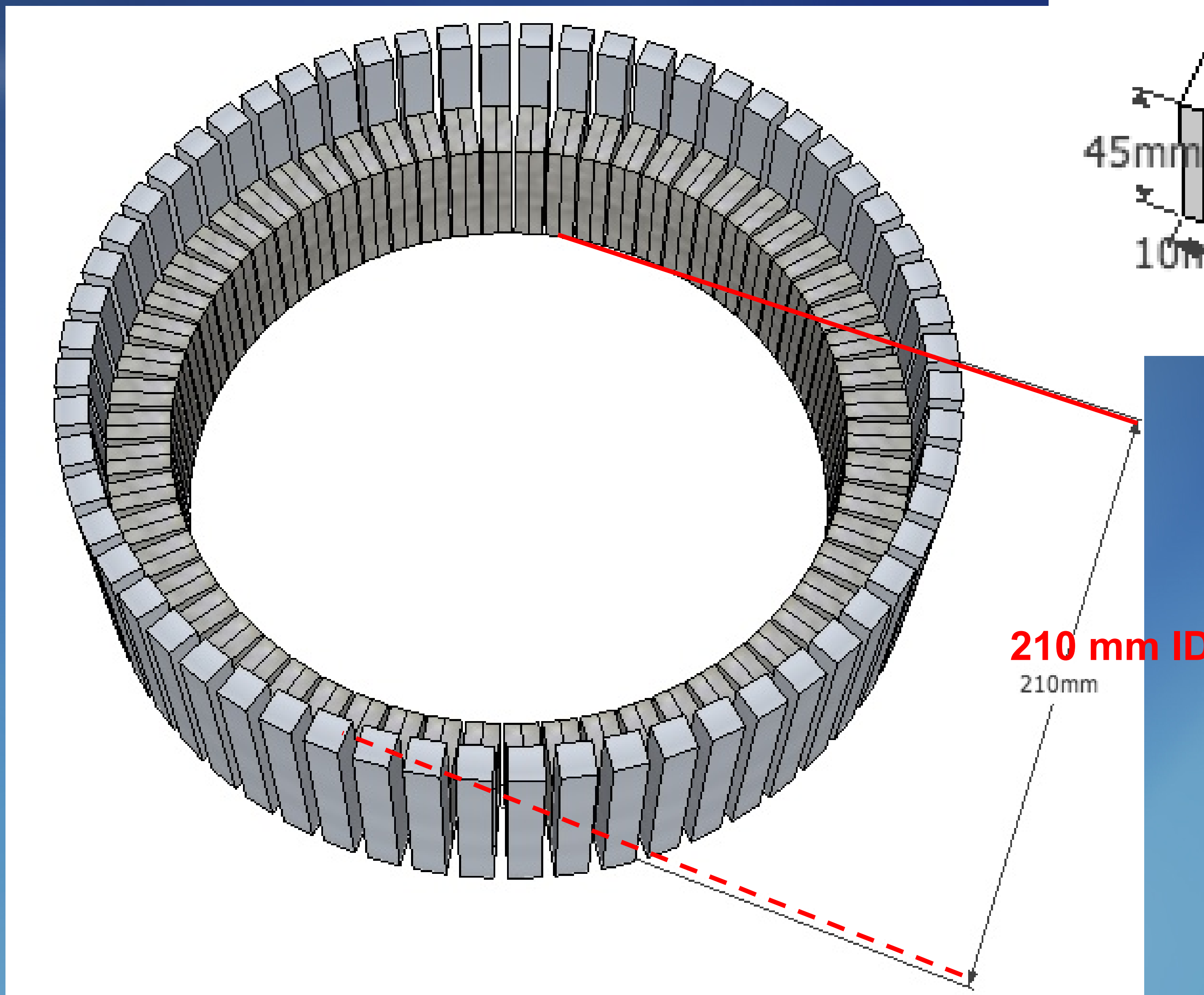

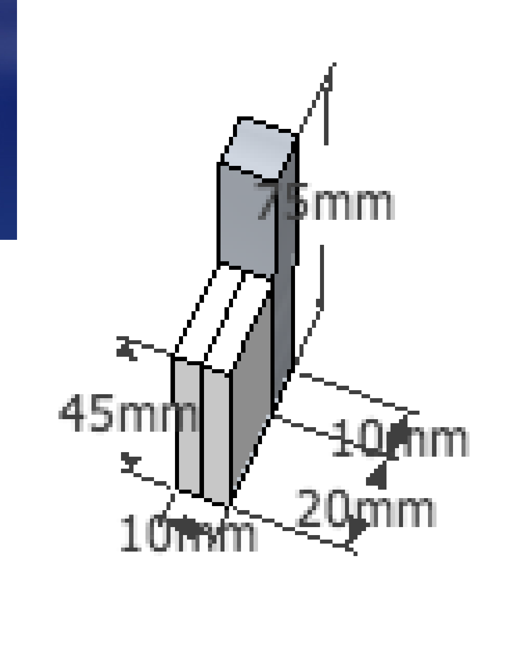

Summary

- Particle physicists have played and still play substantial role in medical imaging: basic concepts, detectors, electronics, simulations, reconstructions. …
- PET was invented many years ago but only in the last decade got full recognition for its unique clinical role when combined with CT and now with MRI
- PET imaging is providing critical assistance with patient diagnosis and treatment, as well as with work on understanding disease origin and cures (in small animal models)
- PET improvements are under way to reach the physical limits of the technique (again role for physicists !): TOF PET, partial angular coverage
- Many new technologies: scintillators, photodetectors, solid state materials – spin-offs from particle physics
- Organ-specific PET imagers-inserts in MRI is the new frontline
- Brain imaging – an obvious focus
- Challenge: ~35k MRI imagers to upgrade to PET/MR
- National laboratories are involved – Fermilab is involved !

Thank you !